MICROCOPY RESOLUTION TEST CHART

NATIONAL BUREAU OF STANDARDS 1963 A
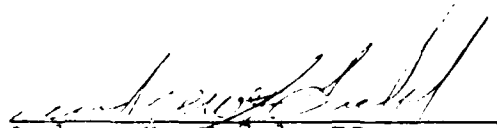
④

March 14, 1988

AD-A192 121

FINAL REPORT

ARC REPORT NO. R88-162

SDIO-SBIR Contract

N00014-87-C-0848

"Radiation Hard Sensors for Surveillance"

DTIC
S ELECTE D
MAR 1 7 1988
∞H

Andrew S. Endal, PI

A. K. Drukier, Co-PI

88 3 15 006

MIL-STD-847B
7 November 198?

REPORT DOCUMENTATION PAGE

1a. REPORT SECURITY CLASSIFICATION	1b. RESTRICTIVE MARKINGS
UNCLASSIFIED	N/A

2a. SECURITY CLASSIFICATION AUTHORITY	3. DISTRIBUTION/AVAILABILITY OF REPORT
N/A	
2b. DECLASSIFICATION/DOWNGRADING SCHEDULE	UNCLASSIFIED/UNLIMITED
N/A	

4. PERFORMING ORGANIZATION REPORT NUMBER(S)	5. MONITORING ORGANIZATION REPORT NUMBER(S)
0001AB	

6a. NAME OF PERFORMING ORGANIZATION	6b. OFFICE SYMBOL (If applicable)	7a. NAME OF MONITORING ORGANIZATION S2010A
Applied Research Corp		Defense Contract Administration Services Management Area/Baltimore

6c. ADDRESS (City, State and ZIP Code)	7b. ADDRESS (City, State and ZIP Code)
8201 Corporate Drive, Suite 920 Landover, MD 20785	300 East Joppa Road Hampton Plaza Bldg., Room 200 Towson, MD 21204-3099

8a. NAME OF FUNDING/SPONSORING ORGANIZATION	8b. OFFICE SYMBOL (If applicable)	9. PROCUREMENT INSTRUMENT IDENTIFICATION NUMBER
Office of Naval Research	N00014	N00014-87-C-0848

8c. ADDRESS (City, State and ZIP Code)	10. SOURCE OF FUNDING NOS			
Dept. of Navy, Code 1512B:JRT 800 N. Quincy Street Arlington, VA 22217-5000	PROGRAM ELEMENT NO.	PROJECT NO.	TASK NO.	WORK UNIT NO.

11. TITLE (Include Security Classification)
Radiation Hard Sensors for Surveillance

12. PERSONAL AUTHOR(S)

13a. TYPE OF REPORT Final & Technical Abstract	13b. TIME COVERED FROM 870915 TO 880314	14. DATE OF REPORT (Yr., Mo., Day) 880314	15. PAGE COUNT

16. SUPPLEMENTARY NOTATION

17.	COSATI CODES		18 SUBJECT TERMS (Continue on reverse if necessary and identify by block number)
FIELD	GROUP	SUB. GR	

19 ABSTRACT (Continue on reverse if necessary and identify by block number)
We report development of a Radiation Hard Sensor for Surveillance. The sensor is being developed by Applied Research Corporation, under an SBIR program. The sensor is based on a Superheated Superconducting Colloid Detector (SSCD). Detection of X-rays, γ-rays and neutrons is monitored by superconducting quantum interference devices (SQUID). Considerable progress has been made in demonstrating that high spatial resolution is possible, and especially that these superconducting detectors are not sensitive to radiation damage up to 35 MRads. We have constructed high quality low noise amplifiers in order to take advantage of the SQUID sensitivity. Multichannel readout capability is presently being built.

20 DISTRIBUTION/AVAILABILITY OF ABSTRACT	21. ABSTRACT SECURITY CLASSIFICATION
UNCLASSIFIED/UNLIMITED ☐ SAME AS RPT ☐ DTIC USERS ☐	

22a. NAME OF RESPONSIBLE INDIVIDUAL	22b. TELEPHONE NUMBER (Include Area Code)	22c. OFFICE SYMBOL
Andrew S. Endal	301-459-8442	

DD FORM 1473, 83 APR   EDITION OF 1 JAN 73 IS OBSOLETE.

Figure 8. Report Documentation Page, DD Form 1473 (1 of 2)

REPORT 0001AC FINAL REPORT AND TECHNICAL ABSTRACT

RADIATION HARD SENSORS FOR SURVEILLANCE

Andrew S. Endal, Principal Investigator
Andrzej K. Drukier, Associate Investigator
Applied Research Corporation
8201 Corporate Drive
Landover, MD   20785
Phone 301-459-8442

11 March 1988

Contract Number: N00014-87-C-0848

Distribution: Scientific Officer
                Administrative Contracting Officer
                Director at Naval Research Laboratory
                Defense Technical Information Center

Prepared For: Dr. Clifford G. Lau
                Office of Naval Research
                Department of the Navy
                800 N. Quincy Street
                Arlington, VA   22217-5000
                        and
                Strategic Defense Initiative Program

Monitoring Organization:
                Defense Contract Administration Services
                Management Area/Baltimore
                300 East Joppa Road-Hampton Plaza
                Towson, MD   21204-3099

Table of Contents

SUMMARY

Applied Research Corporation (ARC) has proposed the development of a new class of solid state particle/radiation detectors called a superconducting superheated colloid detector (SSCD). Using this cryogenic technique, considerable improvement in spatial resolution and subnanosecond time resolution are expected. A new generation of improved γ-ray, X-ray and neutron detectors can be built. One of the biggest advantages is their radiation hardness; we expect that they can operate after an irradiation dose of 1000 MRad, i.e. about three orders of magnitude higher than other particle/radiation detectors.

Our Phase I efforts can be divided into:

- theoretical/analytical studies of diverse radiation hard superconducting detectors;

- experimental studies of SSCD, including the improvements in grain production/selection and in readout electronics.

ARC has studied the use of a superheated superconducting colloid detector (SSCD). The main experimental achievements, we believe, are:

- proof that superconducting particle detectors can withstand irradiation doses of at least 50 MRad;

- considerable improvements in grain production methods, and especially the availability of very spherical grains made of Sn + 1% Sb;

- development of an improved RF-SQUID readout leading to the possibility of detecting a change of state in a single $R \approx 1$ μm grain;

- development of a very low noise preamplifier (noise ≈ 0.5 nV/$\sqrt{Hz}$) appropriate for DC-SQUID's.

- development of very fast ($t_{rise} \leq 10$ nsec) readout electronics sensitive to the change of state of single $R \approx 10$ μm grains;

The experimental results and their implications are described in considerable detail in sections 4 & 5 and in Appendices 1-6. The proof that superconducting particle/radiation detectors are radiation-hard is especially significant because we tested two types of devices (superconducting tunnel junctions and superheated superconducting colloid detector) using two diverse types of radiation (electrons and γ-rays).

Furthermore, much of the successful effort has been in activities which extend the experimental capabilities of ARC and locally collaborating scientists. In an agreement established

between ARC and NBS (Gaithersburg), a dilution refrigerator capable of temperatures below 20 mK was dedicated for very low temperature tasting of the SSCD. This refrigerator is now fully operational in a well- equipped laboratory, and such experiments are currently in progress. We point out that the Gaithersburg refrigerator is unique in the world, being now fully dedicated to very low temperature studies of superconducting particle/radiation detectors.

On the other hand, in an agreement between ARC and U. of Maryland (College Park), a low temperature (T $\geq$ 1K) laboratory has been established on campus. This facility (though quite conventional) provides us with a well laboratory facility in which the prototype detector can be cooled, electronics tested, and irradiation tests performed. Development of the laboratory is now essentially complete, and initial experiments were in started.

We believe that our progress has been rapid and warrants further support. The development of prototype, SSCD-based, high spatial resolution gamma ray/X-ray/neutron detectors seems possible in the time frame of 2-3 years. Furthermore, the rapid progress in SQUID-based readout electronics suggest that application of these radiation-hard detectors can be extended to UV, visible and infrared. The development of 10^4 x 10^4 pixel detectors with micron spatial resolution seems to be possible.

ARC is interested in further development of SSCD and will submit the appropriate Phase-II proposal.

1.1 INTRODUCTION

Applied Research Corporation (ARC) has proposed the development of a new class of solid state particle/radiation detectors called superheated superconducting colloid detectors (SSCD). Using cryogenic techniques, considerable improvement in spatial resolution and sub-nanosecond time resolution are expected. An array of detectors, e.g., $10^4 \times 10^4$ pixels, will provide images with superior quality. The superconducting particle/radiation sensors have been tested as detectors of relativistic particles, gamma and X-rays, as well as neutrons. The development of UV, visible and even infrared imagers seem possible. The proposed new detector uses solid-state electronics which decreases price, increases reliability and facilitates calibration. This new class of detectors will be extremely radiation-hard, i.e. they should function properly after an irradiation dose of about 1000 MRad (more conventional detectors malfunction after irradiation doses about three orders of magnitude smaller).

The research we are presenting in this report involved development of new gamma-ray and X-ray detectors. This program was a collaborative effort including scientists from Applied Research Corporation (ARC), National Bureau of Standards (NBS), and the University of British Columbia (UBC). The research at ARC was supported in part by the DOD-SBIR Phase I contract.

During Phase-I we established the feasibility of the cryogenic X-ray and γ-ray detector, especially as high spatial resolution imagers. Our efforts can be divided into:

- theoretical/analytical studies of diverse applications of SSCD;

- experimental studies of SSCD, including improvements in grain production/selection and improvements in readout electronics.

- irradiation tests.

The background information about the cryogenic particle/radiation detectors, and more specifically about the radiation-hard SSCD is presented in Section 2. The results of our analytical studies of applications are presented in Section 3. In Section 4 we describe the state-of-the-art of the SSCD detector, with particular attention to results obtained in 1987, both by ARC and by other groups. The development of the SSCD at ARC and with collaborating organizations is detailed in Section 5, which describes the motivation, techniques used and major results. The detailed technical reports are provided in Appendices 1-6, and describe our experimental efforts in the following directions:

- study of radiation hardness of superconducting detectors (Appendix 1);

- colloid production/quality assessment (Appendix 2);
- improvements of SQUID readout electronics and irradiation tests (Appendix 3);
- development of multichannel SQUID readout (Appendix 4);
- R&D on the SSCD at $T \leq 100mK$ (Appendix 5);
- development of fast readout electronics (Appendix 6).

Finally, the conclusion provides a synthesis of our results and points to future developments.

2.0 CRYOGENIC PARTICLE/RADIATION DETECTORS

Recent developments in low temperature physics, which open new fields of low temperature bolometry in radiation and particle detection, are:

  a. availability of large refrigerators, including space-born cryostats, operating at $T \leq 0.1^\circ K$;
  b. improvements in Superconducting Quantum Interference Device (SQUID)-based instrumentation;
  c. promises of thermometry with microkelvin precision.

Essentially, two classes of low temperature detectors have been developed, based on crystals (diamond and silicon) and superconductors. Due to their extremely small specific heats, the deposition of energy as small as a few eV leads to a measurable change of temperature in micron-size structures.

During recent years, several groups proposed and developed bolometric particle detectors. The Wisconsin/NASA collaboration[1] obtained dE = 17 eV for E_x = 6 KeV using a silicon bolometer with an implanted thermistor. Thus, even at the present time, bolometric detectors have much better energy resolution than the best semiconductors. It is, however, difficult to operate the crystal bolometers as position sensitive detectors. First, they must be placed in a dilution refrigerator, which is expensive. Second, currently-used sensors require 4-point resistivity and voltage measurements, such that readout of N x N pixels would require use of $4N^2$ wires. Heat escaping along the leads further limits bolometric detectors to 8 x 8 arrays.

Superconducting tunnel junctions have been developed into very sensitive soft X-ray detectors. The energy resolution of conventional solid-state detectors is limited by the statistical fluctuations in the number of created carriers. For example, in silicon with a gap of about 1 eV and a Fano factor of 3, a 5 keV particle creates about 1,000 carriers, and the limit on energy resolution is $\Delta E/E \approx 1 \sqrt{N} \approx 3\%$. In superconductors, the energy necessary to split a Cooper pair is only a few microvolts in low T_c superconductors (W, Os, Ir), and a few millivolts at liquid helium-4 temperatures (Sn, In, Pb, Nb). Superconducting tunnel junctions have been developed[2] with an energy resolution of ca. 40 eV at 4 keV. Unfortunately, the tunnel junctions are small, (10^{-3} cm^2) and thin (t $\leq$ 1µm). There is a possibility of using arrays of such junctions, but the heat diffusion in the substrate limits the geometric coverage of the focal plane to about 10%.

The above described low temperature devices are superior spectrometers and will find many applications in atomic physics and astrophysics. Unfortunately, these are very low mass devices [silicon bolometers $\approx$ 1-10 mg; superconducting tunnel junctions $\leq$ 1 nanogram]. Furthermore, they are not very convenient as imaging devices; their limitations are due to the use of

resistive readout, .i.e. at least two wires have to be attached to each single sensor, which limits the number of distinct pixels to a few tens. In the following we discuss a class of devices in which the readout is by magnetic means; i.e. thousands and millions of physically separated sensors is readout in parallel by only a few channels of very sensitive electronics. These devices use the fact that even very small energy deposition can change the state of a superconductor, leading to a drastic change of its electromagnetic properties. To increase the detector sensitivity, a highly granulated superconducting medium is used.

2.1 Superheated Superconducting Colloid Detector (SSCD)

The first type of detector exploiting the properties of superconductivity was the Superheated, Superconducting Colloid Detector (SSCD). The detector depends on the change of state from superconducting to normal in small grains of a few microns diameter (see ref. 3). The deposition of less than one keV of energy flips the state of the grains. This is easily detectable with ultrasensitive electronics based on a SQUID[4]. This detector has been tested and shown to be sensitive to charged particles, photons and neutrons. It should excel as a high count rate photon detector. It may have some advantages in the detection of high energy particles, e.g., as a shower detector. Furthermore, it may be sensitive to the coherent scattering of weakly interacting particles, e.g., neutrinos.

The basic idea of the SSCD is quite simple. One prepares a colloidal suspension of spherical grains of a Type I superconducting material, which will constitute the detecting medium. Since there are over 20 elements which are Type I superconductors, it is possible to obtain a wide range of material properties. Instead of grains, one can use other micron-size superconducting structures, e.g., arrays of evaporated squares or "dots".

To enable the detection of energy deposited in the grains, one first brings them into the superconducting state by immersion in a cryostat. It is well known that if a large enough magnetic field H is applied to such grains, they will revert to the normal state if:

$$H \geq H_C = (2/3)H_0(1 - T^2/T_C^2) \tag{1}$$

where T is the temperature, T_C is the transition temperature (at zero field) at which the superconducting state is reached, and H_0 is the "critical field". Equation (1) is a thermodynamic relation, analogous to the P(T) equation for the vapor pressure of a fluid. And, in a manner analogous to that for supersaturation of fluid, it is possible for the behavior of pure grains to show superheating. Depending on application, one can use either superheated superconducting grains or grains which return to the superconducting state after heat escapes.

To take advantage of the above principles in radiation detectors, one establishes an ambient magnetic field, H, slightly smaller than $H_{sh}(T)$, where T is the cryostat temperature and $H_{sh}(T)$ is a superheating field. If radiation is absorbed by the grain, it will eventually be converted to heat, which in turn will increase the temperature of the grain by the amount:

$$dT = (3dE)/(4\pi R^3 C_V(T)), \tag{2}$$

where dE is the deposited energy, R is the grain radius, and $C_V(T)$ is the specific heat of the metal. If $H > H_{sh}(T + dT)$, the grain will revert to the normal state. It will remain in this state, even after cooling back to T, unless the magnetic field is reduced to the supercooling point.

The change of state of the grain can be monitored with a superconducting circuit which consists of a pickup coil and output that are connected together (so that whatever current flows in the pickup coil also flows through the output coil). The grain is placed within a pickup coil connected to a SQUID. When the grain changes to the normal state (or "flips"), the magnetic field which had been excluded by the Meissner effect now penetrates freely. Effectively, a magnetic dipole has been removed from the interior of the colloid, and this changes the external field which threads the pickup coil. Due to the quantization and conservation of magnetic flux within a closed loop of a superconductor, a supercurrent is induced in the superconducting circuit. The supercurrent sets up a small magnetic field at the SQUID which is detected by well-known procedures. It should be pointed out that a SQUID can detect and localize a change of state of any single grain in the collection of trillions of grains.

Above, we described an energy- and position-sensitive detector based on superconducting structures. Intrinsically, the detector is very fast; the change of state requires less than 1 nanosecond. The appropriate electronics (Josephson junction flip-flops, used in supercomputers) are ultra-fast and permit tens of picoseconds timing. Optionally, one can use very fast GaAs-Fet preamplifiers operating in liquid helium, which would give sub-nanosecond timing. While these super-fast readout electronics are under development, in most experiments somewhat slower and less-sensitive room temperature preamps based on silicon J-Fet's were used and timing of better than 10 nanoseconds has been achieved (D. Perret-Gallix, CERN; private information).

In this implementation, the detector structure is similar to a "solid-state" multiwire proportional chamber wherein two planes of readout loops permit two-dimensional localization. The signal sharing between closely placed loops permit the use of "center-of-gravity" methods to improve the spatial resolution; we expect that the spatial resolution will be ca. 0.2 x S where the

spacing, S, of the readout wires can be as small as 100 μm. Such readout will however require 2N electronic channels.

We mentioned above that the change of state of a grain is equivalent to the disappearance of a magnetic dipole. This leads to propagation of a spherical wave; the wave amplitude diminishes inversely proportional to the distance from the grain. Thus by using three _identical_ pick up loops, each connected to an ultrasensitive magnetic sensor (DC-SQUID), one can localize the grain which flips. For redundancy, we will use four loops placed around the detector. The spatial resolution of such a system depends on the signal-to-noise ratio; with $S/N \geq 100$ we expect a spatial resolution of ca. 100 μm for a 1 cm^2 detector. We point out that in experiments at IBM, the change of state of a _single_ $R = 5$ μm grain gave a $S/N = 10^6$. Thus, the use of SQUID's is very promising--but depends on the availability/price of multichannel SQUID readout. DC-SQUID electronics featuring 11 SQUID's are commercially available, and systems featuring up to 100 DC-SQUID's are under development. As discussed above, it is our opinion that the development of SQUID electronics appropriate for SSCD readout is the single most important task of further SSCD development, especially in applications requiring very high spatial resolution or recognition of many pixels (512x512 pixel arrays or larger).

2.2 Radiation Hard Superconducting Particle/Radiation Detectors

In this chapter we briefly review the state-of-the art in radiation-hard solid state detectors and provide some arguments as to why superconducting particle/radiation detectors can operate after irradiation with up to 1000 MRad.

Recently, radiation-hard, high spatial resolution detectors were studied for applications at Superconducting Super Colloid (SSC) where irradiation doses of up to 10 MRad are expected. We point out that in many military applications, e.g., when X-ray lasers are used, an even higher irradiation dose is expected.

Radiation susceptibility has been investigated for three different types of tracking devices. These are:

(1) Silicon strip detectors;
(2) Wire chambers;
(3) Glass fiber detectors.

The SSC operating at a luminosity of 10^{33} presents severe and, in some cases, fatal problems for all three of these different tracking methods. Silicon strip detectors (or other types of silicon devices such as silicon drift chambers) would be used to precisely locate secondary vertices and hence should be as close as possible to the interaction point. Optimally located, such devices would receive in excess of 10^6 Rads/year (note that 1 Rad is approximately 3.5×10^7 minimum ionizing particles per cm^2) even for a luminosity of 10^{32}.

2)   "Damage" can be categorized as either atomic displacements or effects from ionization. Minimum ionizing particles primarily cause ionization, but also produce heavy secondaries through spallation and nuclear reactions which create displacement damage.   The displacement damage is important in crystals but not in amorphous films.   On the other hand, radiation damage depends on the amount of energy necessary to remove atoms from the lattice. This energy should be larger for refractory metals; a high melting point characterizes materials with very stiff lattices.

3)   Displacement effects are "bulk" effects and create damage sites throughout a device. They are, therefore, mainly important to "large" volume devices such as detectors, as opposed to microelectronic devices which exist largely on the surface of silicon.   Ionization creates lasting effects in insulators and dielectronics,   e.g.,   surface   effects,   and   thus   primarily influences electronic devices.   Active electronic devices fail with radiation doses two to three orders of magnitude smaller than the doses that degrade detectors. There are no ionization effects in metals wherein charges are not trapped; conductors are self-annealing materials.

4)   Radiation damage is less at very low temperatures and when the devices are off-power.   Unfortunately, due to the rapidly decreasing mobility of carriers, silicon devices have to be operated at temperatures higher than liquid nitrogen. Due to problems with switch-on transients and requirements of calibration and gain stabilization, silicon devices are most often used with power-on.

The proposed superconducting particle detectors are expected to survive a 100 MRad dose because:

a)   they consist of arrays of superconducting, micron-size squares (amorphous refractory metal films) and detection involves only bulk properties;
b)   the devices are operated off-power at liquid helium temperatures;
c)   all "on-chip" readout electronics can use radiation hard, refractory metal (Nb) elements.

The main goal of Phase I was to experimentally study the radiation damage in superconducting metals and devices. Theoretical considerations and preliminary experimental results suggest that superconducting particle detectors can survive a radiation dose of at least 100 MRad. An excellent and very recent review is by F. Ruller-Albenque ("Effects d'irradiation dans les superconducteurs", page 1-70, preprint Lab. des Solides Irradies, Oct. 1987--in following ref. FRA), which quotes 272 references concerned with irradiation effects in superconductors. However, one should remember that there are over 300 superconducting elements/alloys, and that mechanisms of irradiation with photons, electrons, neutrons and heavy ions are

Silicon devices have been shown to operate at up to 2.4 MRad, but more experimental work is needed in this area. The fine granularity of silicon strip detectors and the large area coverage needed suggest that readout electronics should be integrated with the silicon detector itself. Unfortunately, the electronics is much more susceptible to radiation damage than the silicon strips. Tests have shown that 10^3-10^4 Rad are sufficient to render such readout electronics inoperative. Although hardening techniques are available for applications in the nuclear reactor and defense industries, at present it seems unlikely that doses above 10^6 Rads could be tolerated. The cost of implementing this technology has not been estimated and much more work must be done to predict the allowable radiation doses for readout electronics. Broadly speaking, the overall conclusion is that existing detector technology will be able to produce results only if the radiation dose is smaller than 1 Mrad.

In the last two years, there have been many studies of radiation damage to semiconducting position sensitive devices. Some of them were discussed during the Snowmass 86 workshop. For example, R. Klanner et al. (DESY) exposed silicon strip detectors to 3.8×10^{12} hadrons/cm^2 and observed a considerable increase in leakage current from strip to strip over the exposed area. The systematic errors of particle-track position measurements were noted. E. Heijne (CERN) reported on the degradation of silicon detectors for doses larger than 2×10^{11} muons/cm^2. The Rutherford group studied CCD devices and concluded that at 10^5 rads one already has to continuously change the operating conditions to make the devices work. Probably the most worrisome aspect is the fact that "on chip" readout electronics failed at 10^5 rads. Thus, orders of magnitude improvements are necessary. It may be very difficult, if not impossible, to develop radiation-hardened silicon devices.

The ideal microvertex detector would have the following properties:

1) radiation-hard to a few tens of Mrad;
2) spatial resolution of a few microns;
3) sensitivity to minimum ionizing particles and/or, detection of a few keV energy deposited in a micron-size detection element (pixel);
4) fast, nanosecond readout using on-chip radiation-hardened electronics.

The SSCD satisfies all of these criteria.

On the basis of literature on radiation damage, and after study of some military applications, we believe that:

1) A general requirement seems to emerge that devices must tolerate at least 10^8 rads.

to be studied. In the following only some of the observations are quoted.

The proposed detectors are essentially "thermal threshold" devices. If the energy deposited by a particle heats the detector above its critical temperature, there is a change of state which is easily detectable electronically. Thus, the critical temperature and its change under high irradiation doses are of interest. To influence the detector, the T_c change due to accumulated irradiation should be higher than the typical temperature stability of the liquid helium bath (5 mK).

Let us consider the radiation damage due to relativistic electrons and photons. Fig. 1 shows that in typical A-15 type superconductors (e.g. NbTi, Nb_3Ge) there are practically no defects introduced by electrons with $E \leq 0.5$ MeV. For relativistic electrons, the effective change of critical temperature is

$$\Delta T_c \approx \alpha \times 10^{-20} \; ^\circ K/cm^2/electron, \qquad (3)$$

where $\alpha = 0-2$. Thus, to change the critical temperature of a typical A-15 superconductor by 5 mK, one needs 2×10^{18} electrons/$cm^2 \approx 2 \times 10^5$ MRad.

When irradiated with neutrons/protons, the recoil energy of nuclei is much higher. However, the experimental studies of G. Linker (J. Nucl. Materials 72, 1978, 275) shows that for vanadium film irradiated with 3×10^{16} Neon$^+$ions/cm^2 (E = 320 keV), the change of critical temperature is less than 1%. The estimated irradiation dose is 10^5 MRad.

Probably the most important characteristic of superconducting detectors is that of self-annealing when allowed to reach room temperature. Fig. 2 shows the results of studies of niobium films irradiated with oxygen ions (25 MeV) and fast neutrons. Reheating to $350^\circ K$ leads to the disappearance of irradiation damage.

In collaboration with group of Prof. R. P. Huebener, Tubingen University, we initiated a research program in which an electron scanning microscope equipped with a liquid-He stage was used to

1) measure effects due to single electrons on tunnel-junctions, and

2) study irradiation effects.

A Pb-alloy junction was irradiated with 26 keV electrons. No appreciable changes of the tunneling conductivity occurs for about 10^9 electrons striking the 812 μm^2 junction. Thus an energy deposition of about 3×10^{10} ev/μm^2 (or about 35 MRad) doesn't influence the junction performance. This is a surprising

result considering that the oxide between two superconducting layers is only a few angstroms thick (see Appendix 1). In collaboration with Prof. R. P. Huebner's group, we will perform experiments in which lower energy electrons (E ≈ 5 keV) are stopped in the top layer of a superconductor. We believe that in this condition the junctions will survive radiation doses of about 1000 MRad.

In yet another series of experiments being performed by the ARC/UBC collaboration, we are studying the radiation hardness of Sn-SSCD. Both hysteresis curves and QDE are studied for samples before and after irradiation with a cobalt bomb (for preliminary results see Appendix 1; more information will be provided in the Phase-II proposal).

Ad: Cryogenic particle/radiation detectors

1) S. H. Moseley et al., J. Appl. Phys. 56, 1257 (1984)
    D. McCammon et al., J. Appl. Phys. 56, 1263 (1984)
2) D. Twerenbold, Phys. Rev. B34, 7748 (1986)
    D. Twerenbold et al., J. Appl. Phys. 61, 1 (1987)
    F. van Feilitzsch et al., "Workshop on the Superconducting Particle/Radiation Detectors", Torino, November 1987
    A. Lender et al., ibid.
3) C. Valette, Ph.D. thesis, Orsay 1971
    A. K. Drukier, Ph.D. thesis, Copenhagen 1972
    A. K. Drukier, et al., Lett. Nuovo Cimento, 14 (1975) 300
    A. K. Drukier, NIM 154 (1978) 83
    A. K. Drukier et al., NIM 173 (1980) 259
    D. Hueber, C. Valette, G. Waysand, Cryogenics, 387 (1981)
    A. K. Drukier, NIM 201 (1982) 77
    A. K. Drukier et al., "SSCD gamma camera", Proc. Symposium: Radioactive Isotope in Klinik und Forschung, Bad Gastein 1982 p. 213-219
    A. K. Drukier et al., Phys. Rev. D30, 2295-2309 (1984 for review of recent results on SSCD see "Low Temperature Detectors for Neutrinos and Dark Matter", Proc. Workshop, Ringberg Castle, Tegernsee May 12-13, 1987 ed. K. Pretzl et al., Springer Verlay 1987
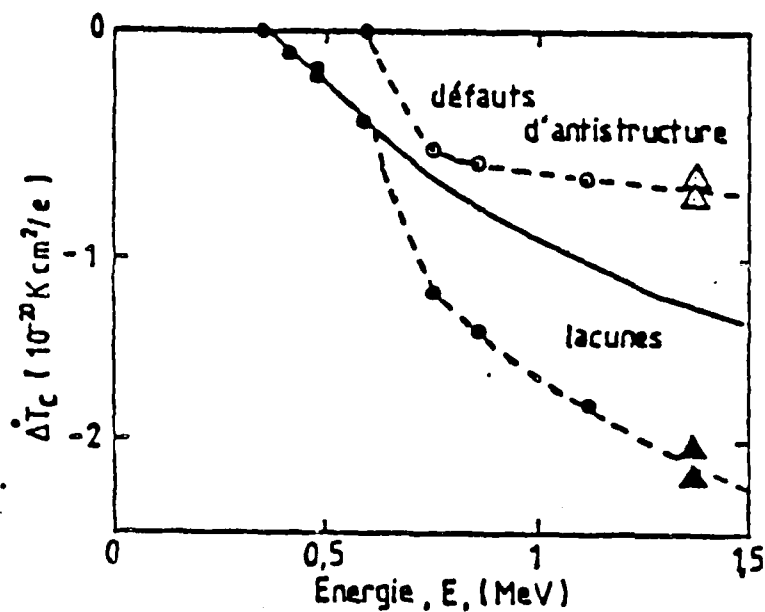   D. Perret-Gallix ,ibid
4) A. Kotlicki et al., ibid p. 37-43.

Fig.1 Change of critical temperature as function of irradiation.
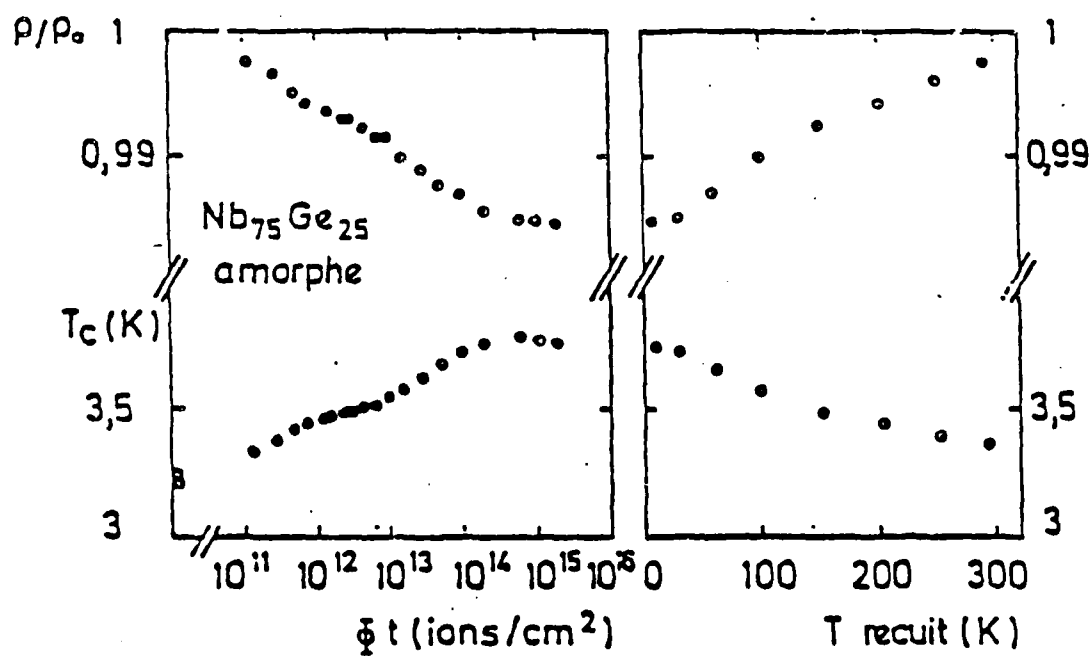
Note scale   dT = O(10^{-20} K*cm^2/electron) .

Fig.2 Self anniling of superconductors when allowed to heat to room temperature.

3. APPLICATIONS OF A SUPERHEATED SUPERCONDUCTING COLLOID DETECTOR

The new cryogenic particle/radiation detector is based on energy sensitive micron-size superconducting structures. When a particle/photon interacts with a superconductor, the energy dissipation leads to an electronically detectable change of state. This generic principle permits the development of a family of detectors characterized by some/all of the following properties:

- very good energy resolution (dE/E≈0.1%);
- submillimetric spatial resolution;
- sub-nanosecond timing;
- high density and photoelectric cross-section.

These properties of granulated superconductor detectors can be used to build devices with important applications. The type of particle and the deposited energy are important in the design of these SSCD imagers; thus, in the following we discuss their application as:

- γ-ray detectors;
- X-ray detectors;
- neutron detectors.

3.1 Applications of SSCD as Gamma-Ray Detectors

The diverse detectors of gamma-rays can be conveniently divided into

- detectors of soft γ-rays ($E_\gamma \leq 200$ keV);
- detectors of hard γ-rays ($E_\gamma \geq 200$ kev).

There are adequate detectors of soft γ-rays, e.g.

- semiconducting, intrinsic Ge diodes;
- liquid noble gas detectors;
- scintillators, mostly NaI(Tl).

The status of instrumentation in the high energy γ-ray range is not good; scintillators are currently used, as well as sandwich detectors. In the following we describe the state-of-the-art in detection of annihilation photons, which with $E \approx 511$ keV is representative of most of the hard γ-ray range. Initially, the annihilation photon detection systems were constructed using NaI(Tl). Its availability, ease of fabrication, and reasonable cost made it an obvious choice in a number of designs using discrete crystals. Its principal disadvantage is a decreasing detection efficiency when using smaller crystals needed for high resolution systems. This limitation places a practical lower limit on the resolution achievable with NaI(Tl)-based systems (about 1 cm³). The development of BGO, with 3 times the stopping power of NaI(Tl), has led to a new generation of high resolution/high efficiency γ-detectors. At present, the lower limit of spatial resolution

is about 4 mm due to the size of the photomultiplier tubes that can be coupled to it. The disadvantages of BGO are increased cost, much lower light output and long crystal fluorescent light decay time. The limitations due to the use of photomultipliers suggest the use of solid state detectors. Unfortunately, Ge has a considerably smaller stopping power and an unfavorable photopeak-to-Compton ratio.

In the recent review of annihilation photon detection systems, S. Derenzo writes "An ideal detector with the best properties...has not yet been found. However, the scintillator properties of many crystals have been discovered rather recently: BaF_2 in 1971, BGO in 1983...and GSO in 1982. Further efforts in this direction are essential if the potentials are to be fully realized.

The ultimate scintillator would have the high atomic number and density of BGO, the high light output of NaI(Tl), and the ultra-fast decay of BaF_2 to combine high detection efficiency, good spatial resolution, high data rates, and the increased sensitivity provided by time-of-flight information".

We argued above that the ideal detector for hard gammas should have the following properties;

1. very high stopping power for annihilation photons;
2. high photopeak-to-total absorption ratio;
3. best possible (about 1 mm) intrinsic spatial resolution;
4. good energy resolution;
5. sub-nanosecond temporal resolution;
6. reasonable cost

To fulfill conditions 1 and 2 the detector should have a very high density, ($\rho \geq 10$ g /cm^3) and should consist of at least one very high atomic number element (Z $\geq$ 80).

We believe that a new annihilation photon detector based on superheated superconducting colloid satisfies all of these conditions and may lead to a major breakthrough in γ-ray instrumentation. The properties of diverse photon detectors are compared with properties of a proposed new, solid state detector in table A.

The basic idea of the SSCD is quite simple; one prepares a colloidal suspension of spherical grains of a Type I superconducting material, which will constitute the detecting medium. Since there are over 20 elements which are Type I superconductors, it is possible to obtain a wide range of material properties. Furthermore, the grains represent only a small percent of the detector weight. The dielectric material between grains (say 90 percent of detector volume) can be a very high density compound of some very high Z element, e.g., UN(14.31 g/cc), UB_2(14.31 g/cc), UO_2(10.96 g/cc), US(10.87 g/cc), Bi_2O_3(8.55 g/cc), PbF_2(8.24 g/cc), Tl_2O_3(10.19 g/cc), HgO(11.1 g/cc), $PtAs_2$(11.8 g/cc), IrO_2(11.67 g/cc), OsO_2(11.37 g/cc), ReO_2(11.4 g/cc), W_2C(17.15 g/cc). From the point of view of

stopping power the optimal are uranium nitride (UN) and di-tungsten carbide (W_2C).

First we observe that the absorption due to the photoeffect is much higher in the new detector than in BGO or CsF; this stopping power is a factor of three smaller in BGO, and a factor ten smaller in CsF. Taking into account that the energy resolution of the new detector is about twice better than for BGO, the photoelectric-to-scatter ratio is far superior for the new class of detectors.

It can be seen that the new detector is much faster than BGO. Actually it may be much faster than CsF scintillators; the electronic sign will be a microvolt pulse with a rise-time of a few tens of picoseconds. Superconducting electronics sensitive to microvolts pulses of picoseconds duration are available commercially.

For a collection of grains with essentially the same radius, the signal is proportional to the number of grains which flip. For high energy photons, e.g., annihilation photons, an energy resolution of $dE/E < 20\%$ is expected.

Ad: γ-ray detectors

Cho Z.H., Farukhi MR: Bismuth Germanate as a potential scintillation detector in positron cameras. J. Nucl M ed 18: 840-844, 1977.

Cho Z.H., Nalciaglu O, Farukhi MR: Analysis of a cylindrical hybrid positron camera with Bismuth Germanate (BGO) crystals. IEEE Trans Nucl Sci NS-25: 925-963, 1978.

Nestor O.H., Huang C.Y.: Bismuth Germanate: A high-Z gamma and charged particle detector. IEEE Trans Nucl Sci NS-22: 68-71, 1975.

Farukhi M.R.: Scintillation detectors for CT applications - An overview of the history and state of the art. Proc Workshop on Transmission and Emission Computerized Tomography, July 1978, Seoul, Korea

Nahmias C., Kenyon D.B., Garnett E.S.: Optimization of crystal size in emission computed tomography. IEEE Trans Nucl Sci NS-27: 529-532, 1980.

Mullani N.A., Ficke D.C., Ter-Pogossian M.M.: Cesium Fluoride: A new detector for positron emission tomography. IEEE Trans Nucl Sci NS-27: 572-575, 1980.

Allemand R., Gresset C., Vacher J: Potential advantages of a cesium fluoride scintillator for a time-of-flight positron camera. J. Nucl Med 21: 153-155, 1980.

Llacer J. Graham L.S.: The effect of improving energy resolution on gamma camera performance: A quantitative analysis. IEEE Trans Nucl Sci NS-22: 309-343, 1975.

G. Charpak et al., CERN preprint, CERN-EP/87-187, October 1987.

S. Derenzo, "Recent Development in PET instrumentation", SPI vol. 671, p. 232-243 (1986)

TABLE A: PROPERTIES OF ANNIHILATION PHOTON DETECTORS

Material	NaI	CsF	BGO	Ge	UNSn	WCSn
Density [g/cc]	3.67	4.61	7.13	5.38	13.61	16.16
Atomic Number*	53	55	83	32	92	74
% per Weight	85	87	65	100	90	94
μ Photo [g/cm^2]	0.019	0.02	0.065	3.3×10^{-3}	0.11	0.065
μ tot [g/cm^2]	0.092	0.10	0.135	0.10	0.178	0.122
X_{photo}	0.053	0.054	0.31	0.012	1	0.7
Statistics	2.500	75	200	$\geq 10^5$	$\geq 10^6$	$\geq 10^6$
dE/E [FWHM]	8%	30%	20%	1%	10%	10%
Photo/All	2.58	0.67	2.41	3.3	6.2	5.3
t[nsec]	1-5	<1	2-10	1-5	<1	<1
dX[mm]*	5mm	5mm	5mm	1mm	0.5mm	0.5mm
dX[mm] system	10mm	10mm	8mm	5mm	1-2mm	1-2mm

UNSn = $U_{0.9} N_{0.05} Sn_{0.05}$

WCSn = $W_{0.94} C_{0.03} Sn_{0.03}$

$X_{photo} = [\mu(x)/\mu(UNS_n)][\mu_{photo}(x)/\mu_{photo}(UNS_n)]$

dX[mm]* = intrinsic spatial resolution

3.2 High Spatial Resolution X-ray Detectors

X-rays of energy from 100 eV to few tens keV are critically important in many applications, including remote sensing, X-ray laser development, tests of FEL concepts etc.

The development of better detectors is essential for further progress. The main detector characteristics which have to be considered are spatial resolution, maximum count rate (overall and local), linearity, and dynamic range. Obviously, quantum detection efficiency (QDE) is very important, especially for $E_x \geq 10$ keV. In practice, however, the response and its stability, which are obviously also directly linked to the signal processing electronics, are very important.

In practice we have three classes of detectors[1]:

a) gas detectors with sub-millimeter resolution and large surface (e.g. 30 x 30 cm^2);
b) TV cameras (512 x 512 pixels with $\phi \leq 5$ cm);
c) solid-state imagers with spatial resolution as good as 25 x 25 µm^2 but very small surface.

It is not possible to specify the "best" detector for diverse applications; different experiments may demand conflicting qualities from the detector. The essential parameters of the detectors are:

a) size: for many applications diameters up to 30 cm are required;
b) spatial resolution: most of the existing detectors have a matrix of 256 x 256 or 512 x 512 but much larger formats, e.g. 4096 x 4096 may be useful;
c) maximal flux: up to 10^8 photons/s can be expected in some applications;
d) homogeneity over the detector surface: for most studies an uncertainty of 1% is sufficient, but others require 0.1% and better;
e) dynamics: usually the dynamic range is below 1000 but can be much higher, e.g. in X-ray laser tests.

No single detector, either now in operation or likely to be constructed in the near future, can satisfy all the demands simultaneously. All proposed techniques are mature and only minor improvements are expected. On the other hand, better and possibly new types of position sensitive detectors will become a must with the new UV and X-ray sources, e.g. Free Electron Lasers. We argue that a new X-ray detector based on energy sensitive superconducting structures may become the best example of next generation focal 2-D detectors, e.g. it can feature the spatial resolution of 4096 x 4096 pixels, with a surface of 20cm x 20cm.

Table 2 shows a comparison of some existing 2-D position sensitive detectors with a new device proposed by ARC. It can be seen that this new detector has much better performance than

existing detectors. For laboratory applications with conventional X-ray sources, the main advantages of the new detector are improved spatial resolution for large detectors. Furthermore the improved energy resolution may be important in some applications. For applications at synchrotron X-ray sources or with X-ray lasers, the most important are orders of magnitude higher count rate and better spatial resolution.

Table 2: Comparison of diverse 2-D detectors of X-rays.

	Gas(MWPC)	TV	CCD	SXD
Size: ϕ[cm]	20	8	5	15
Resolution	512x512	512x512	1024x1024	4096x4096
QDE	85%	70	70	90%
Max. flux [ph/s]	5×10^4	10^8	5×10^5	10^9
Readout time	*	20msec	10msec	1msec
Homogenuity	1.5%	>1%	<1%	0.1%

* Limited by statistics

We and our collaborators believe that within a few years we can develop the following X-ray detectors:

1. Very High Energy Resolution X-ray Detector (VHERD).
   Energy range: 0.1-20 keV
   Energy resolution: dE/E(FWHM)=0.1-0.2% at 5 keV
   Area/No. pixels: 3 mm x 3 mm, 64 x 64 pixels
   Temperature: 0.1-0.5K
   Readout: DC-SQUID's
   Count rate: 10^4 photons/sec

2. High Spatial Resolution X-ray Detector (HSRD).
   Energy range: 0.1-20keV
   Energy resolution: energy threshold with fine tuning
                          $dE_{th}\leq0.1$ keV
   Area: 10 cm x 10 cm
   Spatial resolution: 1024 x 1024
   Temperature: 1.2K
   Readout: DC-SQUID's or Josephson junctions
   Count rate: 10^7 photons/sec.

3. Extreme Spatial Resolution X-ray Detector (ESRD).
   Energy range: 0.1-20keV
   Energy resolution: energy threshold with fine tuning
                          $dE_{th}\leq0.1$ keV
   Area: 10 cm x 10 cm
   Spatial resolution: 4096 x 4096

Temperature: 1.2K
Readout: Magneto-optic
Count rate: 10^9 photons/sec.

The suggested detection scheme is based on the measurement of temperature change in micron-size, superconducting thin films. To increase the device sensitivity, refractory metals with high Debye temperatures are used. Further increases in sensitivity are obtained by using very thin films and small pixels, both made possible by using high atomic number and very high density materials. Each pixel is essentially a structure thermally independent of substrate: heating will occur whenever a photon interacts in the metal. Calculations show that at low temperatures (0.5 - 1.5K), for an energy deposition of a few KeV, the temperature change of a single pixel is easily measurable (larger than 0.01K).

The preferred implementation takes advantage of the properties of Type I superconductors and the very small specific heat of these materials. Each pixel consists of a thick film of a high T_C superconductor (say 3 microns of Re) covered with a thin layer of a low T_C superconductor (say 0.5 microns of Al). This configuration is shown in Fig. 1; the mass of aluminum is about 2 percent of that of the rhenium. However, for T<<Tc, the specific heat of the electrons is suppressed and the specific heats of both layers are comparable. Furthermore, the Kapitza resistance between the two metals is small: when photons are absorbed in the Re, both metals come to thermal equilibrium within a few nanoseconds. Heating will bring the temperature very close to the critical temperature of aluminum. However, this leads to a large change of electromagnetic properties; a magnetic field penetrates metals freely when superconducting currents disappear. The process is fast (a few nanoseconds) and with very sensitive electronics, based on Superconducting Quantum Interference Devices (SQUID's), temperature changes as small as 10^{-5} K are measurable. This structure is a superconducting bolometer based on the Meissner effect.

In the following, the high T_C and low T_C superconductors are called absorber and thermometer, respectively. The choice of rhenium as an absorber is close to optimal; it has a very high θ_D, Z, and density, as well as reasonable T_C. However, other absorbers can be used, e.g., Pb, Tl, Nb, V. Many physical parameters influence the performance of a superconducting thermometer: density, specific heat, penetration depth, critical temperature field. Futhermore, there are trade-offs connected with the choice of the operating point (temperature/field) for radiation energies of interest. Aluminum is only an example of a low T_C superconductor to be used as a thermometer; others are W, Mo, Re, Os, Ir, Cd, Zn. Optionally, one can use a superconducting alloy with an appropriate critical temperature. The first proposed step in our project is an analytical study of diverse combinations of superconducting materials to maximize the temperature increase and electronic signal.

This sensing principle can be generalized to an array of superconducting bolometers. It should be noted that a single superconducting square represents a magnetic dipole. The detected change of flux, due to the change of state, depends on the distance between the superconductor and the SQUID readout loop. With 3 SQUID loops one can establish the position of the irradiated pixel. Such a configuration is a superconducting imaging bolometer.

The application of SQUID's, however, limits the photon flux to about $N \times 10^4$ photons/sec, where N is the number of SQUID's. DC-SQUID electronics featuring 11 SQUID's are commercially available, and systems featuring up to 100 DC-SQUID's are under development. Considerably higher fluxes of photons up to about 10^8/sec can be detected when using a magnetooptic readout. Furthermore, the spatial resolution can be improved, possibly down to 1 micron.

The proposed detector development is based on state-of-the-art techniques used to produce superpure, superconducting films. The development of superconducting photon detectors will require submicron lithography applied to superconducting films of refractory materials. It should be pointed out that the production of CCD imagers requires about ten lithographic operations; our detector would require only one or two etching steps. Thus, the yield of ready devices may be substantially better than for semiconducting devices. Furthermore, superconducting photon imagers are radiation-hardened, which is difficult to achieve with semiconducting devices. Recent experiments (Prof. R. Huebner, Tubingen-private information) have shown that superconducting tunnel junctions are radiation-hard to at least 50 MRad, i.e. about a factor of ten more radiation-hard than any other existing detector. For the superconducting imaging detector, the fatal radiation damage is expected at the level of 1000 MRad (A. K. Drukier, in preparation).

Finally, we should like to mention a new very interesting application of very high spatial resolution, radiation hard X-ray detectors, namely X-ray holography. A number of theoretical studies have suggested the possibility of using soft X-ray holography capable, in principle, of 3-D imaging of biological samples with a resolution of 100-1000A. Moreover, this capability should be applicable to cells and subcellular structures more closely related to their natural state, i.e., without dehydration, sectioning or staining. Furthermore, when X-ray lasers are used, the hologram can be made in less than a microsecond, i.e., study of the protein dynamics are, in principle, possible.

Recently, Livermore teams have made the first X-ray laser hologram. The X-ray holography applicability, e.g., spatial resolution, was limited by the poor coherence properties of the X-ray sources, the low quantum detection efficiency and the sub-optimal spatial resolution of the detectors. More specifically, nuclear emulsions were used which cannot be readout

digitally. Digital readout will considerably facilitate the hologram reconstruction.

In the Livermore experiment, the detector was Kodak 101 X-ray film. The spatial resolution was between 5 and 10 µm, but both the QDE and maximal flux which could be imaged were very bad. A high spatial resolution superconducting colloid with magnetooptic readout will be a much better detector, perhaps permitting the use of much smaller lasers than Nova. This could bring X-ray holography to many biological laboratories, and would be a very important spin-off in the X-ray laser development.

Our discussions with Livermore scientists[3] suggest another important advantage of superconducting X-ray imagers: they can be built of beryllium. A low Z detector is required to minimize the Compton scatter, i.e. to improve the signal/background ratio.

Ad: Applications of SSCD as X-ray detectors

1) A. J. Howard et al., Meth. in Enzymology 114 (1984) 452
   H. E. Huxley et al., Ann. Rev. Biophys., Bioeng 12 (1983) 381
   H. D. Bartonik et al., in "Structural Biologial Applications of X-ray...", Eds. H. D. Bartunik et al., Academic Press, NY 1985
   K. H. Svendson et al., Int. J. Biol. Macromol. 6 (1984) 298
   V. Luzatti, Lecture Notes in Physics 112 (1980) 425
   A. Gabriel et al., NIM 201 (1982) 221
   G. Charpak et al., NIM 201 (1982) 93
   J. R. Helliwell et al., NIM 201 (1982) 153
   U. G. Briel et al., NIMA 242 (1986) 376
   P. Gorenstein et al., preprint CFA No. 2264, March 1986
2) J. E. Trebes et al., Science, 23, 517 (1987)
3) M. Gerossimenko, M. Eckhart, D. Fortner, private information.

3.3 High Spatial Resolution Neutron Detectors

Neutron detectors are important in many applications, including remote sensing. Furthermore, some of the detection challenges are similar in neutron and other neutral particle detectors, e.g. in sensing neutral beams of particles.

Recently, one- and two-dimensional electronic position-sensitive detectors have become the preferred means of data collection in laboratories. A number of such devices have been constructed for neutron applications, since they are capable of increasing the rates of data collection by one or two orders of magnitude compared to a single counter.

The development of better detectors is essential for further progress. The main detector characteristics which must be considered are spatial resolution, linearity, and dynamic range. Obviously, QDE is very important. Furthermore, good photon rejection is necessary to obtain a good neutron-to-background ratio.

In practice we have three classes of detectors:

a) gas detectors with sub-millimeter resolution and large surface (e.g., 30 x 30 cm^2)[2];
b) scintillation detectors[3]; and
c) sandwich detectors, e.g., based on neutron absorption and localization of emitted photons[4].

It is not possible to specify the "best" detector for diverse material and biological studies; different experiments may demand conflicting qualities from the detector. The essential parameters of the detectors are:

a) size: for neutron microscopy size is ca. 1cm^2 but in remote sensing, and fission material detection, diameters up to 30 cm are required;
b) spatial resolution: most of the existing detectors have a matrix of 256 x 256 or 512 x 512, but much larger formats (4096 x 4096) may be useful;
c) quantum detection efficiency;
d) homogeneity over the detector surface: for most studies an uncertainty of 1% is sufficent, but others require 0.1% and better; and
e) dynamics: usually the dynamic range is below 1000 but can be much higher.

Note that we talk here about "system spatial resolution", not the "intrinsic spatial resolution". For example, for thick detectors (gas detectors) the spatial resolution is often degraded by the parallax effect and curved detectors are required.

No single detector, either now in operation or likely to be constructed in the near future, can satisfy all the demands simultaneously; techniques are mature and only minor improvements are expected. We argue that a new neutron detector proposed by ARC may become the best example of the next generation of 2-D detectors.

We describe the development of a new class of neutron detectors based on the measurement of temperature change in micron-size, superconducting structures. Each pixel is essentially a structure thermally independent of its substrate: heating will occur whenever an alpha particle produced by a stopped neutron interacts in the metal.

A possible implementation takes advantage of the metastability of Type-I superconductors and the very small specific heat of these materials. Each pixel consists of a plurality of spherical grains dispersed in highly granulated boron or lithium hybride. Typically, 10% of the detector volume is in superconducting grains. Taking into account the relevant densities (d(Sn) = 7.3 g/cc, d(B) = 2.4 g/cc and d(LiH) = 0.82 g/cc) the specific density of the detector is d_1 = 2.84 g/cc and d_2 = 1.47 g/cc for boron- and lithium-loaded detectors, respectively. Similarly, the fractional weights of the converter are X = 74.3% and X = 44%.

We proposed to use the reactions[10]

a) 10_B + n -> ^{7}Li + α + 2.79 MeV (6.1%)
             -> ^{7}Li + α + 2.31 MeV (93.9%); and
b) ^{6}Li + n -> 3H + α + 4.786 MeV.

The range of alpha particles is much longer than the typical distance between grains, i.e., at least one superconducting grain is heated by the reaction products. Taking into account the detector composition, an average of 0.7 MeV and 2.4 MeV are deposited in the superconductor for reactions (a) and (b), respectively. However, at low temperature, the specific heat of metals is very small, e.g., at T = 1.5K the specific heat of a tin grain with R = 20 microns is only 340 keV/K. Thus, a temperature increase of more than a degree is expected and will bring the temperature above the transition temperature. Change of state from superconducting to normal leads to a drastic change of magnetic properties; magnetic fields penetrate metals freely when superconducting currents disappear. The process of change of state is fast (a few nanoseconds) and with very sensitive electronics, based on SQUID's, temperature changes as small as 10^{-5}K are measurable.

A new 2-D position sensitive neutron detector may be developed which consists of a superheated superconducting colloid loaded with boron or lithium (up to 75% per weight). The preliminary specifications of such a detector are:

-Surface: 1 cm^2
-Spatial resolution: intrinsic: 4096 x 4096 pixels
                                 system: dx$\leq$5 microns
-Efficiency (QDE)   90%
-Photon background rejection: better than 10^{-3}
-System autonomy: 3 days
-Low helium consumption: 10 liter/day

Table 3 shows a comparison of some existing 2-D position sensitive detectors with a new device proposed by ARC.

Table 3: Comparison of various 2-D detectors of neutrons.

	Gas(MWPC)	Scintillators	SIND*
Diameter [cm]	20	100	100
Resolution	512 x 512	256 x 256	4096 x 4096
QDE: Thermal	85%	90%	90%
Timing	1 micro sec.	1 micro sec.	0.1 nsec.
Homogeneity	1%	5%	0.1%
Curved-Detectors	Difficult	Yes	Yes
Photon Rejection	10^3	10^2	10^4

*SIND = Superconducting Imaging Neutron Detector.

It can be seen that this new detector has much better performance than existing detectors, especially for cold neutrons. The main advantages of the new detector is the

possibility of a few microns spatial resolution. Furthermore, we note an improved spatial resolution for large detectors and improved QDE. For time-of-flight measurements much better timing than with scintillators may be possible. For imaging applications the excellent spatial resolution and nanosecond timing will allow new designs of neutron spectrometers.

Finally, we should point out that preliminary experimental studies of SSCD as neutron detectors show a reasonable QDE and very good photon background rejection[5]

Ad: High Spatial Resolution Neutron Detectors

1) "Neutrons in Biology," ed. B. P. Schoenborn, Plenum Press, NY, 1984.
   "Position Sensitive Detectors for Thermal Neutrons," P. Convert, B. Forsyth, eds., Academic Press, 1982.
   Proc. of Int. Workshop on Evaluation of Singe-Crystal Diffraction Data from 2-D Position Sensitive Detectors, Grenoble, (Journal de Physique, Suppl. Fasc. 8, C5-1986), Nov. 1985.
2) J. Alberi, et al., NIM 127, 507-523, 1975.
3) Scintillators, Technical Data, Nuclear Enterprises, 1986.
4) A. P. Jeavons, et al., "A New Position-Sensitive Detector for Thermal and Epithermal Neutrons," preprint CERN 77-01 (Data Handling Division).
5) A. K. Drukier, J. Igalson, L. Sniadower, NIM 154, 91-94, 1978.

3.4   Diverse Applications of SSCD: A Comparison

As usual, the new principle of radiation detection permits a score of fascinating new applications. The judgment of "which to develop first" is subjective, maybe even arbitrary. Two main questions to ask are:

- importance of application;
- feasibility of application.

In table B we present our "crystal ball" prediction. On a scale of 1 to 5 we estimate both the need and difficulty of development. Furthermore, we show the expected development time until production of a working prototype. The technical requirements are quoted and will be described in section 4. More specifically, these are

- SQUID's, fast electronics, and Magnetooptics are three different types of readout;
- SSCD means superheated superconducting colloid detector and SSAD means the superheated superconducting array detector produced by litography.

Table B: Comparison of diverse applications of SSCD

Device	Difficulty	Prototype	T_operation	SQUID's	Fast Electronics	Magnetooptics	SSCD
Gamma detectors	2	1989	1.2°K	yes	maybe	no	yes
X-ray imager (2056x2056 pixels)	4	1990-91	0.3°K	yes	no	yes	no
Neutron detectors	1	1989	1.2°K	yes	no	yes	maybe

SQUID = no but possibly Josephson junction flip-flops

Scale: 5 = highest

4. SSCD -- State of the Art

The change of state of a single grain due to irradiation was observed previously by many independent groups using photons, relativistic electrons, and neutrons. A QDE = 90% for energy deposition of a few keV was achieved. The following aspects of the SSCD development during the last year are briefly described:

1) Grain production and size selection;
2) Electronic readout;
3) Irradiation tests.

This section, however, gives only the most important results worldwide. The experimental achievements of ARC and collaborators are described in section 5 and more detailed descriptions are provided in Appendices.

4.1 Grain Production and Size Selection

Micron size granules were produced from low melting point metals and alloys e.g., $Hg(T_m = -39)$, In $(T_m = 156)$, $Sn(T_m = 232)$, Sn + 1%Sb $(T_m \approx 220)$, $Cd(T_m = 321)$, Pb + 1% $In(T_m = 320)$, $Pb(T_m = 327)$, where all T_m are in $^\circ C$. Reasonable quality grains were produced by ultrasound disintegration of melted metal immersed in silicon oil. When oil is heated on a heating plate, a temperature gradient is established with the bottom $T \geq T_m$ but top layer $T \leq T_m$. The granules of melt rise and close into almost perfect spheres due to surface forces. The method is simple, cheap and quite efficient; kilograms of material can be processed within a week. However, it is rather difficult to control the heat gradient; the cooling is rather fast and many grains crystallize into a polycrystalline state.

Better grains can be obtained by the "standing ultrasound wave" method developed by French groups in collaboration with Extremet Inc., Geneve (see Appendix 2).

The distribution of grain sizes defines the energy resolution of SSCD and may influence the QDE. Thus, it is important to select an essentially monoradial fraction of grains. This can be achieved through a filtration by calibrated meshes [for $\phi \geq 10 \mu m$] and sedimentation. Our effort during Phase I was concentrated on grains with $20 \leq \phi \leq 35 \mu m$, which will be used in detection of high energy photons. By multiple filtration we improved the spatial resolution to $\Delta R/R \approx \pm 5\%$, which is adequate for preliminary tests (see Appendix 2 for details of selection). Further improvement can be obtained when using custom-made, photolithographically-produced calibrated meshes with aperture opening stepped by one micron. This improvement will be achieved in Phase II. For $\phi \leq 10 \mu m$, precision filters are not commercially available and we used selection by sedimentation. The results are promising but other methods, e.g. centrifugation should be tried to compare their efficiency.

After selection, the grains are stored in pure organic
liquids, e.g., trichloroethylene or isopropyl alcohol. We
recently tested some grains produced in 1982; no change in
hysteresis curves was observed, suggesting that the grains can be
stored for long periods of time.

To produce the colloid, grains are mixed with an appropriate
dielectric. Normally, it is a silicon grease or epoxy resin.
In the last case, a machinable solid with perfect mechanical
properties is obtained. Due to increased thermal conductivity,
epoxy so prepared does not crack even when dropped into liquid
helium. For applications in γ-ray detection, we need an SSCD
loaded with a heavy and high atomic number dielectric. The
choice of the loader depends on applications and is limited to
materials which are highly granular. We produced SSCD loaded
with both mercury oxide and lead oxide. The filling factors were
50% of volume heavy oxide, 40% glue, and 10% Sn grains. The
mixture was mechanically stable and appeared homogeneous; the
forthcoming irradiation tests will prove if this homogeneity is
sufficient for detector applications.

We point out that the colloids we worked with have a random
distribution of grains inside the dielectric. This leads to a
spread in hysteresis curves and negatively influences detector
properties. We are developing methods which permit creating
ordered structures of grains (grains in loci of cubic lattice);
this effort will be described in the Phase II proposal.

Finally, we comment on the possibility of producing ordered
arrays of evaporated pixels. This technique is clearly feasible;
already in the 1970's ordered arrays of superconducting dots were
produced (T. Rosenblatt, Rennes, France - private communication).
A reasonable fraction (up to 80%) of these dots show superheating
and hysteresis curves were sharp. Unfortunately, this method is
costly and could not be used in the Phase I effort.

4.2 Electronic Readout

The electronic readout of SSCD senses the change from
superconducting to normal state by the sudden change of
magnetization. A superconducting sphere placed in a magnetic
field is equivalent to a magnetic dipole ("Meissner effect" or
perfect diamagnetism of superconductors). When a particle or
photon heats the grain, there is a change of state within about
10^{-10} sec. However, it takes some time before the
superconducting screening currents decay due to normal state
resistivity. For very pure grains with R ≈ 1μm this time is a
few nanoseconds. For development of very fast detectors it is
necessary to use superconducting alloys, in which the decay time
of screening currents is about one order of magnitude shorter.
This explains why one of the most important improvements in the
last 6 months is observation of superheating in Sn + 1% Sb grains
(D. Perret-Gallix, private information).

When a pickup coil is in the vicinity of a grain changing its state, the electromotive force is proportional to the change of flux ($\Delta\phi \approx \pi R^2 H$) and inversely proportional to the decay time. Furthermore, there are important geometrical factors which define the coupling between grains and loop:

$$\Delta V \approx 10^{-8} \ast (d\phi/dt) \ast (R/L) \approx 10^{-8}(\pi H R^3/Ldt), \qquad (4.2.1)$$

where R is the grain size and L the distance to the pickup loop. Thus, a grain flip induces a voltage pulse with amplitude of tens of microvolts and nanoseconds duration. This pulse can be amplified and detected.

Until recently (see Fig. 1) charge sensitive amplifiers were coupled to the pickup coil via an appropriate transformer. This readout (proposed by Radeka, BNL and Hrisoho, Orsay) was improved upon by TU, Munich and MPI, Munich (W. Gebauer, private information). It is quite sensitive and, for $R = 10\mu m$ grains in a few millimeter diameter loop, permits a $S/N \geq 20$.

The CERN group developed a much faster ($t_{rise} \approx 10nsec$) preamp with comparable sensitivity. It uses a few J-Fet's in parallel, and the preamp is operated at room temperature. Much better performances are expected using GaAs Fet's operating at liquid helium. These are not only faster ($t_{rise} \leq 1nsec$) but also less noisy.

We note that typical pickup coils developed for SSCD readout are of the size required by many applications - about 1mm in diameter and about a centimeter long.

The second, much more sensitive method of SSCD readout is to use ultrasensitive SQUID's. The use of SQUID's is facilitated by the fact that in a given magnetic field ($H_c \leq H_{sh}$) the grains are metastable, i.e., when they change to normal state they stay normal. Thus, there is a semi-permanent change of magnetization. The appropriate figure of merit for different readout methods is the minimal detectable change of flux. For typical "fast electronics" using a low noise preamp, it is $\Delta\phi = 10-50\phi_0$ where $\phi_0 = 2 \times 10^{-7} Gcm^2$. For the best DC-SQUID's, $\Delta\phi \approx 10^{-5}\phi_0$. When operating in a magnetic field, there is a noise component proportional to the field inhomogeneity and vibration amplitude, typically $\Delta\phi$ (vibrations) $\approx 10^{-3}\phi_0$ for $H \approx 100G$ and a loop with $R_{loop} \approx 1cm$. The vibrational noise can be, at least in principle, eliminated by use of a magnetic gradiometer configuration to reach $\Delta\phi \approx 10^{-5}\phi_0$.

Thus the DC-SQUID readout is potentially six orders of magnitude better than "fast electronics". This tremendous potential was confirmed by an IBM experiment in which a change of state of a $R = 5\mu m$ grain placed in 40 Gauss and well coupled via magnetic gradiometer to a DC-SQUID gave $S/N \geq 10^6$. In a 1986/7 experiment at UBC we obtained $S/N \geq 10$ for $R \approx 2\mu m$ grains in about a one centimeter diameter pickup loop. A single grain flip due to radiation was detected.

We believe that the DC-SQUID readout will be used in a majority of applications of SSCD, e.g. in gamma detectors, high spatial resolution X-ray and neutron detectors. When subnanosecond timing is required, a variant of the DC-SQUID technique employing Josephson flip-flops can be used. Thus the improvement of DC-SQUID readout was the major part of our Phase I effort.

To improve SQUID readout one needs to:

a) diminish $\Delta\phi$ vibrations by providing a more homogeneous magnetic field and eliminating vibrations; and

b) develop reliable/inexpensive multichannel DC-SQUID electronics.

We point out that commercially available DC-SQUID's are quite expensive, ca. $15,000. However, these devices are "get it all" devices providing large flexibility. With a well defined application much cheaper devices can be developed (see Appendix 4). Furthermore, commercial SQUID's minimize the SQUID input inductance (2μH in SHE-SQUID's). However, the optimal pick up loop for SSCD readout is a few tens microHenry--we need SQUID's with their input inductance well matched to the pickup loop.

The SQUID readout improvement was performed in collaboration with the groups of Prof. B. Turrell in UBC, Vancouver, (task A) and of Dr. M. Cromar, NBS Boulder, (task B) and is described in Appendices 3 and 4. Generally, we are quite satisfied with our progress:

A) The UBC group designed/built/tested improved a SQUID readout placed in a vibration insulated cryostat. When compared with 1986 we observed noise reduction by a factor of fifty. Thus we reached the noise limits of RF-SQUID's; even more importantly, we now understand the sources of noise. This will permit us to develop in Phase II a gradiometric readout further diminishing noise by a factor of 10-20, and then reach the sensitivity limits of the state-of-the-art DC-SQUID's.

B) In collaboration with the cryoelectronics group in NBS, Boulder, we designed a four channel DC-SQUID readout more appropriate for SSCD applications. The chips will be available to ARC in the spring of 1988 at cost of ca. $1000 dollars/channel. At ARC, we developed/tested a very low noise linear preamp (noise $\leq$ 0.55 nV/$\sqrt{Hz}$) for DC-SQUID readout. Further, we designed a performant but inexpensive phase lock-in amplifier. It will be built/tested in the spring of 1988. We believe it possible to build a four channel DC-SQUID readout for less than $10,000. (See Appendix 4 for further information).

4.3 Irradiation Tests

The sensitivity of SSCD to radiation was well confirmed by diverse groups. The results are, however, still only partially understood theoretically. This is because a variety of

parameters are of importance, which change from experiment to experiment:

-material and grain size;
-grain filling factor in colloid;
-temperature/field in which detector is operated;
-nature and energy of particle;
-type of readout electronics.

A variety of superconducting materials have been tested: $Cd(T_C=0.5)$, $In(T_C=3.4)$, $Sn(T_C=3.72)$, $Hg(T_C=4.15)$, $Pb(T_C=7.2)$ and some alloys, where all T_C are in K. The size of tested grains was usually $5 \leq R \leq 20\mu m$, but recently very interesting measurements on very small ($R \approx 2\mu m$) and very large grains ($R \approx 200\mu m$) were performed at UBC, Vancouver, 1986 and LAPP/CERN, 1986/7, respectively. Among the diverse materials, tin and its alloys are best understood.

The SSCD was usually tested in liquid helium-4 cryostats ($1.2 \leq T \leq 4.2^{\circ}K$) but Cd grains have been studying at $150 \leq T \leq 500$ mK in a dilution refrigerator (TU, Munich, 1984) and Sn at $300 \leq T \leq 500$ mK in a He-3 cryostat (LAPP/CERN, 1986/7).

The SSCD detectors were tested with β^- particles, (Orsay, 1970), relativistic monoenergetic electrons (DESY, 1976), γ photons from radioactive sources (at least 4 groups in the last few years) and soft X-ray photons (LAPP/CERN, 1987). Furthermore, detection of neutrons in a Li-loaded SSCD was reported (A. K. Drukier et al., 1976). Depending on operating temperature, deposited energy and quality of the SSCD, QDE's of 20 to 90% were observed.

The type of irradiation experiment depends crucially on the available electronics. In the preliminary experiments, the collection of grains was placed in a pickup loop and the change of magnetization monitored by means of the frequency change of a cryogenic LC oscillator, where L and C are the distributed inductance and capacitance of the coil, respectively. This method has some advantages: it is simple, inexpensive, and permits detection of small grain ($R \leq 5\mu m$) flips. However, it is relatively insensitive; with a typical oscillator stability of $dv/v \approx 10^{-6}$, about a hundred grains must change their state to give a detectable signal. The typical results (A. K. Drukier, 1980-82, unpublished) are shown in Figure 2. In Figure 3 we show the detected signal versus time; notice the excellent agreement between the size of the signal (dots) and the activity of the short-lived Ga-67 radioactive source (broken curve). Furthermore, when the radioactive source was moved away from the detector, the predicted D^{-2} change was observed (where D is distance between source and detector see Fig. 4). In tests with smaller ($R \approx 5\mu m$) grains, a reasonable QDE$\approx$30% was observed, even if the grains were not selected according to size.

Development of fast electronics (see Section 4.2) leads to a quantitative jump in our understanding of SSCD; the change of

state of a single grain due to photon detection was observed by at least four groups (G. Waysand et al., Paris; F. von Feilitzsch et al., TU, Munich; D. Perret-Gallix et al., LAPP/CERN and L. Stodolsky et al., MPI f. Physik, Munich). In the LAPP/CERN experiments (see Fig. 5), single 6 keV photons were observed to change the state of large (R≈15 μm) grains. Another very important series of experiments was performed by L. Stodolsky et al. (MPI f. Physik, Munich 1986/7), in which a single superconducting grain (R ≈20μm) was irradiated at diverse thermodynamic conditions (temperature and field amplitude/direction). G. Waysand et al. (Orsay, France) developed and tested a hard X-ray imager featuring 128 x 128 pixel spatial resolution. Finally, the coincidence of two small SSCD detectors spaced a few centimeters apart was observed using relativistic electrons (A. K. Drukier et al., 1976). A similar experiment, using relativistic muons and much improved electronics (t_{rise}≈10nsec) is being performed by the LAPP/CERN group with participation of scientists from ARC.

The use of "fast electronics" also has some disadvantages: the experiments have a good S/N ratio only if the grain is reasonably large (R≥10μm). New, more sensitive electronics is being developed which should permit detection of single, R=5μm grains in a few cubic centimeter detector, (G. Waysand, Paris-private information) but we believe that irradiation experiments using SQUID readout are even more promising.

Recent tests carried out at UBC by A. K. Drukier, A. Kotlicki, M. A. LeGros, and B. G. Turrell have demonstrated all aspects of this approach. For these, a pumped ^{4}He cryostat was used to obtain temperatures as low as 1K, and a SHE RF SQUID System 330 was used to monitor grain flipping in magnetic fields. Experiments were done to test the performance of tin (T_c = 3.72°K, H_0 = 309 Gauss) grain flipping in magnetic fields. The grains were prepared by ultrasound disintegration from 99.99% pure tin. Size selection was done by filtering the grains through wire mesh filters. The size distribution of the grains was determined with a laser light scattering technique. Two different types of tests were performed and are described below:

1. In the first test, a microscope was used to select ten grains which had good sphericity and a radii of 15 microns. The grains were arranged in a line on a copper strip which had one end attached to a regulated heat source, and the other thermally connected to the 1°K cryostat pot via a large thermal resistance. With this arrangement, each of the ten grains was at a slightly different temperature and their successive transitions to the normal state as heat was added could be observed. Each transition produced a SQUID signal of about 1 volt. This voltage agrees with the theoretical signal estimates, and the signal/noise was much better than 10.

2. The second test explored the response of the colloidal dispersion of 10^4 tin grains to X-rays from a ^{67}Ga source. The arrangement is shown in Figure 4. The grains had radii of about

5 microns. A 1 cm thick copper block was used to filter the source; when placed over the source it absorbed a majority of the 93 KeV photons. The radiation test was performed at 310G and 2.2 Kelvin; the temperature was about 50 mK below the superheating value. When an X-ray from the Ga source interacts with a tin atom, the most likely scenario is for a tin K-shell electron to be ejected. The range of such an electron (which has a kinetic energy of about 64 keV) is about 22 microns in tin. Typically, this electron will deposit about 10 keV in a grain having a radius of 5 microns, although large fluctuations are possible due to variations in electron path length and energy straggling. Furthermore, about 5% of the K-shell X-rays from decay of the tin atom will interact in the grain, allowing for an energy deposition of 25 keV. From these numbers, we estimate that the most likely temperature increase of a 5 micron radius grain is about 10 mK, and that the maximum temperature is about 50 mK, which should be enough to flip the grain. This is clearly demonstrated by the experimental data (see appendix 3).

Photon absorption and individual grain flip lead to abrupt changes in the SQUID signal. When the copper filter is in place, the flip rate is reduced considerably (leakage of high energy X-rays through the filter will prevent this case from being free of any grain flips). The range of signal sizes is due to the variation in grain sizes. Measurements of the QDE (which is the ratio of the number of grains flipped to the number hit by X-rays) are difficult due to the variation in grain properties, the resulting field dependent width of the phase transition, and the imprecise nature of the radiation source used. Nevertheless, the QDE has been estimated to be 80-90%.

The above results show that the principle of a SQUID readout of the SSCD is experimentally realizable within the current technology. One of the important tasks of ARC in Phase I was to improve upon the preliminary 1986 results. In collaboration with the group of Prof. B. Turrell, UBC we started an experimental program with the following aims:

- diminish the vibrational noise at H=100G by a factor of 5-10;
- make possible the detection of a single, R=1μm grain in a small pickup loop of 2 mm diameter;
- study QDE for photons, e.g., X-rays, soft gammas and annihilation photons.

The preliminary results are excellent and are described in Appendix 3.

4.4 Who is Who in SSCD development

The limited time for Phase I feasibility studies made necessary a careful choice of target tasks. Our choice was motivated by:

- relevance for application;
- requirement that ARC and collaborating groups will not perform experiments which are currently performed by other, mainly European groups.

Thus, we believe that in this report we should provide a short description of the overall picture of R & D not only in ARC but worldwide.

The SSCD was a first example of a low temperature particle/radiation detector. Fortunately, bygone are the times when two stubborn individuals (A. K. Drukier and G. Waysand) tried to prove on a $10,000/year budget that it works. In the last few years (partially motivated by a A. K. Drukier/L. Stodolsky suggestion that SSCD can detect neutrinos) there has been a very rapid increase of interest in the cryogenic detectors. At least 50 people in some ten institutions are currently developing these techniques. More specifically, about 20 people are developing SSCD in America, Europe, Soviet Union and Japan. However, the leading centers of development of SSCD are in Europe. The following is a brief description of their strength/development programs.

a) MPI f. Physik, Munich, W. Germany --
(L. Stodolsky, K. Pretzel, W. Gebauer, A. Fraund, A. Sigass + 2 technician).
Motivation: Development of neutrino/massive weakly interacting particle detectors.
Resources: about $400,000/year; He-4 cryostat, He-3 cryostat, dilution refrigerator on order, good NIM/CAMAC + μVAX excellent mechanical/electronic workshop.

R&D program 1988.

- Improved methods of grain production, especially using alloys;
- Tests of single grain flipping mechanism;
- Improved "fast electronics" readout, especially using cooled preamps; use of DC-SQUID's for grains readout.

b) TU, Munich, W. Germany --
(Prof. R. Mossbauer, F. von Feilitizsch + 4 post docs + 3 technicians).
Motivation: Development of neutrino detectors.
Resources: about $400,000/year; He-4 cryostat, He-3 cryostat; 2 dilution refrigerators

R & D program 1988.

- no R & D on grains until late spring 1988;
- tests of SSCD at very low (T $\leq$ 100mK) temperature using dilution refrigerator + DC-SQUID.

c) F.U. Berlin, W. Germany --
(Prof. E. Klein + 2 post docs)
Motivation: High energy resolution photon detectors.
Resources: $\leq\$20,000$/year; 3 dilution refrigerators, 2 RF-SQUID's

R & D program 1988:

- tests of energy resolution/properties of SSCD at super low (T $\leq$20mK) temperature.

d) Ecole Normale/U. de Paris/Ecole Polytechnique, Paris, France,
(- G. Waysand + 3 physicists + 2 post doc's + 2 technicians).
Motivation: High spatial resolution γ-ray detectors for applications in Nuclear Medicine and Nondestructive Testing; Solar neutrino detection using inverse β decay in In-115; Percolation problems in densly packed collections of spheres.
Resources: about $200,000/year; several He-4 and He-3 cryostats; excellent electronics group; close collaboration with Orsay Superconductivity Group.

R & D program 1988:

- Improvements in grain quality
- More sensitive "fast electronics"
- Development of 128 x 128 pixel imager

e) LAPP, Annency/CERN, Geneve --
(D. Perret-Gallix, L. Gonzales-Mestres + 1 grad.student + 1 technician).
Motivation: Exotic particles detection (m. monopoles and WIMP's); Rauiation hard, high spatial resolution detectors for applications in high energy accelerators;
Resources: ca.$50,000/year; He-4 cryostat + access to a He-3 cryostat; good readout electronics (NIM, CAMAC, Fastbus), especially for very fast timing; Access to electron/muon/proton beams at CERN.

f) U. Torino, Italy -- 3 scientists.
Motivation: Search for exotic particles.
Resources: ?
R & D program 1988: Improvement of "fast electronics", including GaAs Fet's.

g) ARC/UBC/NBS/U.Md/NRL
ARC: A. K. Drukier, T. Girard, C. Nga
UBC: B. Turrell, A. Kotlicki, M. Legros + 1 grad. student
NBS: M. Cromar, R. Ono, J. Colwell, T. Geblutowicz
U.Md: T. Zawistowski
NRL: R. Soulen, M. Kowalski

Motivation: Medical/Biological Applications; Radiation Hard Detectors; Exotic particles searches.

Resources: about $200,000 for 1988: 2 dilution refrigerators + 2 liquid He-4 cryostat; 2 RF-SQUID's + access to the resources of "cryoelectronics foundry" in NBS, Boulder; Expertise in very low temperature thermometry (NBS, Gaithersburg); Good electronic/mechanic workshop (U. Md)

Furthermore, there are groups in Spain (2 scientists), Italy (3 scientists) and USSR (5 + scientists in Moscow/Erevan). It should be pointed out that funds available to European scientists are for experiment instrumentation only; all salaries are fully paid by the participating institutions. Furthermore, the funds have been increasing 50% yearly for the last 3 years.

Please note that the Japanese moved into the field of superconducting particle/radiation detectors only last year, but are fielding the largest team (11 scientists) and are very well equipped. They have a very powerful dilution refrigerator and much experience with SQUID electronics.

The resources in USA/Canada are not negligible, but are definitely less than in Europe (especially since the quoted funds are for both salaries and instrumentation/experiments). The list of people involved in SSCD development looks impressive but most of the scientist/technicians work on these projects only part-time, say 10-20%. Only A. K. Drukier works on SSCD full-time, whereas T. Girard and M. Legros works 80% and 50% of the time, respectively.

Table 1: Understanding of SSCD as Particle/Radiation Detector

	1986	1987	who/where	1988 R&D plans
SSCD at 1 ≥ 1.2°K				
A: Single grain	++	+++	K. Pretzel et al., MPI L. Gonzales, LAPP A. K. Drukier, et al., ARC/UBC	MPI f. Physik, Munich
B: Collection of grains: small filling factors ≤ 10%	++	+++	L. Stodolsky, MPI G. Waysand et al., Orsay A. K. Drukier, et al., ARC/UBC	LAPP/CERN ARC/UBC Orsay
C: Collection of grains: high filling factor ≥ 10%	+		G. Waysand et al., Orsay	Orsay
SSCD at T ≤ 1.2°K				
A. 500 ≤ T ≤ 1.2°K	-	++	D. Perret-Gallix, LAPP	LAPP/CERN MPI/Munich ARC/NBS
B. T ≤ 500°K	+	+	A. K. Drukier, et al., ARC/NBS	ARC/NBS

++++ = excellent ... + = bad

Table 2: SSCD Fabrication/Quality

Tasks	1986	1987	Who/Where	1988 R&D
Grain Production (pure element)	+++	++++	Extramet et Cie. Billiton et Cie.	all groups
Grain Production (alloy)	--	++	Extramet et Cie. LAPP/CERN MPI, Munich	ARC LAPP/CERN MPI, Munich
Size Selection	+++	+++	ARC	ARC
Random dispersion in appropriate dielectric	++	++	ARC	ARC LAPP
Ordered arrays of grains/pixels	+	+	—	ARC T.U., Munich

++++ = excellent ... + = bad

Table 3: Readout Electronics Performance

Type	1986	1987	Who/Where	1988 R&D Plans
LC oscillators	+++	+++	—	—
SQUID's (alloy)	10^{-2} $R \leq 2$ m in $D_{loop} \leq 0.5$ cm	5×10^{-4} $R \leq 1$ m in $D_{loop} \leq 0.5$cm	ARC/UBC	ARC/UBC ARC/NBS MPI f. Physik.
Fast electronics [t_{rise} 1 sec]	50 $R_{min} \geq 15$ m	25 $R_{min} \geq 10$ m	MPI f. Physik Orsay	MPI f. Physik Orsay Torino
Very fast electronics appropriate dielectric	—	50 $R_{min} \geq 15$ m	LAPP/CERN	ARC LAPP/CERN
Magnetooptics	—	—	—	ARC/U. Tubingen

$T \leq 4.2^\circ K$

$T = 300^\circ K$

680pF

HQV 810

(-V)

N=200
L~6µH

$\frac{N_1^2}{N_2^2} = \frac{1}{36}$

C~100pF

Two Layers
$\emptyset_{ext}$= 1mm, l=6mm

copper wire $\emptyset_{ext}$=50µm
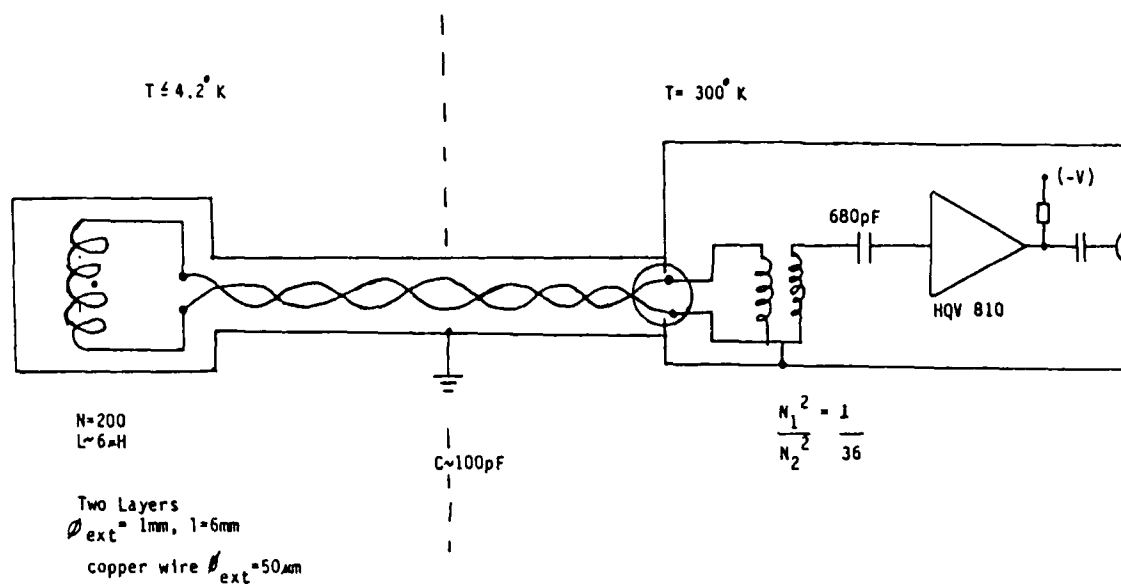
Fig.1 : Fast electronic readout of SSCD
        (Courtesy of MPI f.Physik,Munich).

IRRADIATION TESTS (A.K.DRUKIER)

TESTED : TIN AND INDIUM SSCD (FILLING FACTORS 1-10%)

(GRAINS RADIUS ≈5 MICRONS ,$\Delta R/R$ =30%)

RADIOACTIVE SOURCES : GA-67(80 KEV) ,Tc-99M (140 KEV)

$$E_{DEPOSITED} = \sqrt{2} \cdot R \cdot 1.5 \text{ KEV/MICRON} = 10 \text{ KEV}$$

SECONDARY PHOTONS (20 KEV)

MEASURMENT METHOD : INTEGRATING EFFECT DUE TO SOURCE OVER CA. 1 MIN

MEASURING THE MAGNETIC PERMEABILITY VIA.

RESONANCE FREQUENCY CHANGE IN LC OSCILLATOR

SSC - coil 1 cm , T = 1.63 K

Background
Shielded
Open

Source 2.5 nCi at distance 1 cm from detector
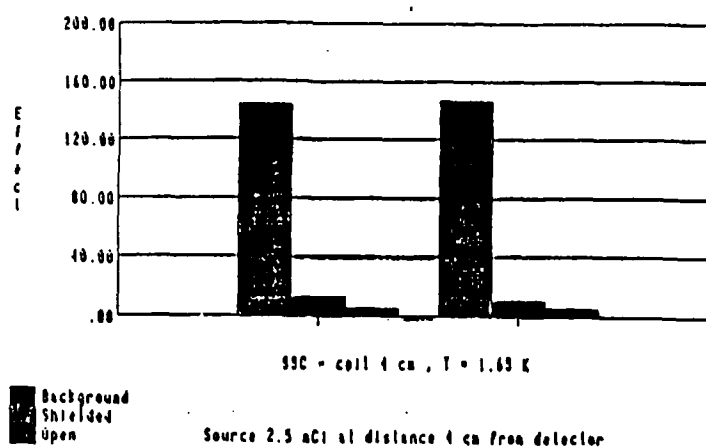
Fig. 2 Irradiation studies using 88 keV gamma source.

SSC IRRADIATED WITH TECHNITIUM

SEC.

ACTIVITIES :0.4,1.8,2.24,2.88 MILLICURIE

• = MEASURED EFFECT , CONTINOUSE LINES = EXPONENTIAL DECAY
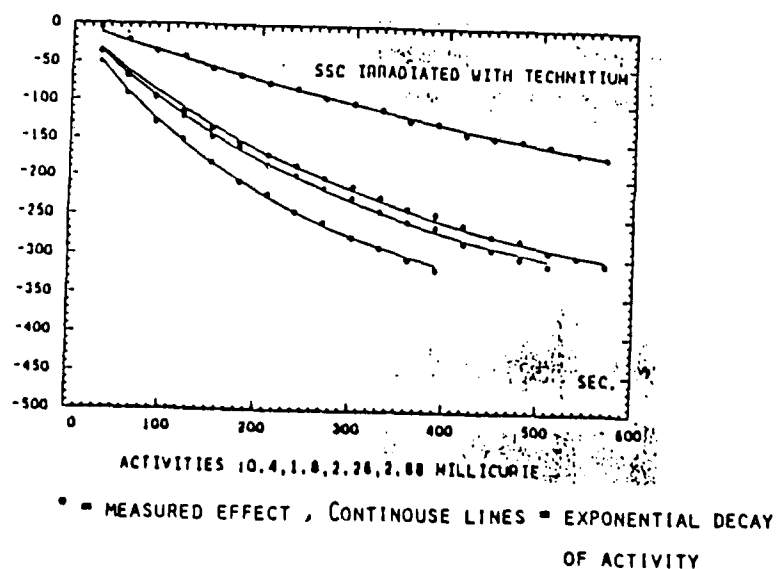
OF ACTIVITY

Fig. 3 Results showing that the effect is proportional
source activity .
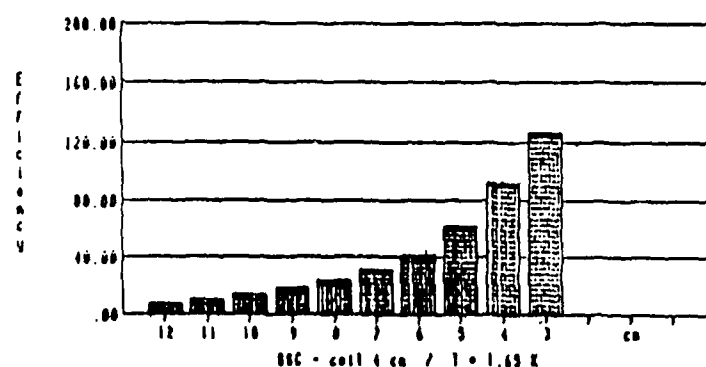
WHEN THE SOURCE IS MOVED OFF DETECTOR EFFECT DECREASES AS R^{-2}

Fig. 4   Effect dependence vs. distance to source.
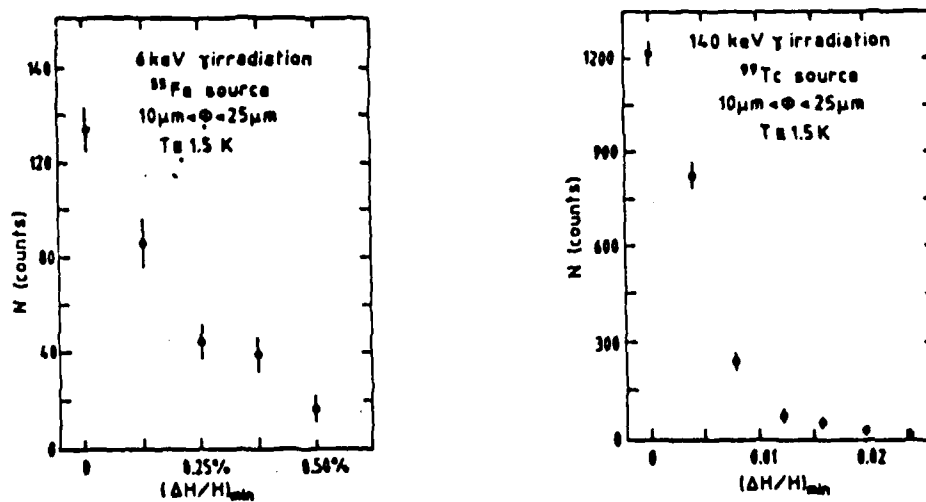
Fig. 5   Irradiation studies of LAPP/CERN group.

5. EXPERIMENTAL PROGRAM OF SSCD DEVELOPMENT BY ARC

5.1 What/Why/Where

Phase I of the SDIO-SBIR project awarded to ARC calls for a feasibility study of a new concept of detectors based on low temperature techniques, and more specifically the development of radiation hard devices using SSCD/SSAD. We believe we have been quite successful with these tasks: our main experimental results are described in this section, and the technical details are provided in Appendices 1 to 6.

One of the important achievements of the ARC team was to obtain collaboration of scientists in universities and large research laboratories. Thus the ARC team (Drs. A. K. Drukier and T. Girard) is efficiently assisted by six excellent scientists on a part-time basis. They provide unique know-how required by our project, e.g., the group at NBS (Boulder) is a leader in cryoelectronics development (SQUID's, Josephson junctions) and one of the three groups worldwide which has operated high T_c superconductor SQUID in liquid nitrogen. The use of high T_c superconductors can considerably facilitate and make cheaper the readout of superconducting particle/radiation detectors. The group at NBS (Gaithersburg) is very well known for development of international standards of temperatures for $T \leq 0.5^{\circ}K$. The group of Prof. B. Turrell, UBC (Vancouver) is well known in fields requiring the use of SQUID's in high magnetic fields and ultralow temperatures, e.g. nuclear orientation studies. Part of the DOD-SBIR funding was used to support the joint ARC/UBC program of development of ultrasensitive SSCD readout. At the U. of Maryland, we have access to the savy of both the high-energy physics group (fast electronics!) and the applied superconductivity group of Dr. G. Park, who specializes in ultrasensitive, large volume superconducting devices (gravity gradiometry). Furthermore, in collaboration with the group of Prof. R. Huebener at Tubingen University, we used their unique facility (electron microscope with a liquid helium cooled focal plane) to obtain the first experimental evidence of the radiation hardness of superconducting particle/radiation detectors.

The successful development of a SSCD gamma camera by the Orsay group shows that even using state-of-the-art SSCD, useful imaging devices can be developed. This gamma camera is used by STEGMA in non-destructive tests of airplanes/rocket engines, and provides reasonable QDE and submillimeter spatial resolution for $E\gamma \approx 100$ keV.

We believe, however, that future engineering tasks will be considerably facilitated by more fundamental R&D in the following sub-fields:

- radiation hardness of superconducting detectors;
- colloid production/quality assessment;
- electronic readout;
- very low temperature ($T \leq 100$ mK) tests.

Furthermore, SSCD has been well tested with electromagnetic radiation ($15 \leq E\gamma \leq 150$ keV), but the irradiation tests should be extended to annihilation photons ($E\gamma = 511$ keV) and to low energy photons ($E\gamma \leq 15$ keV).

The principal technical challenge to the SSCD development is that both the energy threshold,

$$E_{th} \leq \frac{4}{3} \pi R^3 C_v(T) \times \left(\frac{dH_{sh}}{dt}\right) \times \Delta H, \qquad \qquad 5.1$$

and the size of the electronic signal due to grain flipping are proportional to the grain volume. Thus it is very easy to flip small ($R \leq 5$ μm) grains, but the sensing of the change of a <u>single</u> grain is easy for larger $R \geq 10$ μm grains. Let us analyze what kind of improvements that are expected in the next few years.

Better grains, and some innovative techniques of their dispersion in dielectric to obtain "ordered" grains, will narrow the spread of the following parameters in equation 5.1:

- volume of grains;
- temperature barrier ($\Delta T \equiv (dH_{sh}/dT) \times \Delta H$).

The synthetic figure of merit of the colloid quality is the width of hysteresis curve. In other group experiments, $\Delta H_{sh}/H_{sh} \approx 10\%$ was observed. In our experiments, the width of $\Delta H_{sh}/H_{sh} \approx 1\%$ was measured at small fields, and a few percent in high fields (diamagnetic effect!). Further improvement in grains quality will permit

- $\Delta H_{sh}/H_{sh} \approx 1\text{-}2\%$ (5.2a)

- $dE_{th}/E_{th} \approx 2\text{-}5\%$ (5.2b)

- $QDE \geq 90\%$ (5.2c)

Thus improvements in grain production/selection and colloid preparation will lead to about a five-fold improvement upon the state-of-the-art. Another important parameter is the speed with which screening currents decay. Thus, production and quality assessment of grains with different levels of impurities (1-10%) is required to obtain $t_{rise} \leq 1$ μsec.

In some SSCD applications, a considerable increase in electronic sensitivity is possible when using SQUID's. The theoretical analysis suggests an improvement by five orders of magnitude; already the preliminary tests at UBC (1986/7) gave two orders of magnitude improvement. In 1987 we hoped for a further factor of 5-10 improvement, and reached a factor of fifty improvement (see Appendix 3).

The state-of-the-art of electronic readout was described in section 4. When using fast electronics, a further improvement in sensitivity by factors of 2-3 is expected, but may require use of GaAs preamps operating in liquid helium. Rapid progress, however, is expected in the speed of the readout electronics. In 1987 the progress was from $t_{rise} \approx 1$ μsec (MPI F. Physik, 1986) to $t_{rise} \approx 10$nsec (LAPP/CERN, 1987). In 1988 we expect to reach $t_{rise} \approx 500$ psec using GaAs preamps and $t_{rise} \approx 100$ psec seems to be possible using Josephson junction flip-flops.

The specific heat of metals is given by

$$C_V \approx \frac{1}{A} [\gamma T + 1.94 \times 10^3 (T/\theta_D)^3] \ [mJ/mole]$$

For Sn: $A = 118.7$, $\gamma = 1.78$ and $\theta_D = 178$; for Pb: $A = 207.2$, $\gamma = 3.1$ and $\theta_D = 96$. At very low temperatures, $(T \leq 1^oK)$, the specific heat decreases linearly with temperature. The typical temperature reached in pumped liquid Helium-4 cryostats is 1.2^oK; the modern dilution refrigerators can cool large masses (about a kilogram of metal) down to 20 mK. Thus, in principle, for tin the gain of sensitivity is $C_V(1.2^oK)/C_V(0.002^oK) = 73$ by working in a dilution refrigerator (for lead it is a factor of 121). Until last year, it could be argued that the applied use of dilution refrigerators is financially unwarranted, since typically SHE dilution refrigerators cost $200,000. However, in the last year two groups [Argonne National Laboratory, US and Institute Laue-Langevin, France] have developed simple, computer-controlled, one-shot dilution refrigerators which are available commercially for about $50,000. These can be operated for about 12 hours everyday, which is quite satisfactory for many applications. For space-born applications, the group of H. Moseley, NASA/GSFC is developing an adiabatic demagnetization cryostat permitting $T \approx 0.1^oK$ and <u>five year</u> autonomy. Further progress in such cryostats is possible using high T_c superconducting magnets operating in liquid neon or nitrogen. Thus, on the inception of our project it's become evident that very low temperature tests of SSCD are required for a better understanding of the preferred implementation of radiation hard superconducting detectors.

5.2 Plans vs. Achievements

On the basis of the above mentioned arguments and taking into account the available facilities, we decided to try for an <u>extended</u> research scope. The development of SSCD is concentrated in the Washington, DC, area (ARC/NBS, Gaithersburg/U. Maryland, College Park). Some development, coordinated by A. K. Drukier, is subcontracted to the groups of Prof. B. Turrell (UBC, Vancouver), Dr. M. Cromar (NBS, Boulder), and Prof. R. Huebener (Tubingen University).

We organized our activities into five sub-fields. (The expected date of task fulfillment is provided in brackets).

A.   Tests of radiation hardness of superconducting detectors
     [March/April 1988]

     1.   using electron microscope to irradiate superconducting
          tunnel junctions.

     2.   using cobalt bomb to irradiate SSCD.

     The first group of tasks was performed and shows that
superconducting tunnel junctions are radiation hard to at least
50 MRad (see Appendix 1).

     The second group of tests has been slightly delayed and only
preliminary results are available (see Appendix 1). The full set
of results will be described in Phase II proposal.

B.   Grain production/selection [ARC; $\leq$ Dec. 87]

     1.   production of good quality, spherical grains;
     2.   selection of grains with R $\approx$ 20μm and dR/R $\approx$ ±5%;
     3.   production of a SSCD loaded with heavy dielectric.

All of these plans have been fulfilled [see Appendix 2].

C.   Improvements of RF-SQUID readout electronics and tests of
     QDE of SSCD detector [ARC/UBC, Vancouver].

     1.   QDE tests using the 1986 setup [$\leq$ Nov. '87];

     2.   Construction of new cryostat insert; reduction of the
          vibration contribution to SQUID noise [$\leq$ Dec. '87];

     3.   Automatization of tests using PC compatible, 16 bit ADC
          [Jan. '87].

Unfortunately, we could not perform the QDE tests in fall 87,
because the multichannel analyzer used in our 1986 tests broke
down. We had to first implement all readout electronics and
appropriate software using a PC with 16 bit ADC. Due to the
diligence of the UBC group, (especially of M. Legros) both
cryogenics and SQUID readout systems are now operational, and
irradiation studies were initiated at the end of January 1988.
The first results are very encouraging, and are described in
Appendices 1 and 3.

D.   Development of multichannel SQUID readout electronics
     [ARC/NBS, Boulder]

     1.   Production of a chip with four DC-SQUID's appropriate
          for SSCD readout [NBS, Feb. '88];
     2.   Development of a preamplifier with noise $\leq$ 1.5 nV/$\sqrt{Hz}$
          [ARC, Jan. '88];
     3.   Development of lock-in electronics for DC-SQUID [ARC,
          Feb. '88];

4. Assembly of four channels of DC-SQUID electronics [ARC/NBS, March/April '88]

We have been informed that NBS, Boulder is well advanced with the design/mask production for the 4-SQUID chip. At ARC, we have developed a very successful preamplifier with a noise level of 0.5 nV/$\sqrt{Hz}$ at room temperature and 0.4 nV/$\sqrt{Hz}$ when cooled. This is a factor of five improvement over the preamplifier used currently by the NBS, Boulder group. Furthermore, we established that lock-in electronics for SQUID can be built for $1,000/channel; the CAD/CAM development was initiated. These developments are described in Appendix 4.

E. Development of a dilution refrigerator appropriate for SSCD studies; tests at very low temperature (T $\leq$ 100 mK) [ARC/NBS, Gaithersburg]

1. Moving of cryostat to RF-cage [Oct. '87];
2. Assembly/low temperature tests [Jan. '88];
3. Studies of SSCD hysteresis curves [Feb. '88];
4. Irradiation tests at T $\leq$ 100 mK [March, '88];

These tasks are described in Appendix 5. We have been successful with the development of the dilution refrigerator at NBS, the first two tasks being accomplished by the end of October '87. The first hysteresis curves were obtained in December '87. We believe that the first series of SSCD hysteresis curves will be finished in March 1988.

F. Development of fast electronics, and of a facility to test the grains [ARC/U. MD/CERN]

1. Cryostat/Gas handling system [ARC; Dec. '87];
2. Magnetic field/Temperature Stabilization [ARC; Jan. '88;
3. Development of a fast preamplifier [ARC/CERN; spring '88;

These tasks are described in Appendix 3; tasks 1-2 were accomplished on time.

The main experimental achievements, we believe, are:

- experimental proof that superconducting particle/radiation detectors survive irradiation doses of 50 MRad;

- considerable improvements in grain production methods, and especially the availability of very spherical grains made of Sn + 1% Sb;

- production of SSCD colloid loaded with heavy dielectric;

- development of very fast ($t_{rise} \leq$ 10 usec) readout electronics sensitive to the change of state of single R $\approx$ 10 μm grains;

- development of an improved RF-SQUID readout, leading to the possibility of detecting the change of state of a single R $\approx$ 1 μm grain;

- development of a very low noise preamplifier (noise $\approx$ 0.5 nV/$\sqrt{Hz}$) appropriate for DC-SQUID's.

The experimental results are described in considerable detail in Appendices 1-6.

Furthermore, much of the successful effort was focused on activities which extend the experimental capabilities of ARC and collaborating scientists. We should like to point out that the ARC/NBS, Gaithersburg dilution refrigerator is unique in the world, being now fully dedicated to very low temperature studies of superconducting particle/radiation detectors.

Appendix 1:   Experimental Tests of Radiation-Hardness of

Superconducting Particle/Radiation Detectors

Superconducting devices have been discussed as a new family of solid state particle/radiation detectors. Because the energy necessary to break Cooper pairs is typically below 1 MeV, such material appears highly favorable as a solid state particle/radiation detector compared to a semiconductor with a typical energy gap of about 1 eV; diverse superconducting devices, e.g. granulated superconducting bolometers and superconducting tunnel junctions, promise a higher energy resolution. Further, an important advantage of a superconducting radiation detector lies in the fact that the superconducting energy gap is smaller than the Debye energy. Phonons generated by the particle/radiation can therefore contribute to the detector signal, in contrast to the situation for a semiconducting detector, and provides a considerable advantage in detecting beams of neutral particles, e.g. neutrinos or fast neutrons, via nuclei recoil.

Another advantage of superconducting detectors, and more specifically of superconducting colloid detectors (SSCD), is the possibility of excellent spatial resolution. Both detectors with microns spatial resolution and very large (10^4 x 10^4) arrays of detectors, seems possible.

Furthermore, superconducting particle/radiation detectors are expected to be extremely radiation-hard. The most important results of recent ARC efforts was experimental proof that superconducting detectors function properly after irradiation by a few tens of MRad. Two series of experiments were performed:

- in collaboration with the group of Prof. R. Huebener, Tubingen University, we analyzed the radiation-hardness of superconducting tunnel junctions (STJ);

- in collaboration with the group of Prof. B. Turrell, UBC we studied the radiation-hardness of a superheated superconducting colloid detector (SSCD).

These results are also highly significant because we used two diverse sources of irradiation: medium energy electrons with $E_e = 25$ keV, and high energy photons from a cobalt source ($E\gamma \geq 1.5$ MeV).

We begin with a description of the radiation-hardness tests of STJ's. The quasiparticle current-voltage characteristic of a superconducting tunnel junction shows a highly nonlinear behavior, resulting in a sensitive dependence of the magnitude of the detector signal upon the bias point of the junction. In the thermal tunneling regime the current is determined by the quasiparticles which are thermally excited at the operating temperature of the junction. Here the detector signal directly

results from the additional quasiparticles generated by the particle irradiation. In the gap regime the situation is more complicated: in addition to the excess number of quasiparticles, the reduction of the energy gap due to the particle irradiation contributes significantly to the detector signal. This gap reduction is most important for materials having a small quasiparticle diffusion length and results in a distinct maximum of the detector signal for a bias point at the gap sum voltage. For materials having a large quasiparticle diffusion length this effect is less important due to the fast reduction of the excess quasiparticle density due to quasiparticle diffusion. Thus, the STJ configuration is ideally suited to measurements of radiation-hardness: all important parameters are measured during the irradiation. First, it should be rememberd that measurement of voltage/current characteristics of STJ permits a good estimate of not only critical temperature, but also the energy gap and ratio of superconducting/normal electrons. Second, the stability of the tunneling barrier and possible barrier changes occurring during the particle irradiation may be monitored. Third, the degree of spatial homogeneity of the tunneling barrier and of the thermal coupling to the substrate may be evaluated.

Experimentally the electronic response of superconducting tunnel junctions to particle irradiation can be investigated using a scanning electron microscope equipped with a liquid-He stage. We have utilized such a system extensively for imaging spatial structures in a tunnel junction by means of low

temperature scanning electron microscopy (LTSEM)[1-3]. In these experiments the junction is scanned with the electron beam and a proper junction response signal is recorded as a function of the coordinates of the beam focus, while the backside of the substrate carrying the junction is in direct contact with liquid He. In addition, the LTSEM principle can serve in quantitatively evaluating the application of tunnel junctions as cryogenic particle detectors. We report on recent experiments of this second category performed with Pb-alloy junctions.

Experiments were performed using thin-film superconducting tunnel junctions fabricated by standard vacuum deposition techniques. Both the base and the top electrode consisted of Pb-In alloy containing 10% weight In (deposition by flash evaporation). The substrates were single-crystalline sapphire disks of 20 mm diameter and 1 mm thickness. During the deposition of the junction electrodes the substrates were in good thermal contact with a metallic plate cooled with liquid N_2. The natural oxide of the base electrode, served as the tunneling barrier (oxidation at room temperature at O_2-pressure of about 30 mbar; oxidation time 12 - 18 h). The tunneling area was defined by a square window of 28.3 μm side length in a SiO film thermally evaporated upon the base electrode. Microfabrication was performed using photolithographic techniques.

The geometry of the tunnel junctions is shown schematically in Fig. 1. A barrier-parallel magnetic field could be applied by

passing an electric current along the base electrode. On each substrate two electrically-separated tunnel junctions were prepared. A total of 10 junctions have been investigated. The characteristic parameters of these junctions are listed in Table 1.

The electron beam irradiation experiments at low temperatures were performed using the unique facility developed by Prof. R. Huebener group: low temperature scanning electron microscopy (LTSEM).[1-3] Here the substrate carrying the tunnel junction detector at the top is mounted on the low-temperature stage of a scanning electron microscope (SEM) in such a way that the detector can be irradiated directly with the electron beam, whereas the bottom of the substrate is in direct contact with the liquid helium bath. The schematics of LISEM are depicted in Fig. 2. The electron beam of the SEM can be periodically modulated up to frequencies of about 5 GHz. Further, short beam pulses can be obtained. The coordinate point of the beam focus can be chosen arbitrarily. Typical beam parameters are the following: voltage = 25 kV, power = $15^{-5} - 10^{-8}$ W, diameter < 1000 A, pulse width $\geq$ 10 ns. During most experiments the temperature of the liquid-He bath was 4.2 K.

The beam-induced response signal generated in a tunnel junction depends upon the junction bias condition. If the junction is voltage-biased on the quasiparticle voltage-current characteristic, the beam irradiation causes a current signal δI_q.

Correspondingly, a voltage signal δV_q results for current-biased operation. To increase sensitivity it is convenient to modulate the beam and to measure the modulated response signal using a lock-in amplifier. A more detailed description of the electronic principles for signal detection in LTSEM of superconducting tunnel junctions can be found elsewhere. [4]

LTSEM can deliver a very large radiation dose in short times: a few minutes irradiation leads to a few tens MRad exposure. The effects of irradiation can be divided into:

- changes of superconductor properties, e.g. drift of T_c;

- destruction of the oxide barrier.

In the first studies described below, we expect that the dominating effect is due to possible changes of the tunneling barrier under particle irradiation, since it is a highly delicate object with a thickness of only a few atomic layers. Further, the tunneling rate depends exponentially upon the height and width of the barrier potential. This argues against the use of STJ as radiation-hard devices, but the experimental results show, to our surprise, that device withstand well radiation of up to 50 MRad.

For investigating possible changes in the tunneling conductance due to the electron beam irradiation, the electron

beam was scanned over the tunnel junction for an extended period. After time intervals of about 1-5 min the beam was turned off and the tunneling characteristic was measured, repeating this procedure many times. In these experiments the total area scanned was about 9 times larger than the tunneling window, the latter being in the center of the scanned area. The He-bath temperature was 4.2 K. Holding the beam voltage constant at 25 or 26 kV, the beam current was kept small in the beginning (typically 30 - 100 pA) and subsequently was raised gradually (up to about 1 nA) until no appreciable changes in the tunneling conductance could be observed.

Typical results are presented in Figs. 3-5, and show the tunneling conductivity in the normal state versus the number of beam electrons which have struck the tunneling window. (This number was calculated from the irradiation time, the beam current, and the fractional portion of the total scanned area taken up by the tunneling window of $28.3 \times 28.3 \ \mu m^2$ area. At the top of Fig. 3 and 4 the different values of the beam current and the corresponding irradiation times are indicated). In Figs. 3-5 the tunneling conductivity is normalized to the conductivity at the beginning of the particular irradiation run. The latter conductivity values are indicated in the figure legends.

Figure 3 refers to the first irradiation of tunnel junction 2/6/I. The normal conductivity is seen to initially increase during the irradiation to pass through a maximum and then to

approach gradually a conductivity value smaller than that at the beginning. A similar result has been observed in a second irradiation run with the same tunnel junction, if the junction has been warmed to room temperature between runs (see Fig. 4. Between the first and second irradiations the junction was held at room temperature for 3 - 4 days). If the junction was maintained below 77 K between two subsequent irradiations, the second irradiation generally effected a monotonic increase of the tunneling conductivity. Typical results are shown in Fig. 5 for such a case.

The fact that appreciable changes of the tunneling conductivity do not occur below the irradiation level of about 10^9 electrons striking the area of the tunneling window represents an important result of our measurements. With a window area of 812 μm^2 and beam energy of 26 keV, this threshold level corresponds to an energy deposited per window area of about 26 . 10^9 eV/μm^2. From this relatively large energy value per area of the tunneling window we conclude that the stability of the tunneling barrier does not appear to represent a serious problem for usual particle detector applications. Actually, a proper operation seems possible after irradiation with 50 MRad, i.e. more than one order improvement in radiation-hardness when compared with semiconducting devices.

In this first series of studies using the LTSEM, the electron energy (E_e = 25 keV) was chosen so that they cross the

oxide barrier and are absorbed in the bottom electrode. To test the influence of irradiation on superconducting properties, the ARC/TU collaboration is performing a second series of tests with lower electron energy such that the electrons are stopped in the top layer of STJ and the effects of the oxide barrier can be neglected. We expect that in this situation, the tunnel junction will be radiation-hard to a few hundreds MRad. We hope to include the preliminary results of these measurements in Phase-II proposal.

The second type of study of radiation-hardness of superconducting detectors was performed by ARC/UBC collaboration using superheated superconducting colloid. The SSCD properties were measured before and after about 10 MRad irradiation with high energy γ-photons from a radioactive source ("Cobalt-bomb"). The SSCD preparation is described in Appendix 2, and SQUID-based readout electronics in Appendix 3. In this appendix we provide only the data concerning the radiation-hardness of SSCD.

Figure 6 shows that after 8.5 MRad irradiation, SSCD functions correctly as γ-ray detector. Each one of the steps is due to a change of state of a single (R $\approx$ 5 μm) grain absorbing a single photon from Tc^{99m} radioactive source. Please note the excellent singal to noise ratio, S/N $\geq$ 20, even for this relatively small grains in low magnetic field (H $\approx$ 93G $\ll$ $H_{sh} \approx 400G$). The preliminary estimates show that the QDE of SSCD is the same before and after 8.5 MRad irradiation.

The enclosed hysteresis curves (see Fig. 7 a/b and 8 a/b) show that irradiations of 8.5 MRad do not influence the width of transition. This is confirmed by measurements of single grain flips due to γ's from a Tc^{99m} radioactive source. We continue this study and hope to present in the Phase-II proposal the results for SSCD irradiated to about 50 MRad.

References

1) R. P. Huebener, Rep. Prog. Phys. 47, 175 (1984).

2) R. P. Huebener, Advances in Electronics and Electron Physics, P. W. Hawkes, ed., Vol 70, 1987.

3) J. Bosch, R. Gross, and R. P. Huebener, Josephson Effect-Achievements and Trends, A. Barone, ed., World Scientific, 1986, p. 174.

4) R. Gross, Thesis, University of Tubingen (1987)

   R. Gross, R. P. Huebener, and U. Klaβ, "Electron-Beam Irradiation of Josephson Tunnel Junctions" to be published in Proc. Workshop on Superconducting Particle Detectors" Torino, Oct. 26-29, 1987 ed. A. Barone.

| Sample No. | Thickness [nm] | | Oxidation Time [h] | $\sigma_n [\frac{1}{\Omega \cdot cm^2}]$ | $\frac{\sigma_n}{\sigma_{SG}}$ |
	Base Electrode	Top Electrode			
1/I	280	320	16 (at 670 HPa)	$6.3 \cdot 10^4$	8.0
1/II				$1.0 \cdot 10^4$	7.5
2/I	212	511	18	$5.7 \cdot 10^4$	2
2/II				$2.9 \cdot 10^4$	7.4
4/I	200	668	14	$7.2 \cdot 10^4$	8.0
4/II				$1.1 \cdot 10^5$	8.6
1/6/I	190	590	15	$3.2 \cdot 10^4$	6.4
1/6/II				$1.0 \cdot 10^5$	4.4
2/6/I				$1.6 \cdot 10^4$	6.4
2/6/II				$2.2 \cdot 10^4$	6.2

Table 1: Sample characteristics. σ_n is the normal tunneling conductivity. σ_{SG} is the sub-gap tunneling conductivity.

Fig.1

Tunnel-Area

Top-Electrode

SiO-Window

Base-Electrode

(a)

Oxide Layer

Top-Electrode

SiO-Window

Base-Electrode

Sapphire

(b)
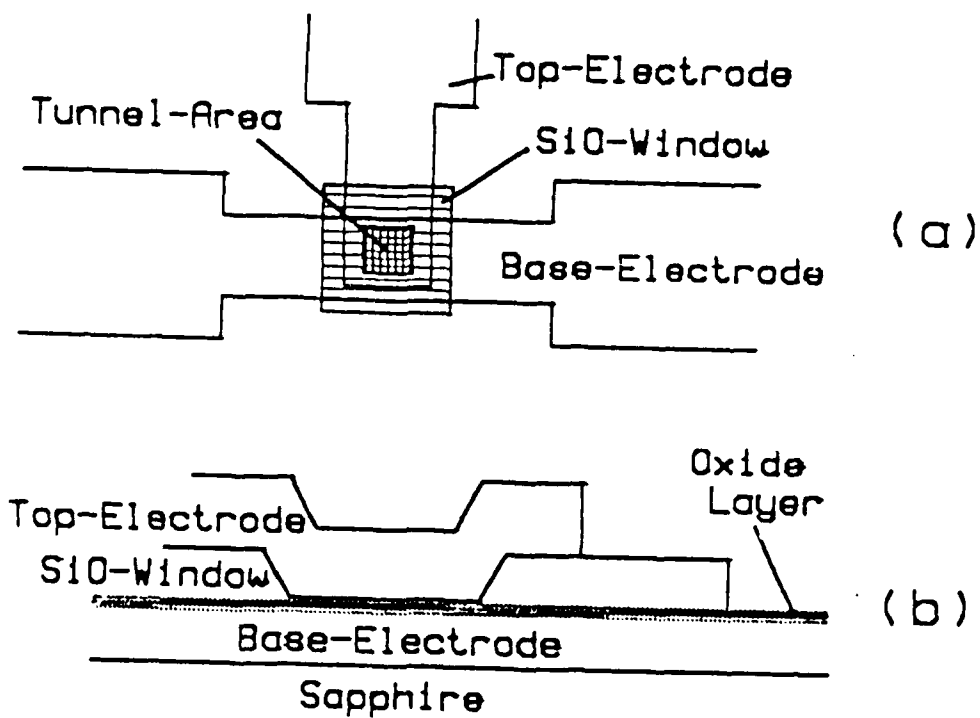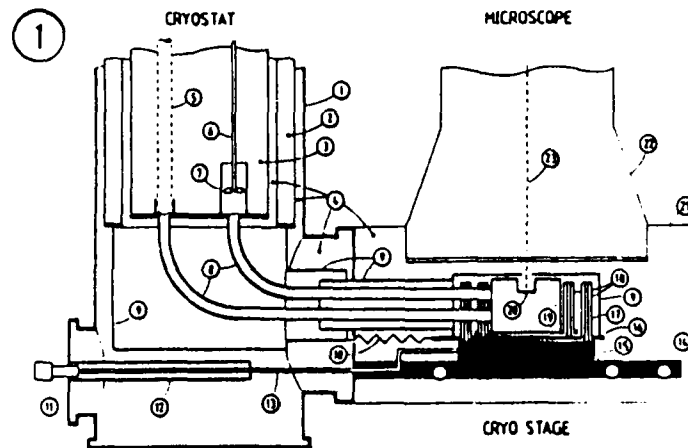
Principle of the low-temperature stage.
(1) outer vacuum case, (2) LN_2-reservoir, (3)
LHe-reservoir, (4) vacuum space, (5) position of
LHe-transfer siphon, (6) driving shaft, (7) circu-
lation pump, (8) LHe-transfer tubes with bellows,
(9)LN_2-shield, (10) flexible thermal coupling
(copper ribbon), (11) shift control, micrometer
screw, (12) mechanical vacuum feedthrough with
bellows, (13) push rod, (14) microscope mounting
plate, (15) x-y micropositioning stage, (16)LN_2-
base plate, (17)LHe-base plate, (18) thermally
isolating spacers, (19) LHe-tank, (20) sample,
(21) microscope chamber, (22) microscope column,
(23) electron beam (from Ref. 18)
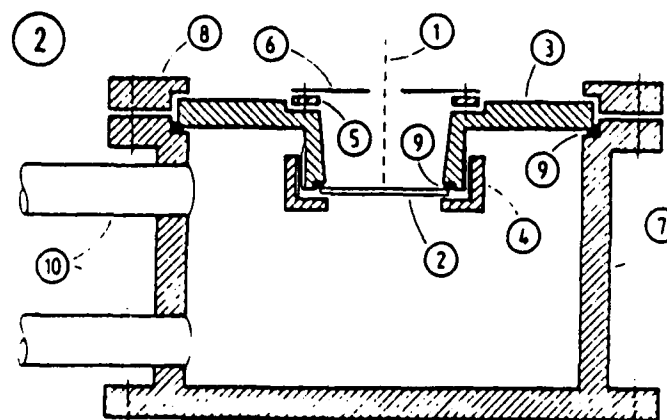
Sample mounting. (1) electron beam, (2)
sample, (3) sample holder, (4) clamping screw,
(5) copper ring for wire heat sinking, (6) ther-
mal shield, (7) LHe-tank, (8) clamping ring, (9)
indium seal, (10) LHe-tubes (from Ref. 18)
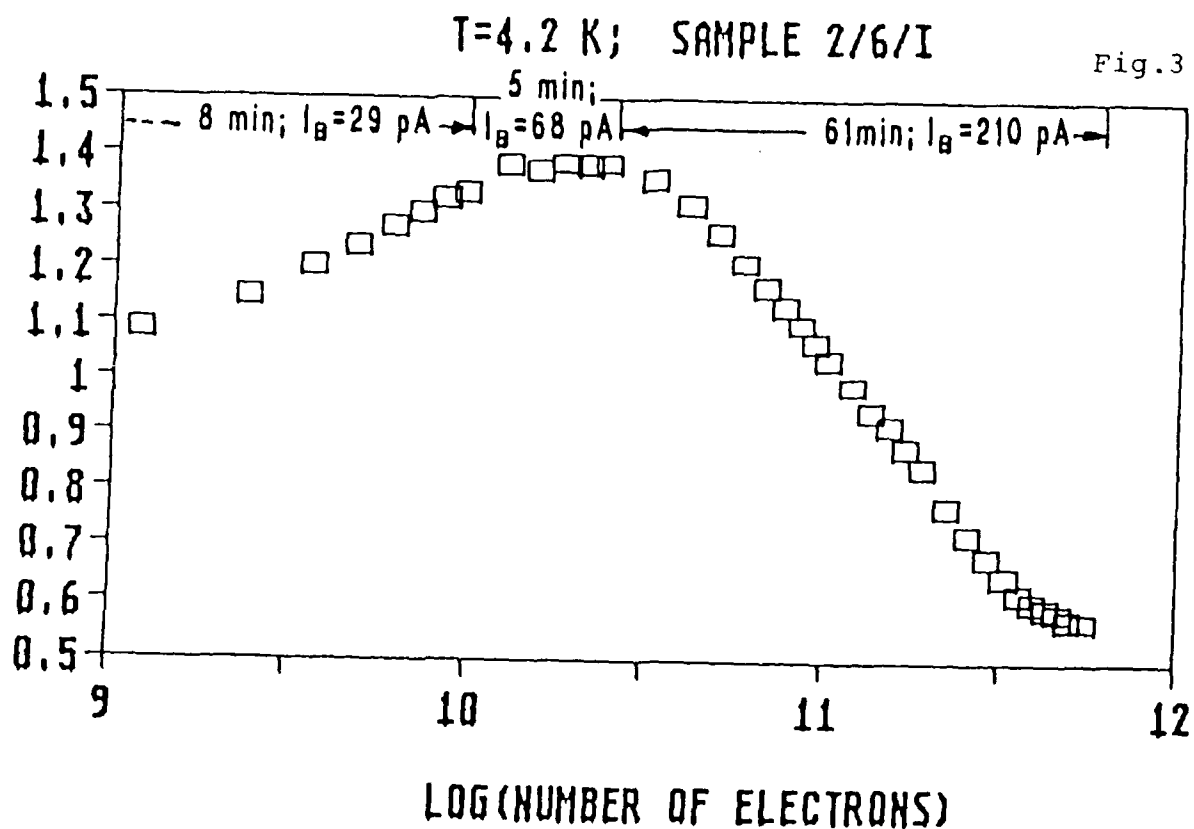
T=4.2 K; SAMPLE 2/6/I

Fig.3

Plot with y-axis "NORMAL CONDUCTIVITY/CONDUCTIVITY(B)" ranging from 0.5 to 1.5, and x-axis "LOG(NUMBER OF ELECTRONS)" from 9 to 12. Annotations: 8 min; I_B=29 pA →|← 5 min; I_B=68 pA →|← 61min; I_B=210 pA →

T=4.2 K; SAMPLE 2/6/I

Fig.4

Plot with y-axis "NORMAL CONDUCTIVITY/CONDUCTIVITY(B)" ranging from 0.7 to 1.3, and x-axis "LOG(NUMBER OF ELECTRONS)" from 9 to 12. Annotations: 14 min; 112 pA →|← 52 min; 184 pA →|← 22 min; 840 pA
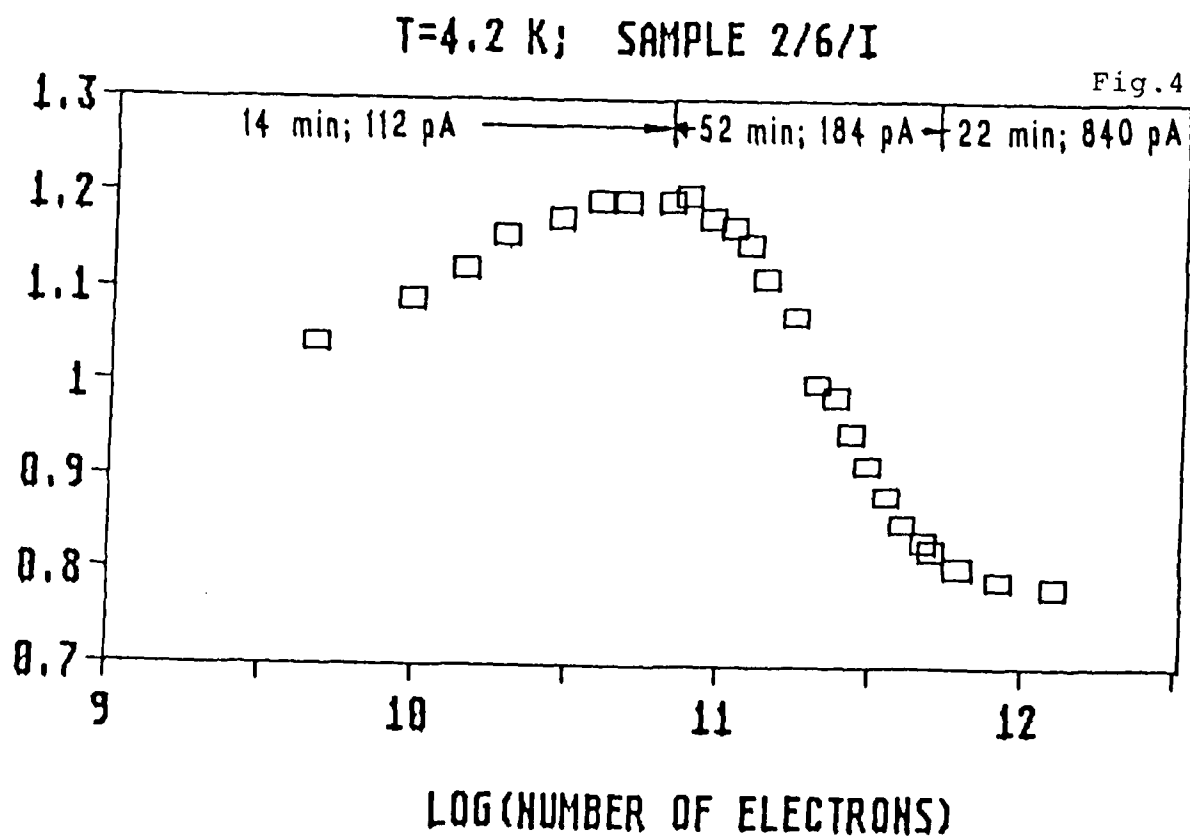
T=4.2 K; SAMPLE 4/I

Fig.5
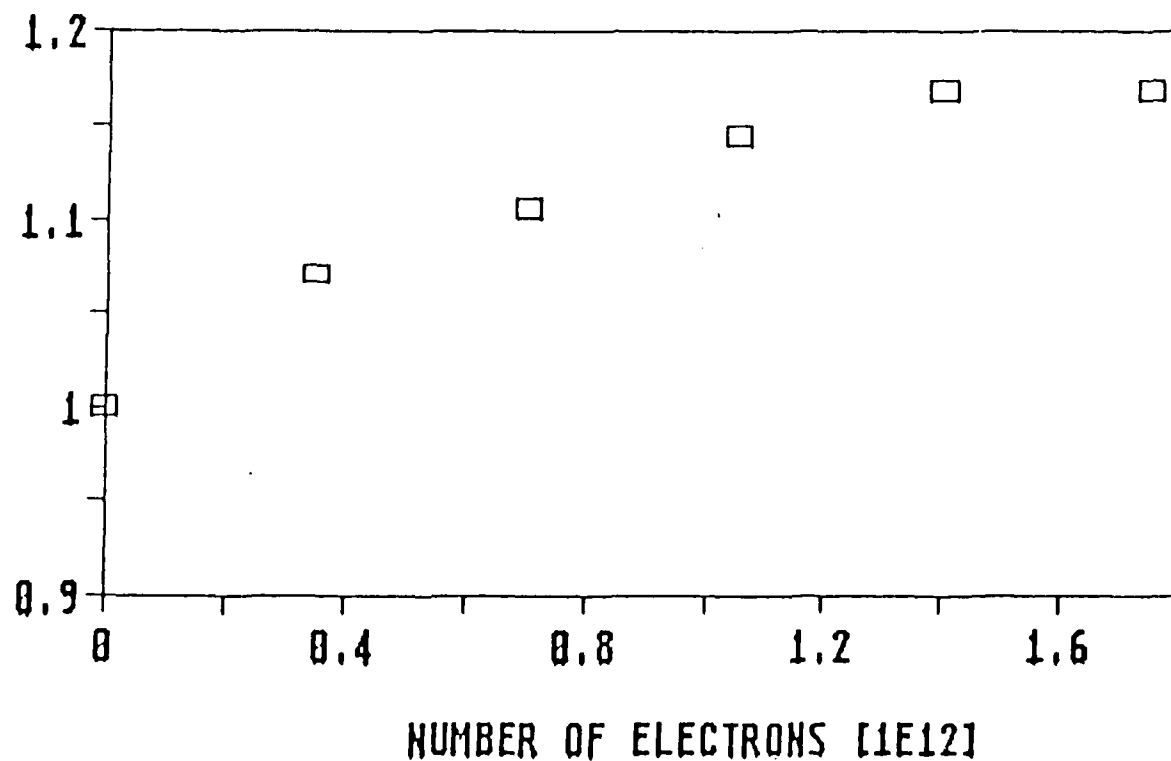
RUN # 57₆ : B = 93 gauss

March 9, 1988, 17:25

Fig.6
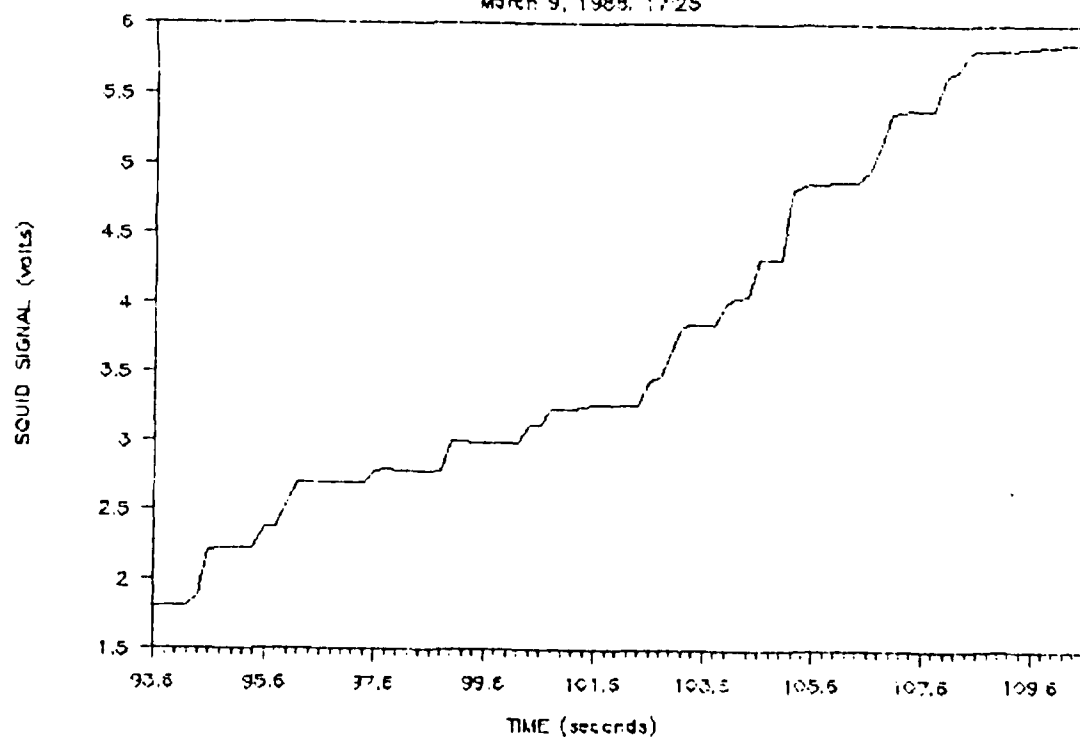
HYSTERESIS 20 : B = 63 gauss

Feb. 22, 1988; 8:33 pm

Fig.7
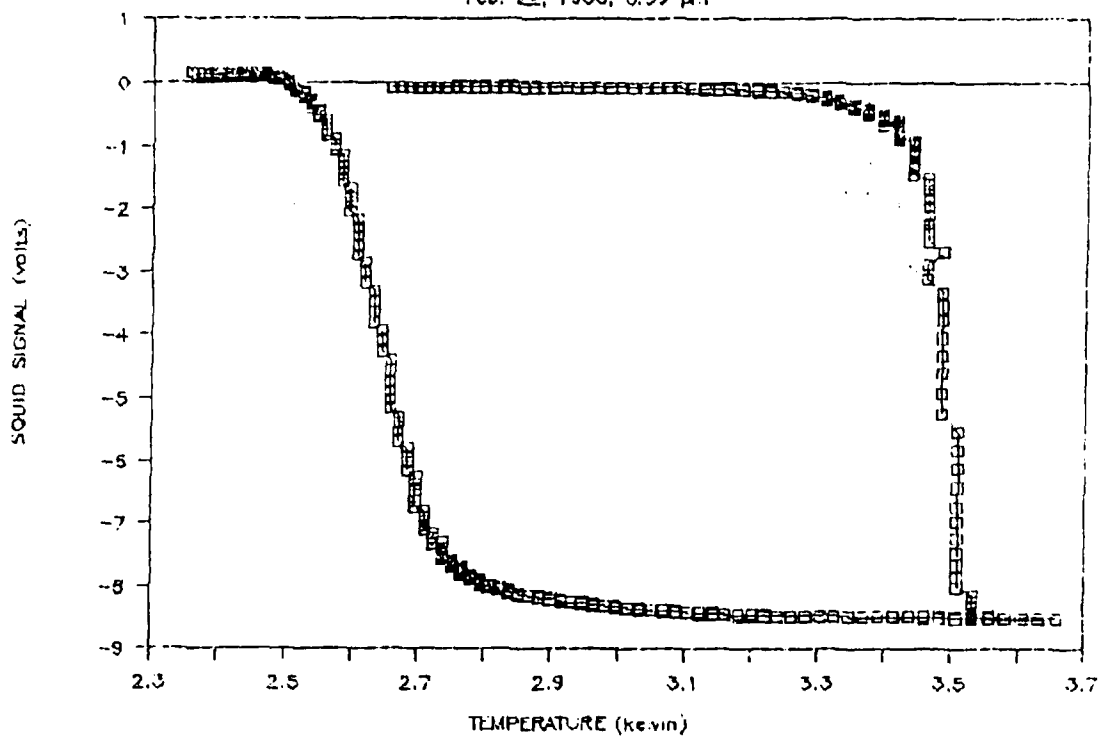
Before irradiation

HYSTERESIS 41 : B = 63 gauss

Mar. 8, 1988; 16:55
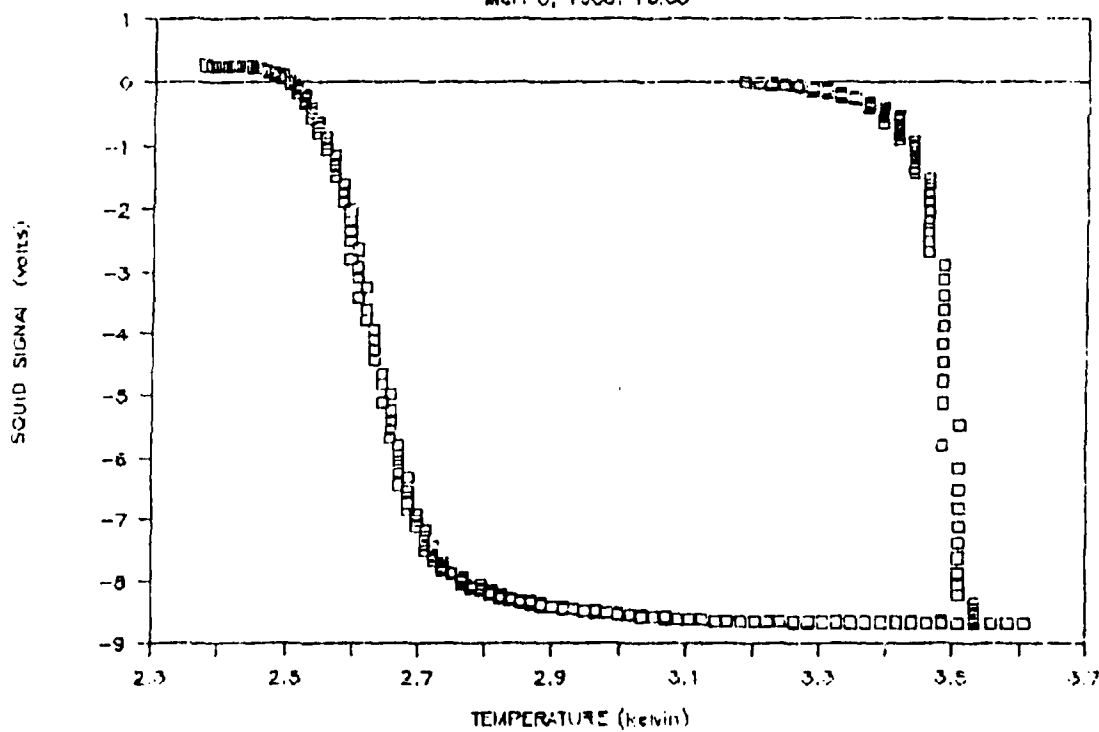
After 8.5 MRad irradiation

HYSTERESIS 27 : B = 93 gauss

Feb. 23, 1988; 13:25

Fig.8
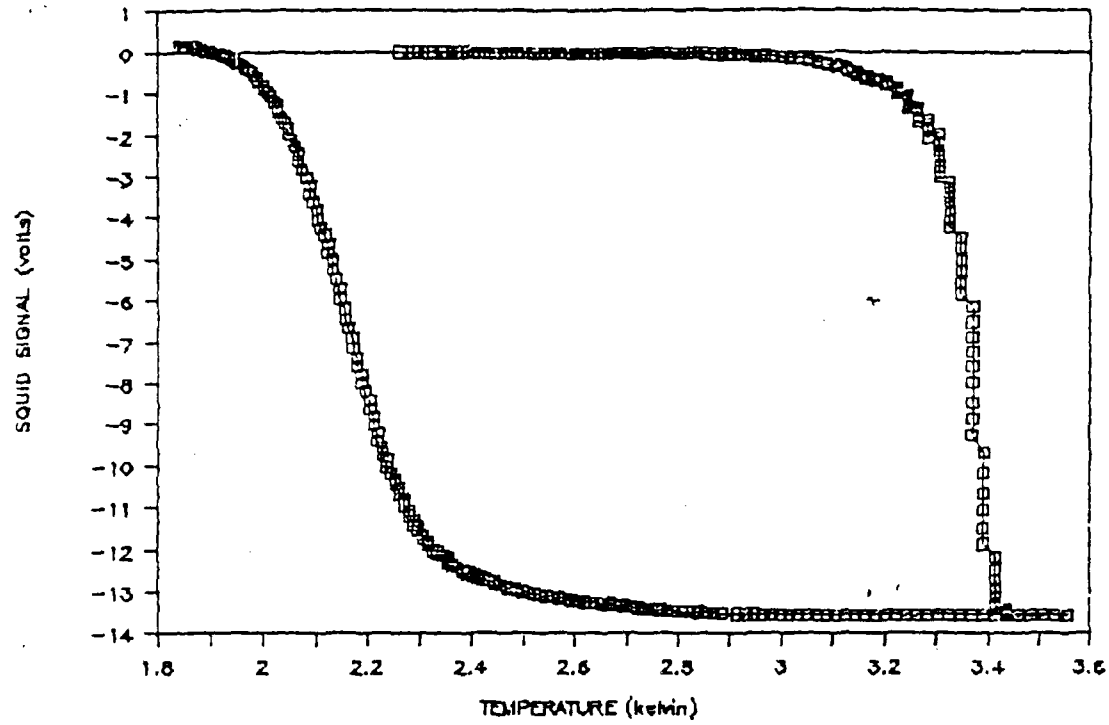
Before irradiation

HYSTERESIS 43 : B = 93 gauss

Mar. 8, 1988; 17:21
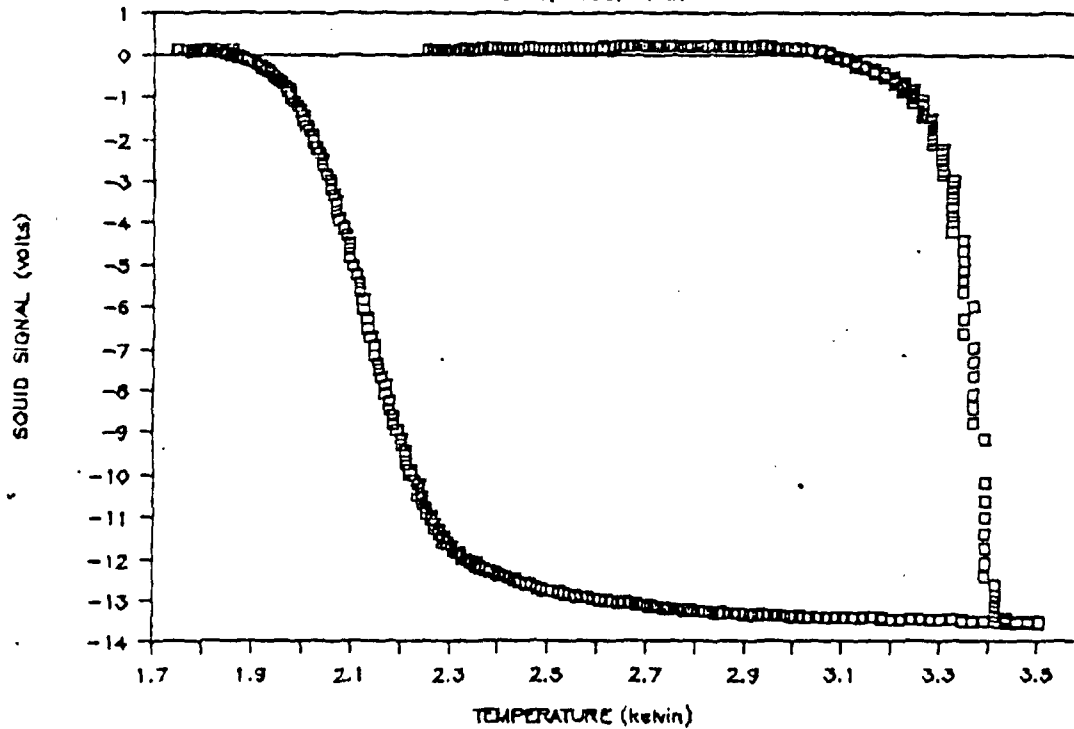
After 8.5 Mrad irradiation

Appendix 2:

Preparation of the Superheating Colloid

The preparation of the SSCD material consists of the following steps:

a) Grain production;
b) Grain selection according to size;
c) Dispersion in appropriate dielectric.

Spherical grains of an appropriate size ($5 \leq \phi \leq 30$ μm) were produced from diverse low melting point materials e.g. Hg, In, Sn, Sn + 1% Sb, Pb + 1% In and Pb. The two most successful methods were:

- ultrasound disintegration;
- capillary wave disintegration.

A third, "ink jet", method looks very promisirg but has not been tested with superconducting metals.

In ARC, we have operational a set-up in which grains are produced by ultrasonic disintegration of melted tin. Tin is placed in silicon oil and melted; a strong ultrasound source breaks it into tiny droplets. The surface forces close grains into spheres. The advantage of this method is the simplicity and commercial availability of the required ultrasound sources; the method is reasonably efficient and we can process about one kilogram of Sn per week. Furthermore, very small grains ($\phi \leq 5$ μm) can be readily produced which are of importance in some applications, e.g. in X-ray detection. The disadvantage is that the process of grain cooling is rather fast, which leads to creation of polycrystalline structures (see enclosed electron-microscopy of a produced grain). Some improvement of grain quality is observed (K. Pretzel et al., private information) when the alloy Sn + 1% Sb is used. Furthermore, it is possible to remelt the grains by flow in a sedimentation column filled with silicone oil, wherein a fraction of the liquid is heated over the melting point of the metal.

Grains of excellent sphericity and reasonable surface smoothness have been produced commercially by Extramet Cie, Geneva, Switzerland. (see (Photo 1) The proprietary process involves creation of ultrasonic standing waves in a pool of melted metal supported on a piezeoelectric crystal. This process of "capillary wave" disintegration is used in many applications e.g. home humidifiers. However, appropriate temperature of melt, piezoelectric, and frequency are required to obtain spherical grains. We obtained from Extramet two samples (each ca. 100g) of grains with sires of $15 \leq \phi \leq 25$ μm and $25 \leq \phi \leq 40$ μm, respectively. According to a recent test at CERN (D. Perret-Galix et al., private information), these large grains are

better than those of the same size produced by ultrasound disintegration. Extramet is working on the production of smaller ($\phi \leq 5$ μm) grains.

Almost perfect but very large ($100 \leq \phi \leq 400$ μm) grains wer produced by Billeton et Cie, Nanterre, France. Superheating was observed in such $\phi \approx 400$ μm grains, an unprecedent achievement showing that the grain surface is almost perfectly even for these macroscopic objects (please remember that the existence of defects destroys metastability).

Some effort of the ARC team was in the selection of grains according to size. After production, the grains were removed from the silicon oil and cleaned in pure (99.9%) trichloroethylene. For selecting the grains, we used:

- filtration by calibrated meshes;
- sedimentation in liquids.

We used old wire-wrapped sieves with nominal diameters of 50, 45, 40, 36, 28, and 25 microns. Furthermore, we have Microplate Test Sieves from Endecotts Ltd., England, with diameters of 20, 15, 10, and 5.0 microns. Recently, we were informed that Microplate Test Sieves of 12.5 and 7.5 microns can be custom made. We discovered that the filtration of small diameter grains requires that the process takes place in the ultrasonically-agitated liquid. We used a mixture of mineral oil and trichloroethylene. A small amount (< 50 cc) of grains suspended in trichloroethylene was placed inside the filter and immersed in about 500 cc of trichloroethylene which was constantly agitated by an ultrasonic cleaner. Typically, the filtering takes about 10 minutes and is repeated about ten times. The results of filtering by wire-wrapped sieves are shown in Fig. 1 and Table 1. One observes that relatively good size selection ($\Delta R/R \approx \pm 5\%$) has been achieved. Furthermore, contamination with small grains is less than 5%. About 5 grams of grains per fraction is available.

To select grains with $\phi < 25$ microns we used both filtration and sedimentation. The sedimentation liquid was 75% trichloroethylene + 25% mineral oil (by volume). The sedimentation column is about 1.5 m long and for each run 20 different fractions were obtained. The sedimentation time is strongly dependent on the grains' size (see Tab. 2).

Typically, the grains were first filtered, then sedimentated and then once more filtered. Usually, the first few fractions and the last fractions were removed (fractions F1-4 and F19-20 in our example). Further filtering removes the small/big grain contamination (see Fig. 2a/b).

The properties of the selected grains are given in Fig. 3. It should be noted that the number of slightly oval (less than 10% deviation from sphere) increases but there are practically no irregular grains. On the other hand, the resolution in size is worse than for big grains. It would be further improved with the

purchase of 7.5 and 12.5 μm filters, and when more than one sedimentation is performed for $\phi < 5$ μm grains.

Grain size was estimated by counting under an optical microscope. Furthermore, the UBC group developed a method in which size distribution is measured using coherent light scattering. The observed Frauenhofer rings (see Fig. 4) suggests good sphericity and reasonable size distribution. The theoretically expected (random distribution of monoradial, ideal spheres) and observed light curves are compared in Fig. 5. The size distribution measured with coherent light and using optical microscopy are in good agreement (see table 4).

Further improvement of the grain size selection is possible using centrifugation. We decided not to concentrate on this until obtaining the good grains produced by Extramet, which became available to ARC at the end of 1987. We are currently working on improved grain selection.

To test the quality of the produced grains, we measured the hysteresis curves of a SSCD consisting of R=5-10 μm grains prepared from 99.99% pure tin. In the past, these curves were studied at constant temperature with an externally applied, variable magnetic field. The availability of a RF-SQUID readout system (see Appendix 3) permits a more sensitive measurement in which the field is constant and temperature varied. The hysteresis curves at H=0.5, 31, 90 and 155 Gauss are shown in Figures 6a, b, c, and d, respectively. Notice that a large collection of more than 10^4 grains was used. We observe, especially at low field, very sharp hysteresis curves. For example, with only the geomagnetic field the width of the superheated transition is $\Delta T \approx 50$ mK, i.e. $\Delta T/T \approx 2\%$. This is a factor of three to five improvement over the hysteresis curves studied by other groups.

The above measurements are a part of a larger program in which the hysteresis curves for diverse materials (Sn, Sn + 1% Sb, In, Cd) will be experimentally studied. The dependence of the hysteresis curve on grain size and filling factor will be elucidated.

Furthermore, we are developing two methods of ordering the grain distribution. The goal is to produce a SSCD with a transition width better than 0.5%. Overall, we are confident that the preparation of an adequate quality SSCD can be achieved within the 2 year time-frame of our future development.

TABLE 1: Big Grains ($\dot{\phi} > 25$ μm)

Size *	R [μm]	V [μm³]	ΔR/R [FWHM]	Oval**	***
40 < φ < 45	22.4	4.92×10^4	11.3 %	7 %	13
36 < φ < 40	20.4	4.15×10^4	13.6 %	1 %	12
32 < φ < 36	19.0	2.90×10^4	11.0 %	5 %	16
28 < φ < 32	17.2	2.17×10^4	17.6 %	7 %	16
25 < φ < 28	16.1	1.87×10^4	11.0 %	6 %	16

*   nominal size of filter in microns
**   fraction of oval/irregular grains
*** number of filtrations

TABLE 2: Sedimentation Time vs. Grain Size

Size [μm]	Time [min]
20 < φ < 25	15
15 < φ < 20	30
10 < φ < 15	45
5 < φ < 10	90
φ < 5	180/300

TABLE 3: Small Grains ($\phi < 25$ μm)

Size [μm]	R [μm]	V [μm³]	ΔR/R[FWHM]	Oval
20 < φ < 25	11.1	6.08×10^3	12.5 %	6 %
15 < φ < 20	7.1	1.53×10^3	17.3 %	16 %
10 < φ < 15	6.3	1.26×10^3	15.0 %	25 %
5 < φ < 10	3.4	199.	25.0 %	11 %
φ < 5	2.0	43.	10. %	18 %

TABLE 4: Diameter of Grains

Fraction	Microscope	Laser
45 ≥ φ ≥ 40	44.8 ± 5.6%	46. ± 5.2%
40 ≥ φ ≥ 36	40.8 ± 6.8%	38.9 ± 4.3%
36 ≥ φ ≥ 32	36.0 ± 5.5%	36.5 ± 6.8%
32 ≥ φ ≥ 28	34.0 ± 9.8%	33.7 ± 5.8%
25 ≥ φ ≥ 20	22.2 ± 6.1%	18.0 ± 8.3%
20 ≥ φ ≥ 15	17.2 ± 8.6%	17.4 ± 8.6%

all diameters in μm
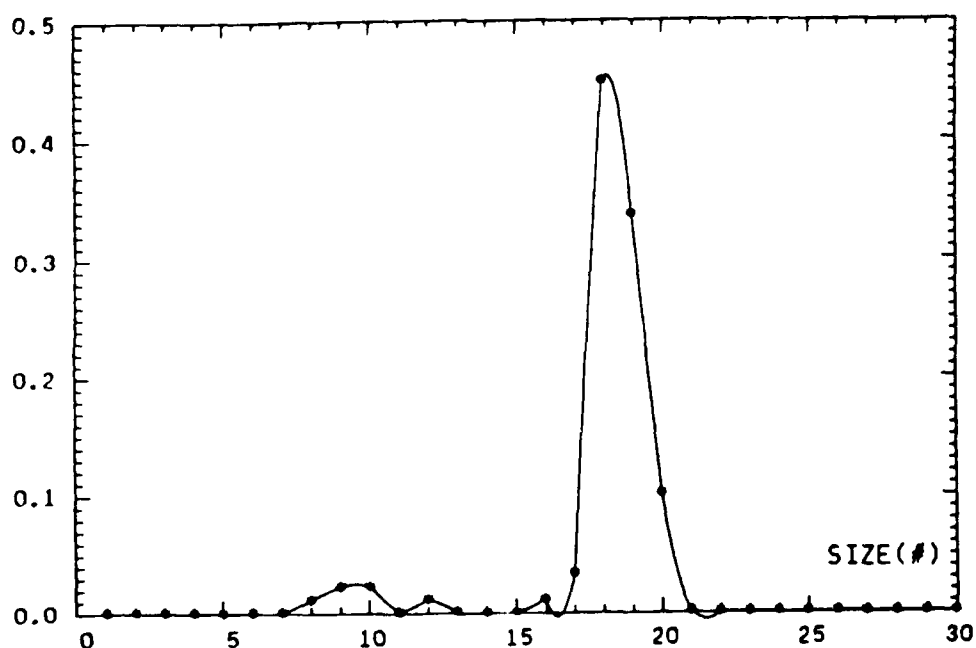
SIZE DISTRIBUTION N(%):40>D>45 MICRONS

SCALE : 1 # = 2.5 MICRONS

FIG. 1A
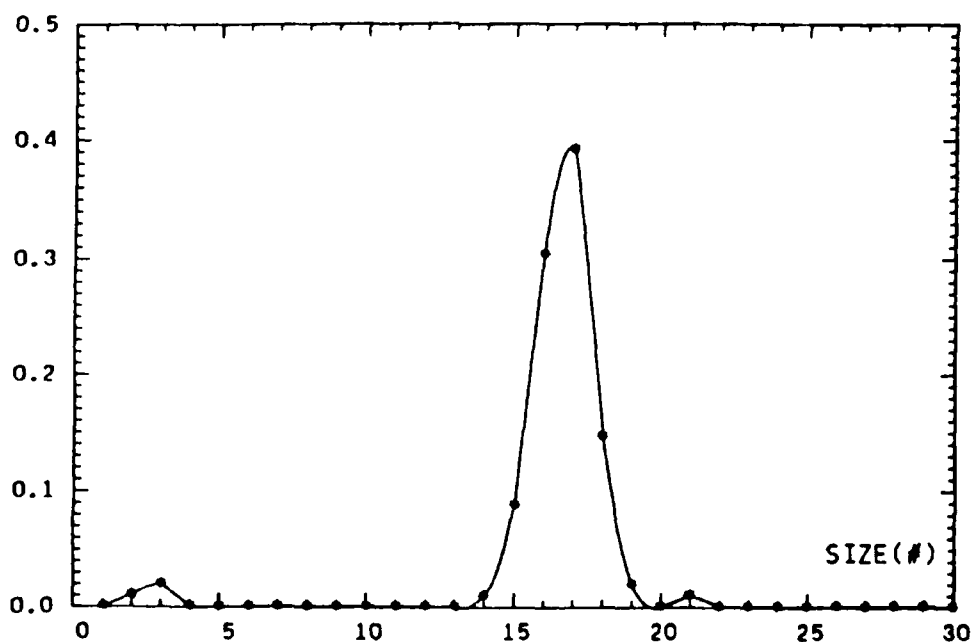
SIZE DISTRIBUTION N(%):36>D>40 MICRONS

SCALE : 1 # = 2.5 MICRONS

FIG.1B

A2.7
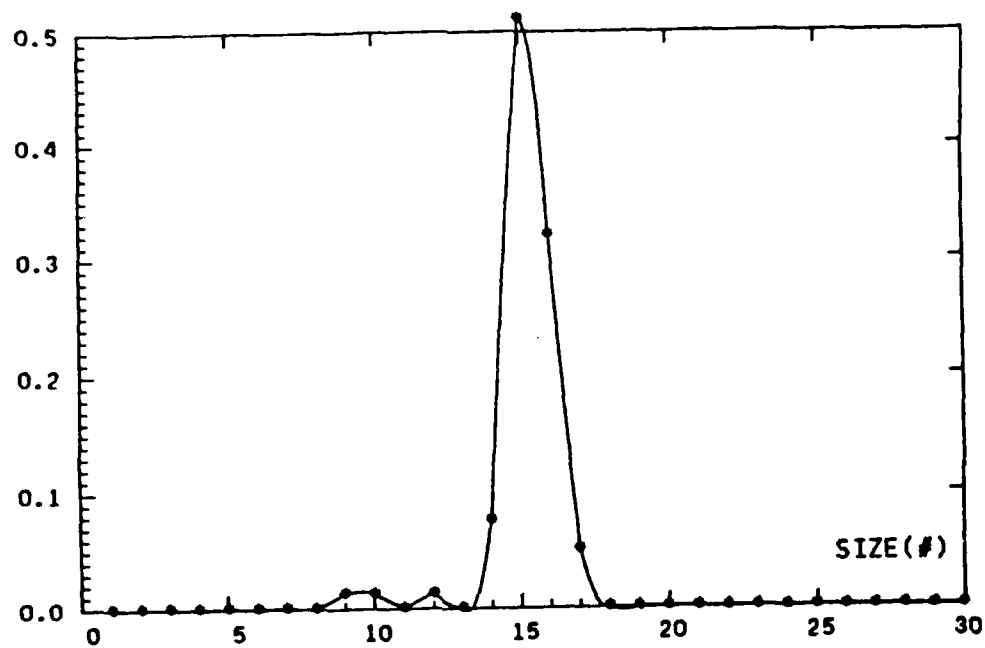
SIZE DISTRIBUTION N(%):32<D<36 MICRONS

SCALE : 1 # = 2.5 MICRONS

FIG.1C
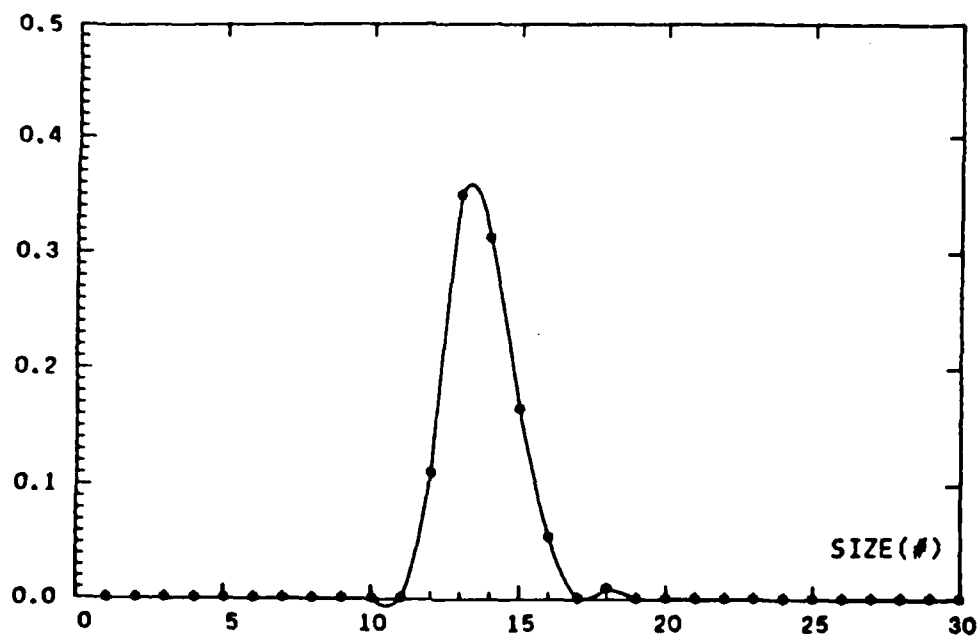
SIZE DISTRIBUTION N(%):28<D<32 MICRONS

SCALE : 1 # = 2.5 MICRONS

FIG.1 D
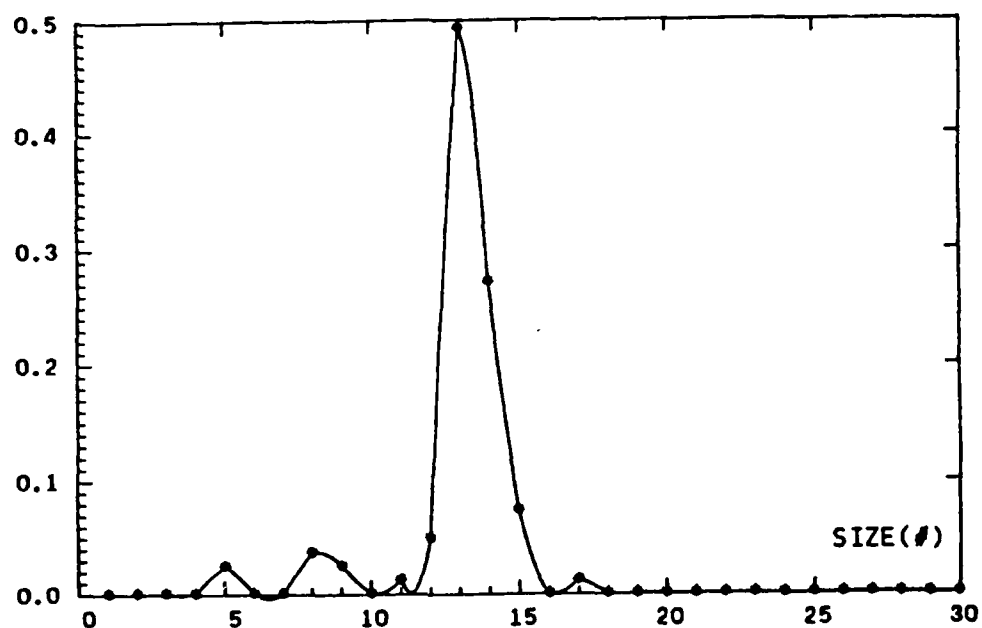
SIZE DISTRIBUTION N(%):25<D<28 MICRONS

SCALE : 1 # = 2.5 MICRONS

FIG.1E

SIZE DISTRIBUTION N(%):10<D<15 MICRONS:F7-18 ONCE

SCALE : 1 # = 1.2 MICRONS

FIG.2A

SIZE DISTRIBUTION N(%):10<D<15 MICRONS

F7-18; ONCE;FILTERED

SCALE : 1 # = 1.2 MICRONS
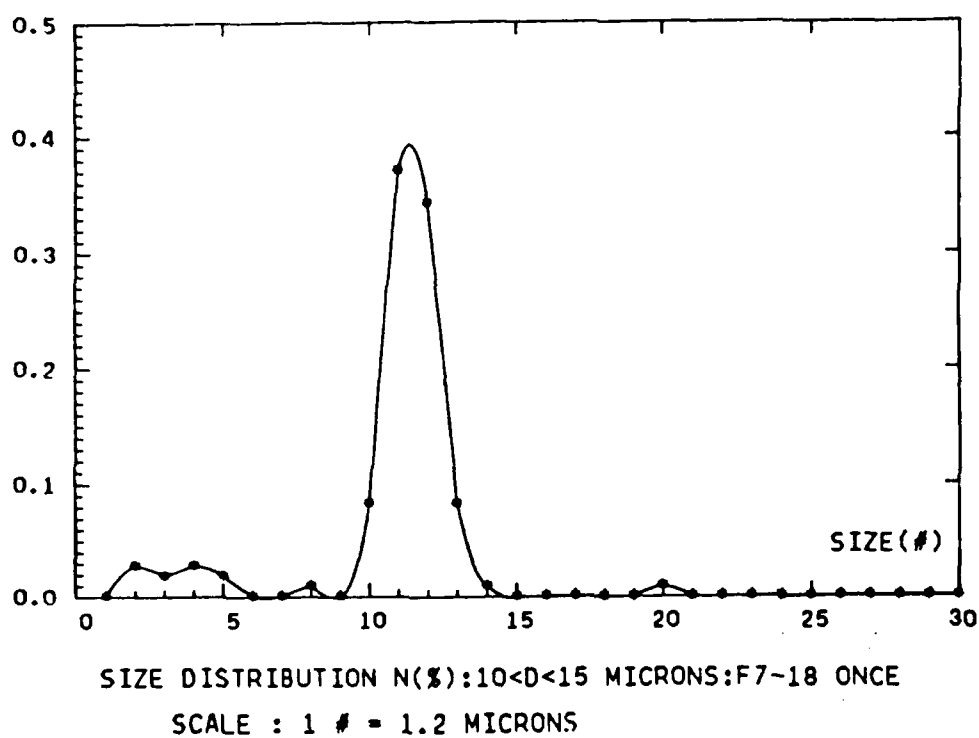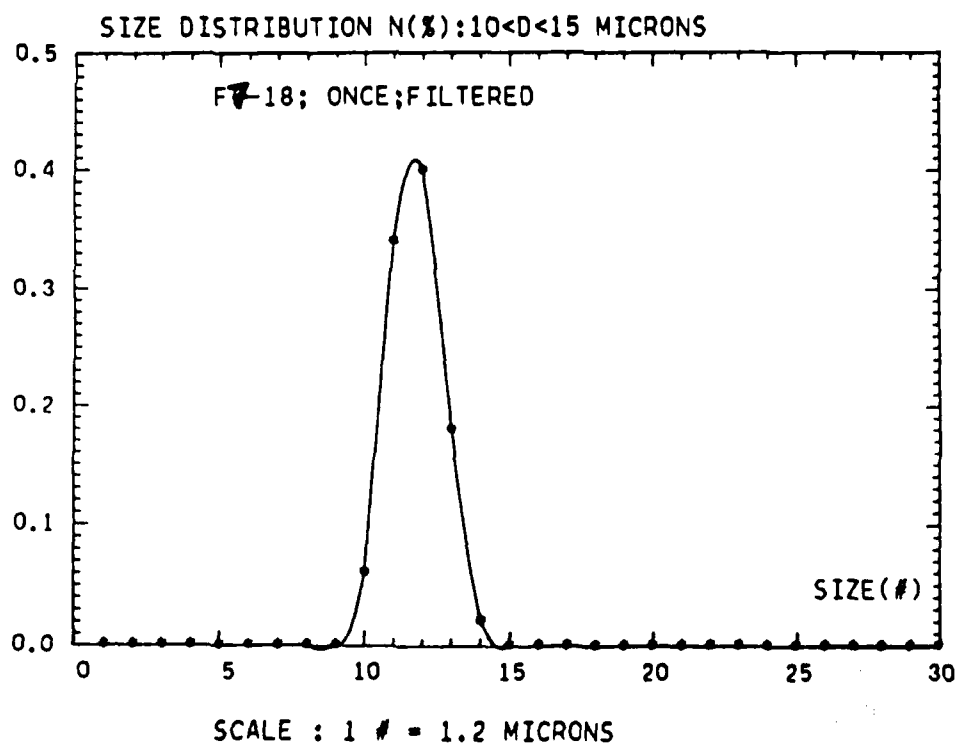
FIG.2B

SIZE DISTRIBUTION N(%): 5.<D<10. MICRONS

1ST SEDIMENTATION FILTERED

SIZE(#)

SCALE : 1 # = 1.2 MICRONS

FIG.3

SIZE DISTRIBUTION N(%): D<5. MICRONS

2ND MEDIUM

SIZE(#)

SCALE : 1 # = 1.2 MICRONS

FIG.3

SIZE DISTRIBUTION N(%):D<5 MICRONS

2ND SMALL

SIZE(#)

SCALE : 1 # = 1.2 MICRONS

FIG.3

SIZE DISTRIBUTION N(%):D<5 MICRONS

2ND VERY SMALL

SIZE(#)

SCALE : 1 # = 1.2 MICRONS
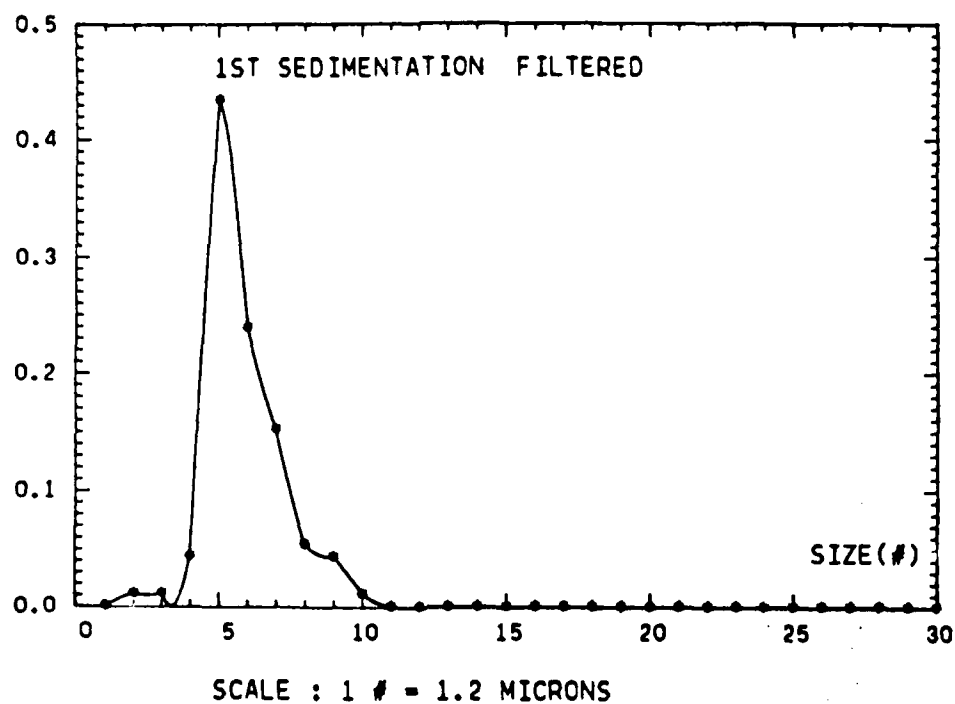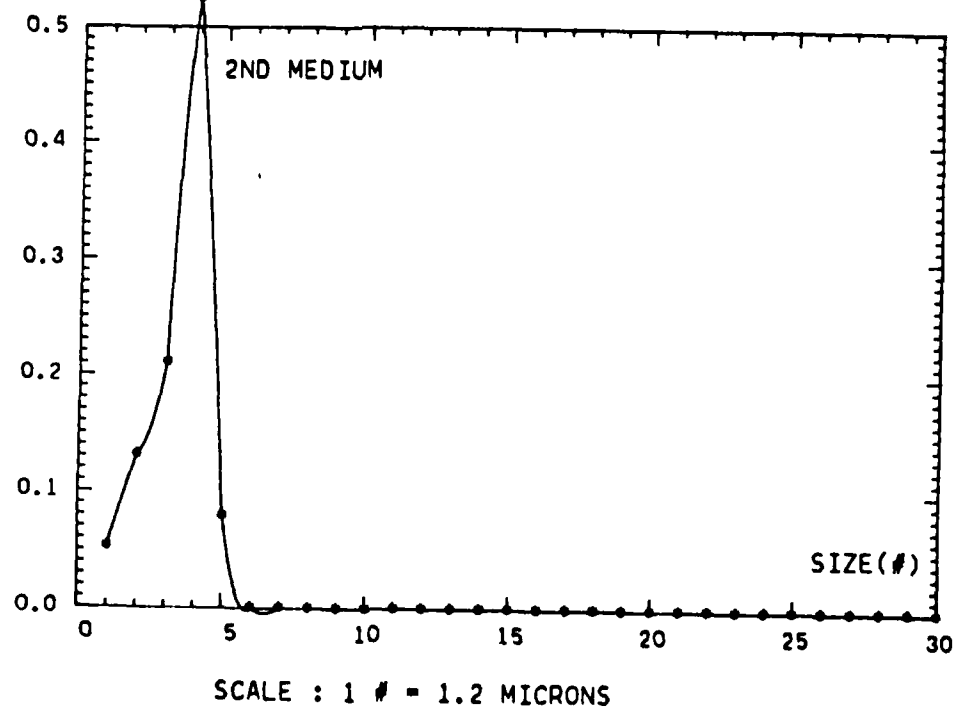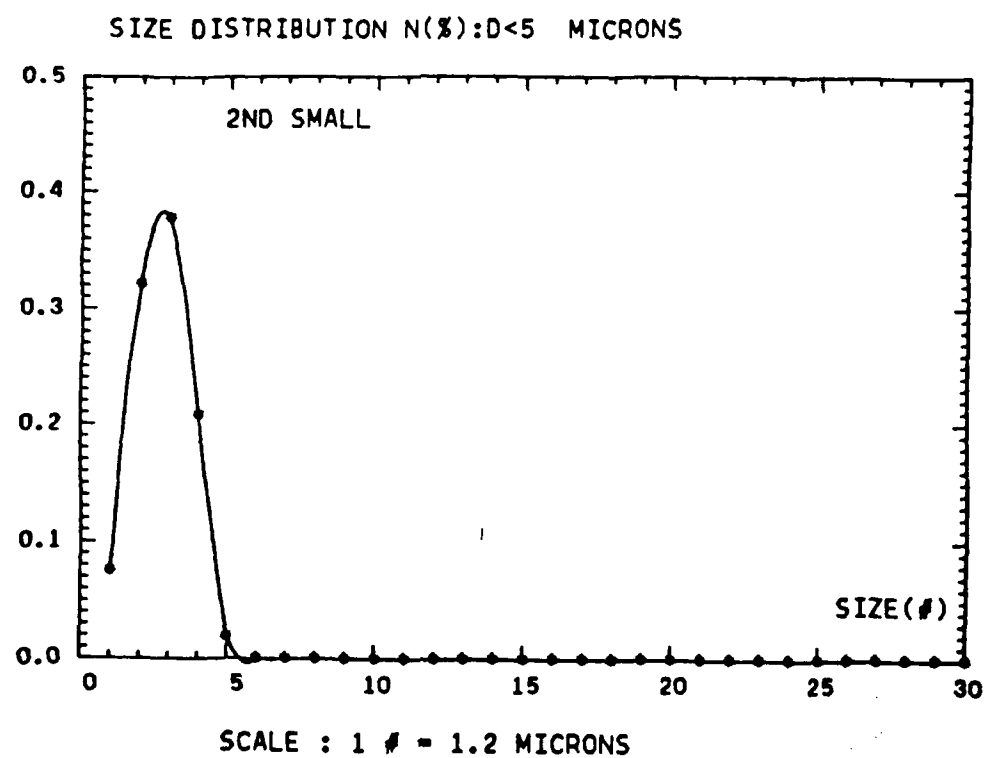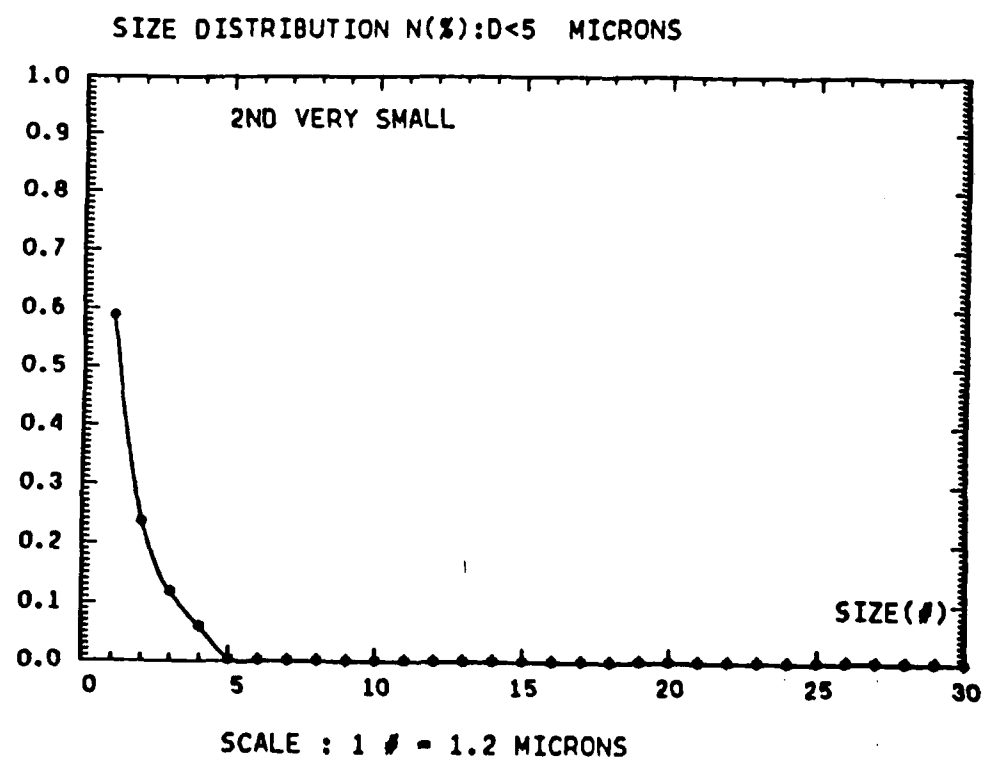
FIG.3
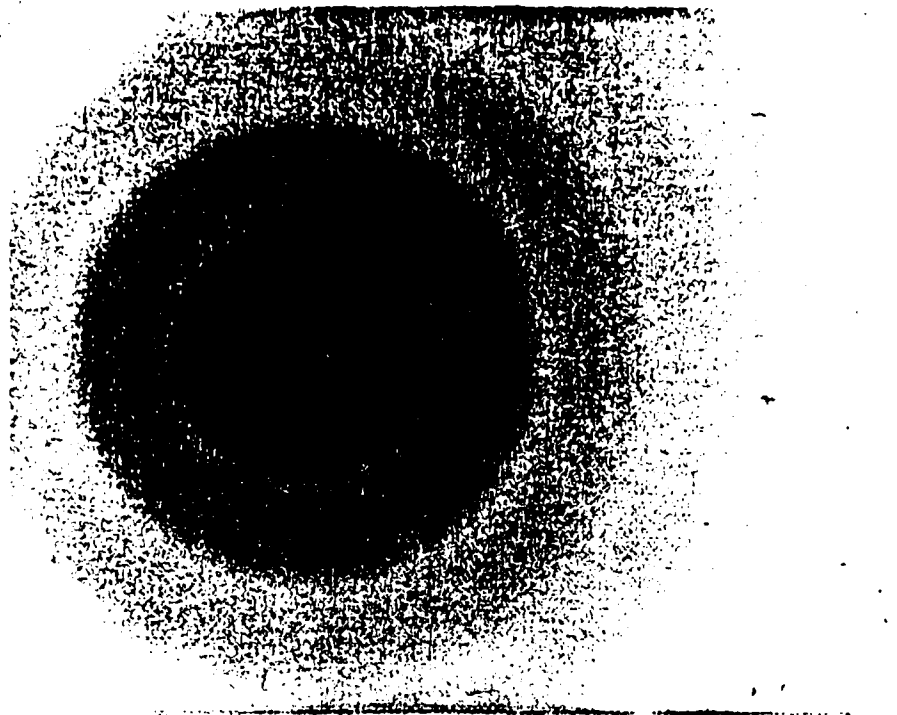
Fig.4
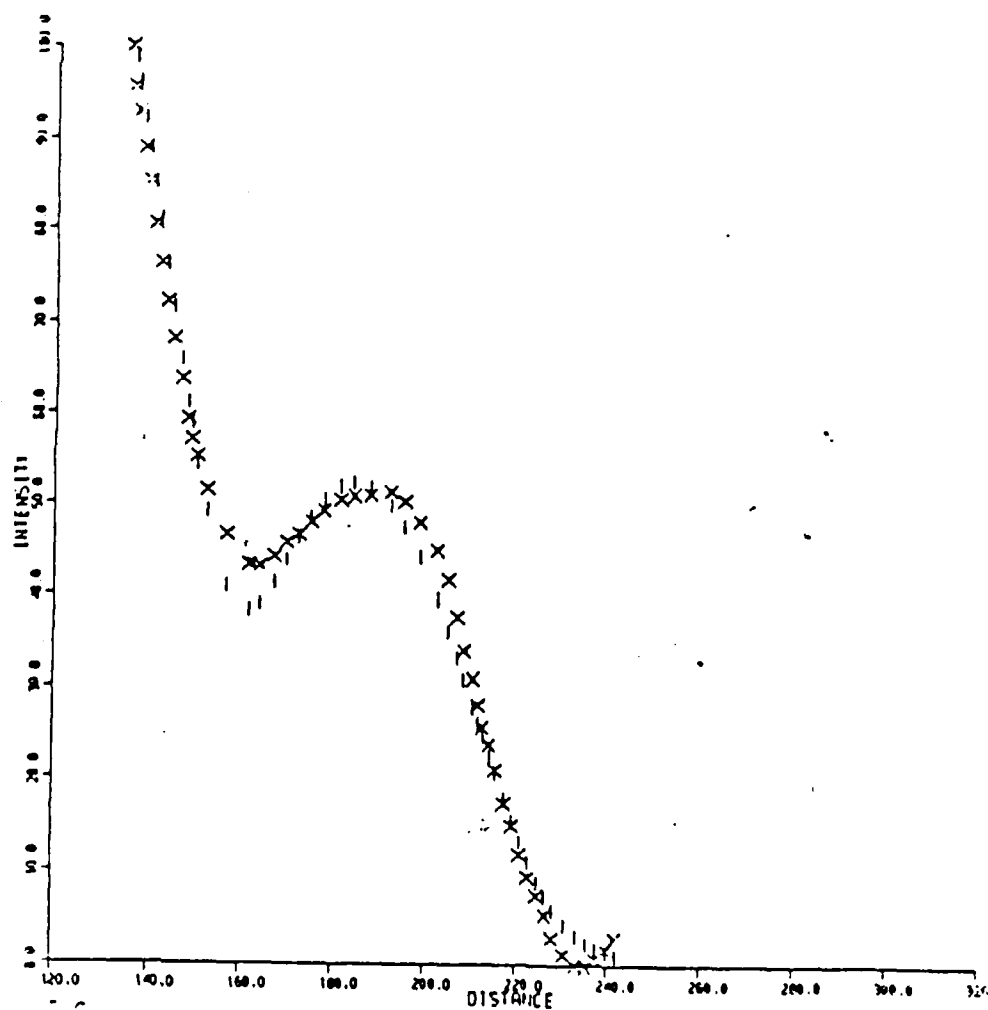
Fig.5

HISTERESIS CURVE:earth's magnetic field
February 12, 1989 (a)

Fig.6a

TEMPERATURE (Kelvin)
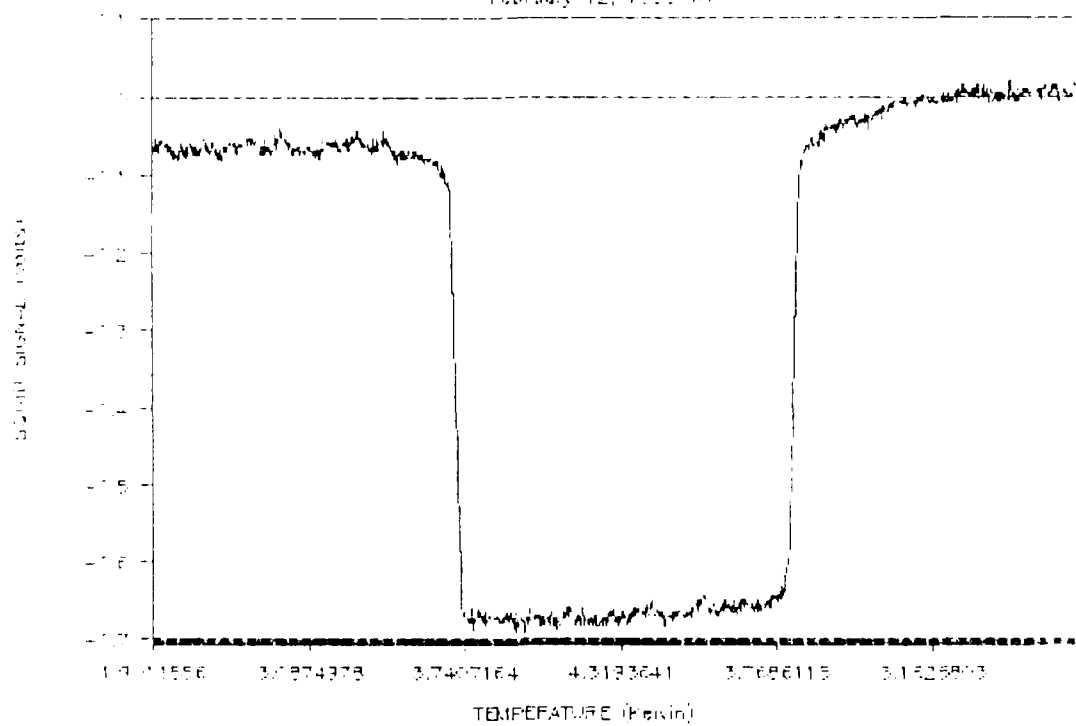
HISTERESIS CURVE : 9.3 gauss
February 12, 1989 (a)

Fig.6b

TEMPERATURE (Kelvin)

HISTERESIS CURVE : 93 gouss

February 13, 1989   (b)

Fig.6c

TEMPERATURE (Kelvin)

1.9779407 2.5579559 3.0337374 3.4603824 3.8257329 3.4603824 3.1514233 2.5814572

HISTERESIS CURVE : 93 gouss

February 12, 1989 (a)

Fig. 6d

TEMPERATURE (Kelvin)
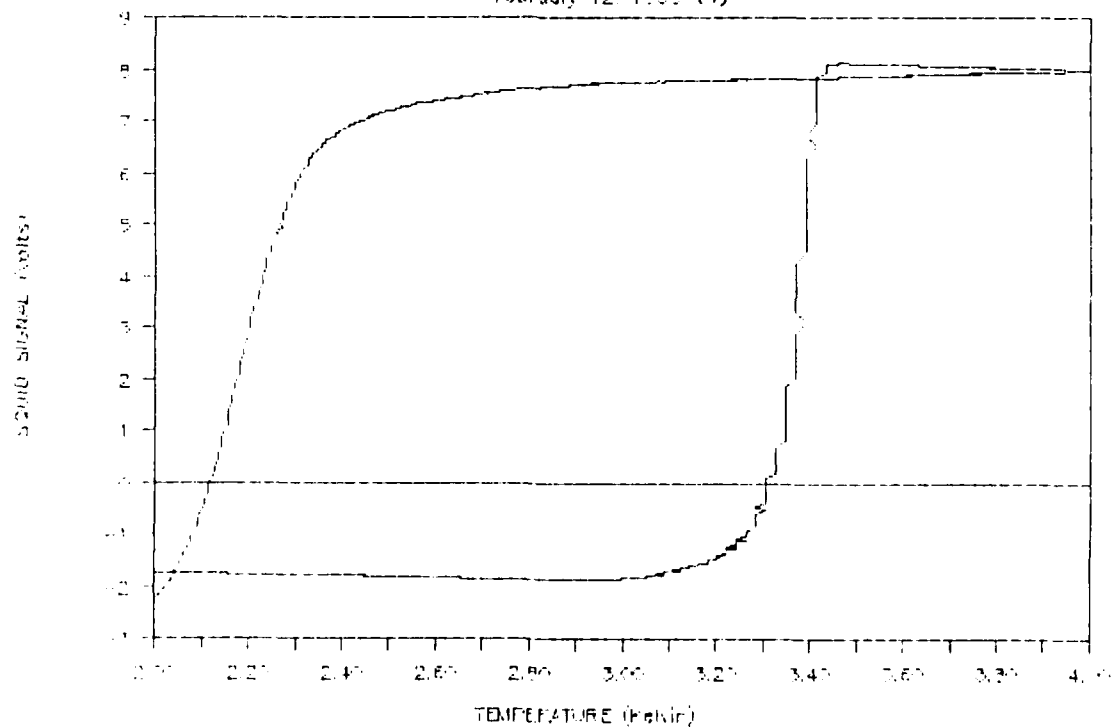
Photo. 1
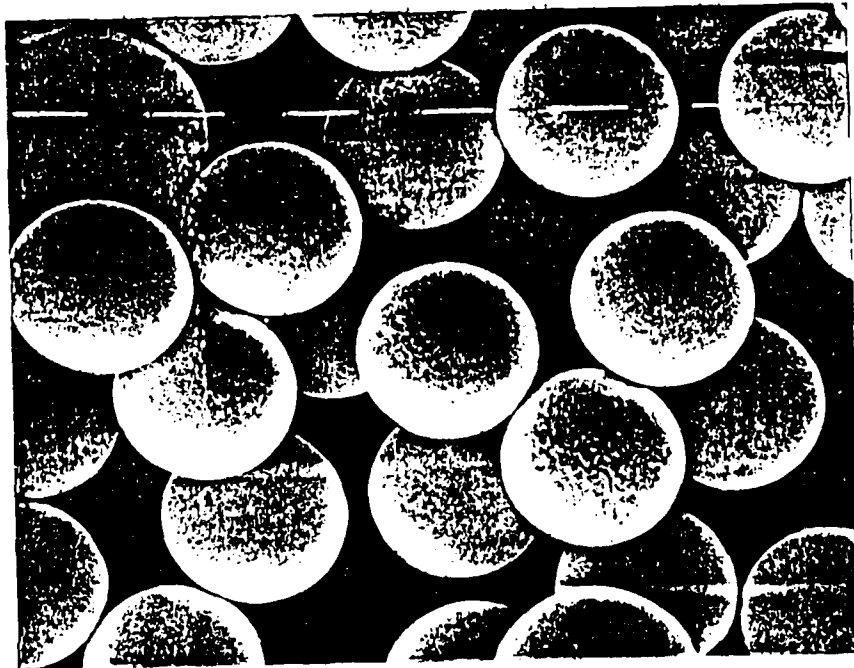
APPENDIX 3:   Improvements of RF-SQUID Readout Electronics and
                Preliminary Results of Irradiation Experiments

Technical Report of ARC/UBC, Vancouver collaboration

     In section 4.2 we pointed out that SQUID readout electronics
are potentially orders of magnitude more sensitive than fast
electronics. We also described (see sections 4.3 and 5.1) that,
at $T \geq 1.2$ K, and for minimum ionizing particles, a much better
QDE is possible for smaller ($R \leq 5$ μm) grains. At the moment,
only ultrasensitive SQUID electronics permit the detection of a
change of the state of a single, $R \leq 5$ μm grain. This is why the
development of a RF-SQUID readout appropriate for SSCD is of
major importance.

     In this Appendix we describe:

- results of a first series of UBC, Vancouver experiments;

- improvements of RF-SQUID electronics;

- preliminary irradiation tests with new electronics.

     The results of the first series of experiments were very
promising and we planned to continue the irradiation studies for
different grain sizes, using the same experimental set-up to
study the colloid quality. Installation of the improved RF-SQUID
readout was intended only in fall 1987. Unfortunately, the
failure of a 10-year old, 12 bit multichannel analyzer essential
for our data acquisition forced a change in plans. A new data
acquisition system, based on a PC-compatible 16 bit ADC, was
developed. The new system influenced almost all elements of our
experimental set-up and we opted for a thorough overhaul. The
new system and first experimental results are described in
section A3.1 and A3.2 respectively. In general, the new RF-SQUID
readout is about fifty times more sensitive than the one used in
our 1986 experiments.

A3.1   The RF-SQUID readout developed by UBC, Vancouver in 1986.

This section consists of the paper by M. Legros et al., presented at the "Workshop on Low Temperature Detectors for Neutrino/Dark Matter", Ringberg Castle, Tegernsee, May 1987.   In the following this paper is quoted as UBC, 1987.

SQUID Detection of Superheated Granules

M. Le Gros[1], B.G. Turrell[1], M.J.C. Crooks[1], A. Kotlicki[2],
and *A.K. Drukier*[3]

[1]Department of Physics, University of British Columbia,
 Vancouver, B.C., Canada, V6T A6
[2]Institute of Experimental Physics, Warsaw University, Hoza 69,
 PL-00-681 Warsaw, Poland
[3]Harvard-Smithsonian Center for Astrophysics, 80 Garden St.,
 Cambridge, MA 02138, USA

1. Abstract

We report two tests designed to study the practicality of a superheated superconducting colloid detector using a SQUID readout system. In the first test, the individual 'flips' of ten $15\mu m$ radius tin grains were observed as the temperature was swept through the superheated superconducting — normal phase transition. In the second test, we were able to observe transitions induced by 90 keV γ-rays in a colloid of 5 μm radius grains in epoxy.

2. Introduction

The last few years have seen an increasing interest in the development of low-temperature particle detectors, which include the superheated superconducting colloid detector (SSCD) [1-7], the superconducting tunnel junction [8], the crystal bolometer [9-11] and the hybrid detector [12]. Our own interest is in the SSCD, and in this paper we will discuss recent investigations performed at the University of British Columbia. Although this detector was developed for applications in high-energy physics and photon detection, it is also a promising candidate for detecting neutrinos [13] and weakly interacting massive particles (WIMPS) [14-16]. The ideal SSCD consists of a large number of identical micron-sized grains immersed in an appropriate dielectric and prepared in a superheated superconducting state.

The deposition of a few keV of energy into a given grain will then 'flip' it into the normal state, thereby producing a change of magnetic flux which can be detected in a pick-up coil. The energy needed to flip the grain depends on the grain material, size and operating temperature.

Two tests were performed. In Test 1, the flipping of individual 15 μm radius grains was detected as the temperature was swept, while in Test 2, the effect of low-energy γ-radiation on a colloid sample of 5 μm radius grains was investigated. The experiments were performed in a standard $1K$ pumped ^4He cryostat. A superconducting solenoid supplied an external field B on the sample, and both this field and the temperature of the sample were computer-controlled, allowing the sample to be taken through various paths in the B-T phase diagram. The changes in flux produced by grain flips were detected by a SQUID connected to the pick-up coil, which, together with the $1K$ cryostat and the solenoid, were shielded in a superconducting lead jacket. The signal is proportional to the magnetic field and the grain volume, and depends on the geometry of the pick-up coil and the various inductances in the detecting system.

3. Experimental Tests

In this section, we describe the two tests. The samples used in these tests were selected from batches prepared by ultrasound disintegration of 99.99% pure tin. Size selection was performed by filtering the grains through wire meshes.

3.1. TEST 1. SINGLE-GRAIN SIGNAL

In this experiment, a line of 15 μm radius grains was mounted on a copper strip, one end of which was attached to a regulated heat source, while the other end was heat-sunk to the 1K pot via a large thermal resistance. With this arrangement, the temperature could be swept with each of the ten grains being at a slightly different temperature. The ten grains were selected using a microscope so that good spheres of the same size were used. Each grain was mounted on a piece of teflon tape which was then placed on copper cold finger so that there was no electrical contact between the grain and the copper. Good thermal contact between grain, tape and copper was effected by using high thermal conductivity grease which also encapsulated the grain.

Signals were detected using a commercial SHE System 330 RF SQUID mounted in the 4.2K bath. The output voltage of the SQUID was digitized using a multichannel analyser (Tracor 1710) with 12-bit digitizer, controlled by the computer. As well as recording the output voltage, the SQUID re-sets were recorded using a home-made flux counter.

Figure 1 shows the signals obtained from the ten 15μm radius grains as the temperature was swept in the cycle $ABCDA$ in the phase diagram Fig. 2 [17], where A is below the supercooling transition point D, and C is above the superheating transition point B. The small temperature dependence of the SQUID signal in the A and C regions was due to paramagnetic impurities in the copper cold finger and the noise came from vibrations transmitted through the cryostat mounts. These were subsequently reduced to a level at which 5 μm radius grain signals could be observed with a signal/noise ratio of 10.
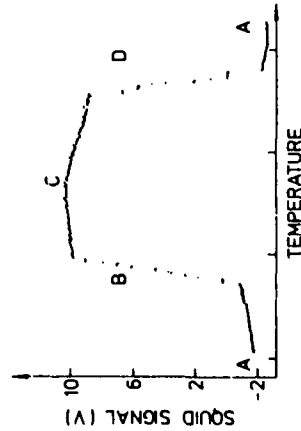
Fig. 1. The sequential phase transitions of ten 15 μm radius grains. The points $ABCD$ are shown on the B-T phase diagram, Fig. 2.
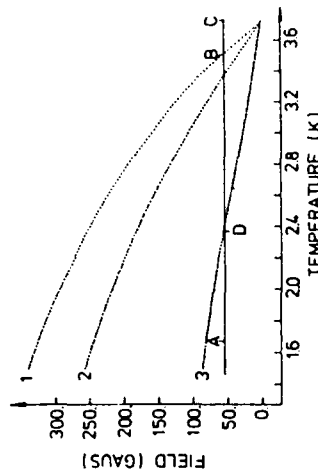
Fig. 2. The B-T phase diagram of the grains [17]. Boundary 1 represents the superheated transition line, boundary 2 is the thermodynamic transition line and boundary 3 is the supercooling transition line.

3.2. TEST 2. RADIATION TEST

For this experiment, a sample was prepared consisting of about 10^4 μm radius grains embedded in an epoxy resin (Emerson and Cummings Stycast 1266). This sample was loaded into a copper capillary connected directly to a temperature-regulated copper block. The source of γ-radiation was a ^{67}Ga sample placed inside the cryostat, and a 1 cm thick copper block could be moved by magnetic remote control to absorb the γ-rays. When the block was in place the 90 keV γ-rays were strongly attenuated (to about 2% of the unblocked radiation), while the higher energy γ-rays suffered only small attenuation. However, the low-energy γ-rays have by far the highest probability of flipping a grain. The experimental set-up is shown in Fig. 3.

It should be noted that no grain selection was made other than the initial filtering by the meshes. Thus there were significant variations in both the size and shape of the particles. These variations, coupled with inhomogeneity of the grain distribution within the epoxy, which cause a spread of dipolar fields, produce a relatively large spread in the individual grain transition temperatures, as can be seen in Fig. 4. The effective colloid transition width increases with field. A typical radiation test comprised the following sequence of operations:

(1) The colloid sample was collected in $B = 0$ to $T < 1.9K$ ensuring that all the grains were superconducting.

(2) The external field was then increased to the required value.

(3) The temperature was then swept slowly upward until the SQUID signal indicated the beginning of the superheated phase transition.

(4) The temperature was stabilized, and, after the SQUID output indicated that the sample had equilibrated and that thermally-induced transitions had ceased, the γ-ray aperture was alternately opened and closed while the SQUID output was recorded.
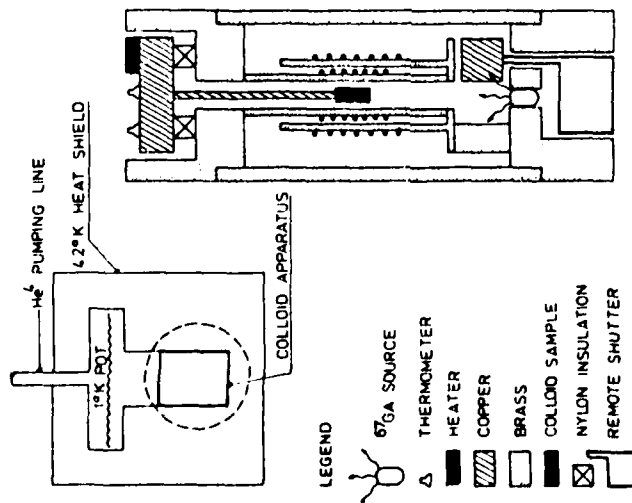
Note that in the 'opening' and 'closing' operations in Step 4 the temperature had first to be lowered to off-set heating effects and then re-set. The shutter magnet was activated only in these operations and was off during the measurements. Also the SQUID was deactivated by a heat-switch on the pick-up circuit during opening and closing and whenever the field was changed, e.g. in Step 2.

The results of a radiation test at $B = 0.031T$ and $T = 2.2K$ are shown in Fig. 5 and Fig. 6 which show slow and fast scans respectively. In Fig. 5B, the aperture is closed and the signal (change in voltage) is due to low-probability transitions induced by high-energy γ-rays which pass through the shutter. In Fig. 5A, the aperture is open. For the fast scan with open aperture shown in Fig. 6A the individual grain flips can be seen.
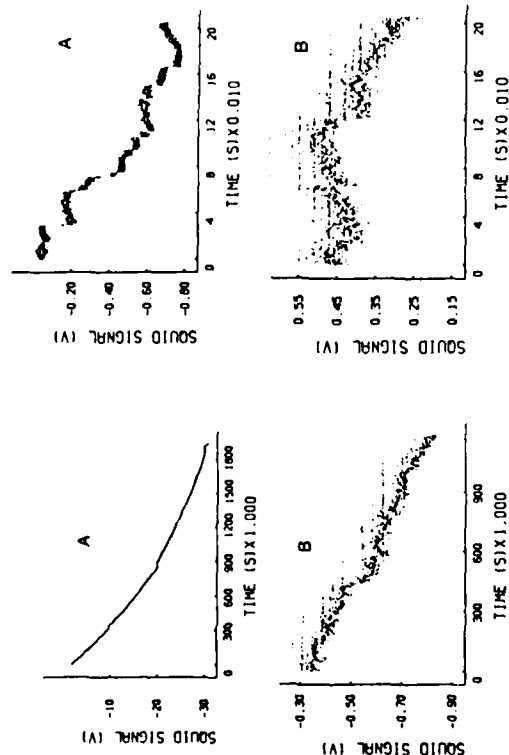

Fig. 5. The SQUID signal from the superheated colloid with the γ-ray shutter open (A) and closed (B). The field $B = 0.031T$ and temperature $T = 2.2K$.

Fig. 6. A faster scan showing the SQUID grain × 100. In (A) the shutter is open; in (B) it is closed. Note the single grain flips in (A).

While observing grain flips the temperature was reduced until the flipping ceased. By this procedure we estimated the maximum temperature gain caused by a γ-ray hitting a grain to be approximately 50 mK. Thus the only grains that can be driven normally are those with their transition temperatures within 50 mK of the quiescent temperature. This means that the effective grain filling factor f_s is much less than the mass filling f_m. For example, for $B = 0.031T$

41

Fig. 3. The design of the apparatus for Test 2. The coils around the colloid sample are the pick-up coil and the superconducting solenoid.

LEGEND

67GA SOURCE
THERMOMETER
HEATER
COPPER
BRASS
COLLOID SAMPLE
NYLON INSULATION
REMOTE SHUTTER

Fig. 4. The deconvoluted SQUID signal for the colloid at $B = 0.031T$. Point A is a typical temperature setting for the radiation Test 2.

40

we estimate $f_e/f_m = 0.05$. Taking this into account, the fraction of γ-rays absorbed and the solid angle presented by the colloid sample, we define a quantum detection efficiency (QDE) as the ratio of the grains that can and do flip when hit by a γ-ray to the number that can flip. We then estimate the QDE ≈ 85%.

4. Conclusion

We have built a practical SQUID read-out system that is sensitive enough to detect individual 5 μm radius grain transitions. Also we have demonstrated that a stable superheated colloid state can be prepared which becomes unstable under irradiation of 90 keV γ-rays. For this SSCD we estimate the QDE ≈ 85%.

This is very encouraging to the prospect of building a SSCD to detect neutrinos and dark matter. The greatest problem to overcome is the production of a homogeneous colloid of grains that are defectless and have uniform size and shape.

5. Acknowledgments

6. References

[1] H. Bernas, J.P. Burger, G. Deutscher, C. Valette, and S.J. Williamson: Phys. Lett. 24A, 721 (1967)

[2] A.K. Drukier and C. Valette: Nucl. Instr. and Meth. 105, 285 (1972)

[3] A.K. Drukier, C. Valette, and G. Waysand: Lett. Nuovo Cimento 14, 300 (1975)

[4] A.K. Drukier and L.C.L. Yuan: Nucl. Instr. and Meth. 138, 213 (1976)

[5] D. Huber, C. Valette, and G. Waysand: Nucl. Instr. and Meth. 165, 201 (1979)

[6] A.K. Drukier: Nucl. Instr. and Meth. 173, 259 (1980)

[7] A.K. Drukier: Nucl. Instr. and Meth. 201, 77 (1982)

[8] N. Coron, G. Dambier, G.J. Focker, P.G. Hansen, G. Jegoudes, B. Jonson, J. Leblanc, J.P. Moalic, H.L. Ravn, B.H. Stroke, and O. Testar: Nature 314, 75 (1985)

[9] E. Fiorini and T.O. Niinikoski: Nucl. Instr. and Meth. 224, 83 (1984)

[10] S.H. Moseley and J.C. Mather: J. Appl. Phys. 56, 1257 (1984)

[11] D. McCammon, S.H. Moseley, J.C. Mather, and R.F. Mushotzky: J. Appl. Phys. 56, 1263 (1984)

[12] B. Cabrera, L.M. Krauss, and F. Wilczek: Phys. Rev. Lett. 55, 25 (1985)

[13] A.K. Drukier and L. Stodolsky: Phys. Rev. D30, 2295 (1984)

[14] M.W. Goodman and E. Witten: Phys. Rev. D31, 3059 (1985)

[15] I. Wasserman: Phys. Rev. D33, 2071 (1986)y

[16] A.K. Drukier, K. Freese, D.N. Spergel: Phys. Rev. D33, 3495 (1986)

[17] J. Feder and D.S. McLachlan: Phys. Rev. 177, 763 (1969)

A3.2   Improvements in RF-SQUID readout and preliminary irradiation studies.

The RF-SQUID system developed by UBC, Vancouver in 1986 improved the sensitivity of electronic readout by about a factor of 50 in comparison with state-of-the-art fast electronics. However, we were still about two orders of magnitude worse than the resolution of the best RF-SQUID's. Further improvement would be possible using a DC-SQUID.

Let us first analyze the available signal. Figure 3 of the UBC, 1987 paper shows that in order to diminish the relative movement of the pickup coil inside the inhomogenous magnetic field, a SQUID pickup coil and magnetic coil wound on the same brass kernal was implemented. However, due to the coupling between the two coils, their mutual inductance is larger than the pickup self-inductance. Thus, we were mismatched with the SHE-SQUID input coil, which diminished the signal by about a factor of two. In the new set-up, the coupling between the pickup and magnetic coils is negligible.

Figure 5 of the M. Legros et al. paper permits identification of the first source of the noise: digitation jitter. In the experimental situation of the irradiation experiments, the dynamic range of the 12 bit ADC was too small. In the improved system, a 16 bit ADC was used.

The noise of SQUID's operating in a magnetic field is dominated by vibrations/displacements of the pickup loop in an inhomogeneous field. There are four ways to diminish this source of noise:

- a better mechanical design to improve the vibrational damping;

- the creation of a very homogeneous magnetic field;

- the use of a magnetic gradiometer;

- the use of an array of SQUID's to reject the common mode vibrations in off-line data processing.

In our 1987 effort we concentrated on the first two techniques.

A major source of noise was discovered when, by accident, we switched off the pump before switching off the SQUID; the noise diminished by a factor of about two. Thus in the new system we modified the gas handling system and improved the pump vibrational insulation with more sand and gummi pads. However, further improvement requires the purchase of a more modern pump and movement of the pumping station to another room.

At the same time, we developed an improved cryostat insert featuring better vibration insulation. In 1986, the 1.5 K pot was rigidly suspended on a single metal tube used for vacuum

pumping. The new setup features three support rods, and the pumping line is decoupled from external vibrations.

The magnetic field homogeneity was also improved. In the 1986 setup, the field homogeneity was about 10^{-2}/cm, whereas the best NMR spectroscopy coil features a homogeneity of 5×10^{-9}/cm and very large, whole body NMR magnets have 10^{-6}/cm. Thus, in principle, the vibrational component of SQUID noise can be eliminated by better engineering of the magnetic field. The goal of the 1987 development was to reach $\Delta H/H \approx 5 \times 10^{-3}$; a further improvement by a factor of five will be attempted during Phase II.

Actually, the improvement of magnetic field homogenity is not so easy in the UBC setup because of

- the requirement of shielding external magnetic fields;

- the small diameter of the cryostat;

- the need for "heat switches".

Due to financial limitations we opted for superconducting shields. In the small cryostat ($\phi \leq 4$ inches) this required accounting for all mirror images. In 1986 we used Pb foil as a magnetic shield but observed that the mechanical deformations lead to considerable field inhomogenity. In 1987 we electro-plated the cryostat interior with Pb to obtain a reproducible, spherically symmetric shield. Most probably, the best (but somewhat expensive) solution is use of an external mu-metal shield.

Finally, due to the limited slew rate of our 10-year old RF-SQUID, we had to use heat switches. To shield the DC current necessary to operate a heat switch, we used a superconductor. We tried to minimize the field distortion in the 1987 setup, but further improvements will be introduced in 1988. When using a high slew rate DC-SQUID, heat switches may be unnecessary. Optionally, RF heating with copper shields will be used.

Overall the development goal for Phase I was a factor of five improvement in S/N. Thus, our system should be sensitive to a change of state of a single, $R = 1$ μm grain inside a readout loop of about 0.5 cm^3. We expect a QDE $\geq 90\%$ for $T = 1.2$ K and minimum ionizing particles, i.e., for energy depositions of a few keV.

A3.3 Results

The development of the data acquisition system was finished in the early fall of 1987. The first low temperature runs in the beginning of December 1987 showed good temperature stability and improved noise reduction.

The spectrum of the noise at H=0 and H=300 Gauss shows that the overall noise is comparable but at the higher field the sharp noise peaks at 440G and 880 Hz were observed. Further modifications of the insert permitted the elimination of the vibrational noise at 440 and 880 Hz (see Figures 1a, and b). The noise component at 130 Hz is due to the vibration of the dewar itself, and can be easily filtered.

Thus in 1986/7 we reached the limiting sensitivity of RF-SQUID electronics, i.e. our noise is 2-5 x 10^{-4} ϕ_o. This is a factor of 2,500 improvement over previous readout electronics. The improvement achieved during the SBIR-Phase I project is a factor of 50, i.e. much higher than expected.

This very low noise level permits a very good signal/noise for the change of state of even very small (R $\approx$ 1-2 μm) grains. The estimated energy threshold of such grains is ca. 1 keV at T = 1.2K and $\leq$ 50 eV at T = 0.05K.

The irradiation studies were initiated and are described in the main-body of this proposal.

In the future, we expect further improvement in SQUID readout sensitivity. A multichannel DC-SQUID readout is being developed and is described in Appendix 4.
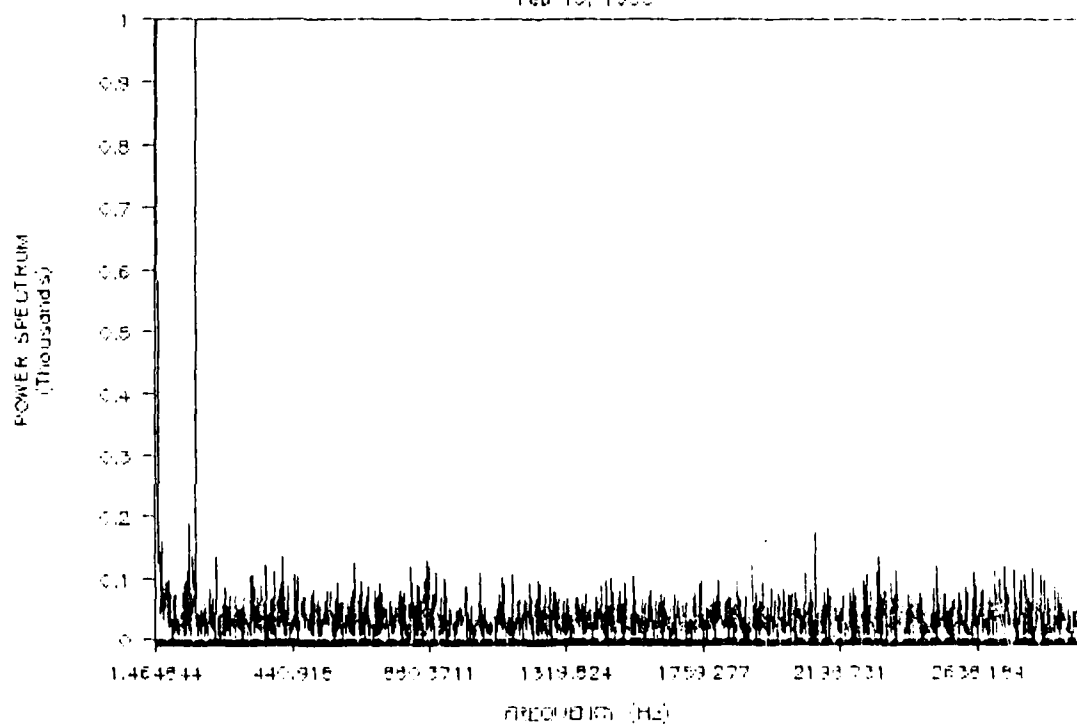
NOISE SPECTRUM – zero field

DATE. February 13, 1989
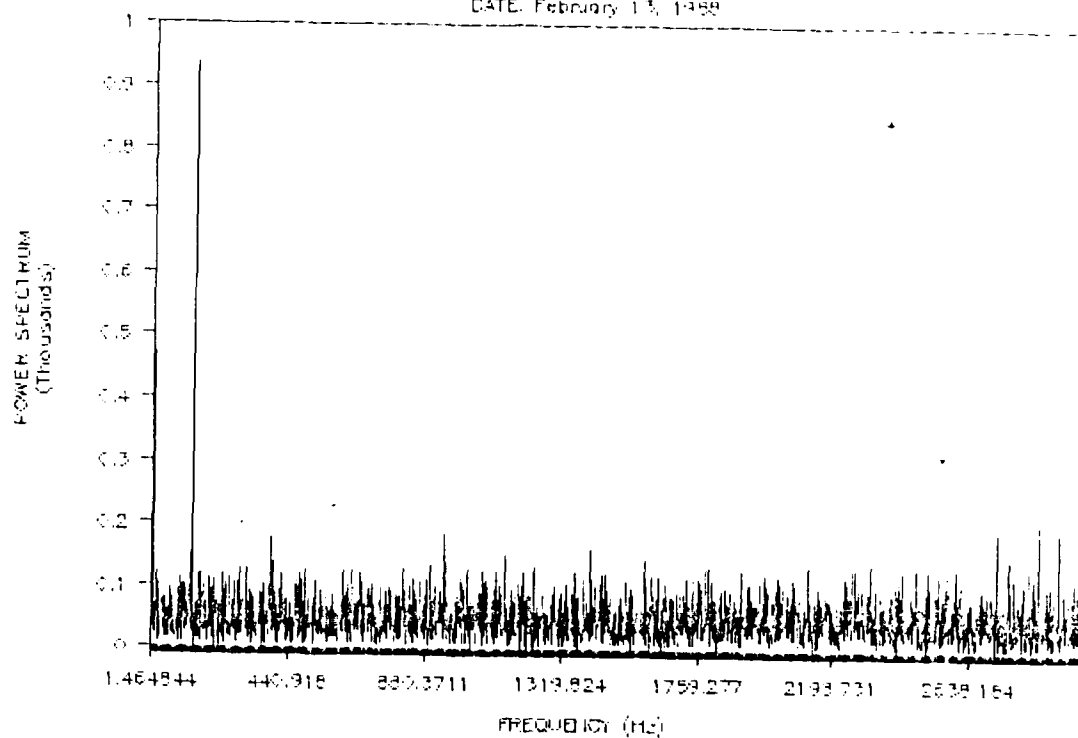
NOISE SPECTRUM – 300 gaues

Feb 13, 1989

Appendix 4: <u>Development of Inexpensive Multichannel DC-SQUID Readout.</u>

The DC-SQUID readout is potentially six orders of magnitude better than "fast electronics". As described in section 4.2 and Appendix 3, this tremendous potential was confirmed by IBM and UBC, Vancouver, experimental results. We believe that the DC-SQUID readout will be used in many applications of SSCD.

Commercially available DC-SQUID's are quite expensive, about $15,000 - $20,000 per channel. In some applications of SSCD, four or more channels are required. However, when the application is well specified, which is the case in SSCD readout applications, improvement of array performance and considerable economy is possible.

In collaboration with the group of Dr. M. Cromar, NBS-Boulder, we are developing the electronics for a multichannel DC-SQUID. The schematics of a single channel is shown in Figure I. For clarity of future descriptions, it can be divided into three parts:

- a low temperature thin film, niobium edge junction coupled to a double transformer;
- a low noise preamplifier; and
- a phase lock-in amplifier.

NBS-Boulder, has excellent facilities for cryoelectronics development and the group of Dr. M. Cromar is among the leaders of the field. They will deliver to us five chips, each featuring four DC-SQUID's, with an estimated price below $1,000/channel. The technology used by the NBS group and their DC-SQUID's results are described in the next section of this Appendix.

ARC will develop room temperature electronics for multichannel DC-SQUID systems. More specifically, the performance of the low noise preamp developed by the NBS group (see Fig. 2) is limiting the overall system performance. ARC's task was to improve the preamp noise from 2.5 nV/√Hz to below 1.5 nV/√Hz. Actually, the preamplifier developed by ARC is much better than preliminary development specifications: at room temperature, the noise is 0.5 nV/√Hz; when slightly cooled, 0.4 nV/√Hz. The schematic of this amplifier is shown in Fig. 3. Notice that the preamp is rather inexpensive: the cost estimate is $175 (see Table 3). Further technical details of this preamp are described in section 3 of this Appendix.

The next step in the development of a multichannel DC-SQUID is the development of the lock-in amplifier. We have performed a cost analysis and believe that further development will require about $5,000 for R & D, and about $2,000 for each lock-in. The tentative date for full development of the lock-in is summer 1988.

Thus, in collaboration with NBS-Boulder, we designed and partially developed the multichannel DC-SQUID readout. With a typical noise of $\Delta\phi=5\times10^{-5}\phi$, it is somewhat better than commercially available SQUID's and close to the best DC-SQUID's produced by IBM. The considerable advantages for a SSCD readout loop are:

- the possibility of direct coupling to a gradiometric magnetic loop evaporated on the same substrate;
- somewhat higher input inductance (the design is for 5µH) sufficient to facilitate good matching to a SSCD; and
- a factor of 8 lower price/channel than commercially available DC-SQUID's.

A4.1: The Development of DC-SQUID's in NBS-Boulder.

The enclosed recent paper of NBS-Boulder, provides information about their capabilities. For further information about their fabrication process, please note references 1, 2, 3, and 5 of the enclosed paper.

Very low noise, tightly coupled, dc SQUID amplifiers

B. Muhlfelder,[a] J. A. Beall, M. W. Cromar, and R. H. Ono

National Bureau of Standards, Electromagnetic Technology Division, Boulder, Colorado 80303

We have fabricated and tested thin film, niobium edge junction, double transformer, dc superconducting quantum interference devices (SQUID's) that were stable under room-temperature storage and thermal cycling and that had very good noise performance. The input inductance, approximately $1.7 \mu H$, was large enough to facilitate good matching to many experiments. When the SQUID was operated as a small-signal amplifier, the minimum detectable energy per unit bandwidth (S_e) was 5×10^{-33} J/Hz at 100 kHz, referred to the SQUID loop (uncoupled). The minimum detectable energy per unit bandwidth was 1.8×10^{-31} J/Hz at 100 kHz, referred to the input coil. The SQUID's had good characteristics for flux-locked operation since the small signal S_e was low over a substantial range of bias current and magnetic flux. For operation in a flux-locked feedback circuit, S_e was 6×10^{-32} J/Hz at 1 kHz.

This letter describes a new thin-film dc superconducting quantum interference device (SQUID) amplifier that incorporates recently developed design and fabrication techniques. These devices have very low noise and excellent reliability, and couple well to sources with inductances in the microhenry range. Applications that require such very low noise amplifiers include inductive monopole detectors, biomagnetic sensors, and Weber gravitational wave detectors.

A double transformer (DT) design was used to transfer energy from the signal source to the SQUID. As shown schematically in Fig. 1, a second transformer was placed at what would have been the input terminals of a single coil configuration. This approach provides both a large input inductance and a small SQUID inductance while requiring only a moderate number of turns in the coils.[1-3] The DT dc SQUID was fabricated with very low capacitance edge junctions and thin-film coils in a reliable Nb base electrode technology.

References 1–7 provide a framework for the design of a useful dc SQUID amplifier. They imply that $L1$ (Fig. 1) should have low inductance; the Josephson junctions should have low capacitance; the coupling to the signal source should be large without adversely affecting the performance of the SQUID; and finally, the device should be mechanically rugged and electrically stable. A model based on resistively shunted Josephson junctions with capacitance and thermal noise[4] was extended to include the lumped element representation of the stripline formed by $L1$ and the groundplane.[3] Optimization of the present design was based on computer simulations of this extended model.

In previous work,[1-3] we noted and studied electrical resonances in the $L1$-groundplane stripline. In the present design we have reduced the size of $L1$ so that the resonances occur at frequencies that do not adversely affect the SQUID characteristics.

The current-voltage characteristics of a DT dc SQUID for two different values of external magnetic flux are shown in Fig. 2. As noted above, the curves are smooth and free of resonance structures. The junction critical current I_c, the shunt resistance R_s, and the modulation parameter β_L are listed in Table I. The modulation parameter $\beta_L \equiv 2L_1 I_c / \phi_0$ was inferred from the change in the total critical current with applied magnetic flux.[8] We estimated the junction capacitance C_J using the first LC resonance of a SQUID with no shunt resistors.[9] This capacitance was a factor of 4 smaller than that of our earlier devices. The hysteresis parameter $\beta_c = 2\pi I_c R_s^2 C_J / \phi_0$ was computed assuming this value of C_J for SQUID's with shunted junctions. The values of β_c and C_J for the SQUID corresponding to Fig. 2 are also given in Table I.

Table I also contains the coil parameters for the DT dc SQUID. A drawing and micrograph of the device are shown in Fig. 3. The inferred inductances of $L3$ and $L4$ were within 30% of the predictions. The calculated bare inductance of the input coil $L4$ was $5 \mu H$. Shielding currents in $L2$-$L3$ reduced L_1', the effective inductance at AA' (Fig. 1). For zero circulating current in $L1$, and for L_3/L_1 equal to 0.54, the predicted input inductance was $1.7 \mu H$. The current required in $L4$ to couple one flux quantum into $L1$ was $2.0 \mu A$.

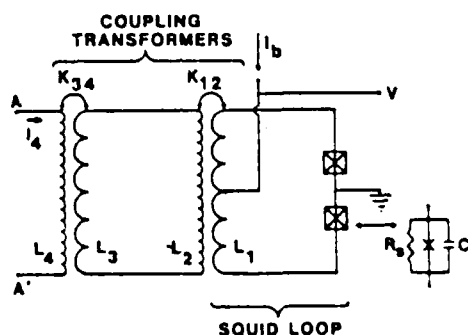FIG. 1. Electrical schematic diagram for the DT dc SQUID. The input terminals for the device are at AA'. The signal current is I, and the output voltage is V. The mutual inductance coupling coefficients for the two transformers are k_{12} and k_{34}. I_b is the bias current.

[a] Present address: Relativity Gyro Program, Hansen Laboratory, Stanford University, Stanford, CA 94305.
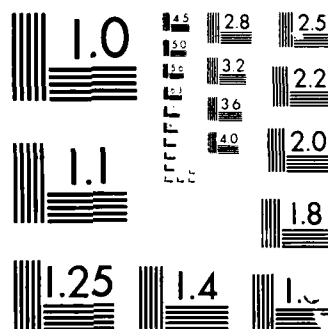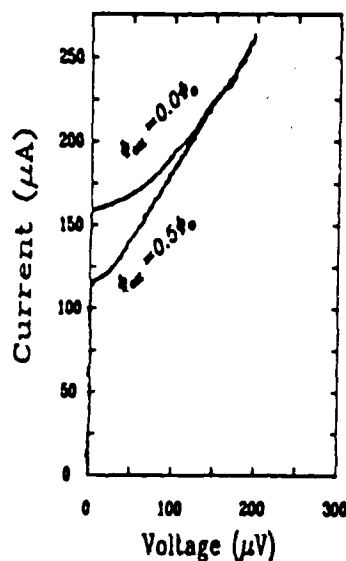
MICROCC   RESOLUTION TEST CHART
NATIONAL BUREAU OF STANDARDS 1963-A

FIG. 2. Current-voltage characteristics of a DT dc SQUID for $\phi_{ex} = 0.0$ and $\phi_{ex} = 0.5\phi_0$.

This implies that M'_{14}, the effective mutual inductance between $L\,1$ and $L\,4$, was 1.0 nH.

The measured value of L_1 was a factor of 2 higher than expected and the measured value of the mutual inductance between $L\,1$ and $L\,2$ was a factor of 2 lower. The reduction in the mutual inductance between $L\,1$ and $L\,2$ caused a reduction in the coupling efficiency between $L\,1$ and $L\,4$ resulting in degradation of the coupled sensitivity of the SQUID. One contribution to these discrepancies may have been stray inductance in $L\,1$. A second contribution may have been the vertical structure with the coil $L\,2$ lying beneath $L\,1$ which in turn lay beneath the groundplane. This resulted in a groundplane that was not flat, rather than the planar structure assumed in the stripline model.

We have measured the SQUID noise at 100 kHz with the input coil unterminated. A tank circuit at low temperature was used to match the output impedance of the SQUID to the input impedance of a commercial low noise amplifier. The best noise performance was observed for $I_b/I_c = 2.0$

TABLE I. Measured and inferred SQUID and coil parameters.

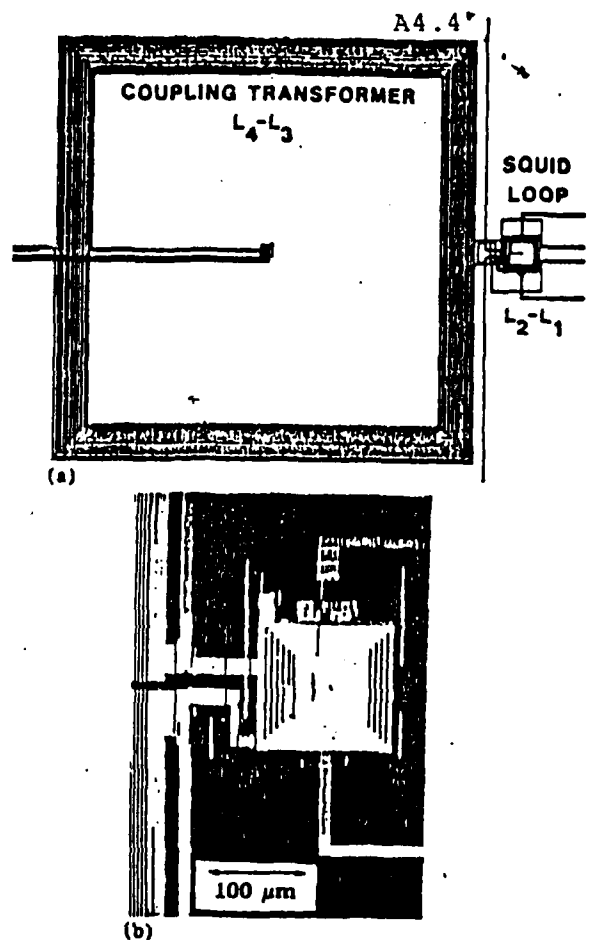| Parameter	Value
β_L	1.7
R_s	2.1 Ω
I_c	77 μA
$-C_J$	0.09 pF
β_c	0.09
Number of turns in $L\,4$	40
Number of turns in $L\,3$	1
Number of turns in $L\,2$	5
Number of turns in $L\,1$	1
$k_{13}^2 L_3$	42 pH
L_3/L_1	0.54
L_4'	1.7 μH
L_1	23 pH

(a)

100 μm

(b)

FIG. 3. (a) Line drawing of the DT dc SQUID. The matching transformer for the SQUID is labeled $L\,4$–$L\,3$ and is represented by the large square coil (1.7 mm × 1.7 mm). The single turn secondary lies over the coil and is not shown in this drawing. $L\,1$ and the coupling coil $L\,2$ are directly to the right of the transformer. (b) Scanning electron micrograph of the SQUID loop region. The bias current and output voltage leads extend off to the right of the figure. The coupling coil $L\,2$ lies beneath $L\,1$ which in turn lies beneath a groundplane.

and $\phi_{ex} = 0.10\phi_0$, where I_b is the bias current and ϕ_{ex} is the externally applied magnetic flux. For these conditions the flux-voltage transfer function, $\partial V/\partial\phi_{ex}$, was 620 μV/$\phi_0$. The power spectral density of the equivalent magnetic flux noise, referred to $L\,1$, at this bias point was $S_\phi = 2.3 \times 10^{-7}$ ϕ_0/Hz$^{1/2}$ corresponding to a minimum detectable energy per unit bandwidth $S_e = S_\phi/2L_1 = 5 \times 10^{-33}$ J/Hz. The noise was low for a wide range of bias conditions. We measured S_e to be less than 1.4×10^{-32} J/Hz for $0.05 < \phi_{ex}/\phi_0 < 0.15$ and $1.9 < I_b/I_c < 2.0$. This was the best performance we measured, but several other devices with similar dc characteristics had $S_e = 7 \times 10^{-33}$ J/Hz. Computer simulations similar to those described above[3] predicted $S_e = 4 \times 10^{-33}$ J/Hz, in fair agreement with our measurements.

Although the matching between the source and input impedances must be considered when comparing the sensitivities of different SQUID's for a particular application, the coupled minimum detectable energy per unit bandwidth

(i.e., referred to the input coil) is one reasonable measure of performance. We measured this to be $S_e^c = S_\phi / 2k_{14}^2 L_1 = 1.8 \times 10^{-31}$ J/Hz, where k_{14} is the effective coupling constant between $L1$ and $L4$ and is given by $k_{14}^2 = M_{14}^2 / L_1 L_4 = 0.027$.

We also operated the SQUID in a flux-locked configuration. The magnetic flux in the SQUID was monitored by observing the voltage across the SQUID as the flux was modulated. A change in average flux caused room-temperature feedback electronics to couple a corresponding but opposite flux into $L1$, thereby fixing the total flux. We measured the system's transfer function by applying a known flux signal to the SQUID.

Having determined the transfer function, we measured the equivalent flux noise of the SQUID at low frequencies. The noise was at least a factor of 10 greater than the noise we measured at 100 kHz in the open loop configuration. Some of this increase in noise may have been the result of inadequacies in the room-temperature electronics. In most cases the noise spectrum was flat for frequencies between 500 Hz and the feedback system rolloff at 2 kHz. The power spectral density of the noise increased for frequencies below 500 Hz and did not fit a simple power law as a function of frequency. In the flux-locked mode, the lowest S_e was 6×10^{-32} J/Hz at 1 kHz and 8×10^{-31} J/Hz at 1 Hz.

These devices proved to be insensitive to stray magnetic fields and variation in source impedance. Suppression of the SQUID's maximum critical current due to trapped flux was rarely observed in these devices, possibly because of small junction area (0.25 μm $\times$ 2.0 μm), low ambient magnetic field, and shielding of the magnetic field by the groundplane. The input coil and signal source impedance can affect the high-frequency dynamics and performance of tightly coupled SQUID's. This was not the case in the present devices since their current-voltage characteristics were nearly unaffected when the signal source impedance was changed from an open to a short circuit.

To fabricate these SQUID's, we developed a thin film, niobium base electrode technology. The device shown in Fig. 3 has a vertical structure containing six metal and five insulator layers. Electron beam lithography (EBL) was used to define the entire circuit geometry except for optically defined large area pads (not seen in Fig. 3) that mated to the cryogenic test probe. Dry etching through EBL resist masks

yielded a high percentage of continuous thin-film coils with 40 turns of 2-μm wires and spaces. The Josephson junction area and capacitance were minimized by using an edge geometry[10] in which the junction was formed by depositing a Pb alloy over the sloped edge of an oxidized Nb film. This process yields SQUID's that are both more stable and have less uncoupled noise than our earlier DT dc SQUID's. Most of the Nb devices exhibited electrical characteristics that were unchanged after many thermal cycles, six months room-temperature storage, and exposure to the atmosphere and moisture. This improved reliability distinguishes these devices from the previous Pb-alloy-based SQUID's. A detailed description of the fabrication process will appear elsewhere.

In summary, the double transformer configuration provided a large input inductance, 1.7 μH, while allowing a low inductance for $L1$ and a smooth current-voltage characteristic in the operating region. In the open loop configuration the uncoupled minimum detectable energy per unit bandwidth was 5×10^{-33} J/Hz and the coupled minimum detectable energy per unit bandwidth was 1.8×10^{-31} J/Hz. The coupled sensitivity can undoubtedly be improved by redesign of the $L1$-$L2$-groundplane structure. The niobium base electrode, edge junction fabrication technology produced reliable SQUID's that rarely exhibited the effects of trapped flux. Thus, the DT dc SQUID may be an attractive amplifier for biomagnetic sensors, Weber gravitational wave detectors, and inductive monopole detectors.

[1] B. Muhlfelder, W. W. Johnson, and M. W. Cromar, IEEE Trans. Magn. MAG-19, 303 (1983).
[2] B. Muhlfelder, J. A. Beall, M. W. Cromar, R. H. Ono, and W. W. Johnson, IEEE Trans. Magn. MAG-21, 427 (1985).
[3] B. Muhlfelder, Ph.D. thesis, University of Rochester, 1984. Available from University Microfilms, Ann Arbor, Michigan.
[4] C. D. Tesche and J. Clarke, J. Low Temp. Phys. 29, 301 (1977).
[5] M. W. Cromar and P. Carelli, Appl. Phys. Lett. 38, 723 (1981).
[6] D. J. Van Harlingen, R. H. Koch, and J. Clarke, Appl. Phys. Lett. 41, 197 (1981).
[7] M. B. Ketchen and J. M. Jaycox, Appl. Phys. Lett. 40, 736 (1982).
[8] R. L. Peterson and C. A. Hamilton, J. Appl. Phys. 50, 8135 (1979).
[9] Y. Song and J. P. Hurrel, IEEE Trans. Magn. MAG-15, 428 (1979).
[10] P. Vettiger, D. Moore, and T. Forster, IEEE Trans. Electron Devices ED-28, 1385 (1981).

A4.2:   Bipolar Low Noise Preamplifier for DC-SQUID.

During   the   development   of DC-SQUID signal conditioning and
processing   electronics   (see   Fig.   1),   it   became necessary to
improve the preamplifier developed at NBS-Boulder, (see Fig. 2).
We examined both the noise and signal bandwidth limitations.

This bipolar preamplifier design is of particular interest
because   it   is,   in principle, optimal for low source impedances
such   as   that   of DC-SQUID.   The   disadvantage   of   bipolar
transistors,   however,   is   that   they   will   not   work at liquid
nitrogen temperatures.

The   improvements   introduced   by   the ARC team were on three
fronts:

-   a less noisy power supply;
-   emitter-coupled transistors used as first stage; and
-   optimization of operating temperature (the idea being that
    the   lowest   temperature   where   the amplifier can operate
    satisfactorily will also result in the lowest noise).

These   efforts   resulted in a preamplifier running at dry ice
temperature   (192K) with a total noise of 0.4 nV/√Hz (referred to
the   input when driven from a 10 Ω source), a gain of 1000, and a
bandwidth of 0.1Hz-430kHz.   The preamplifier schematics are shown
in Fig. 3.   Following are the theoretical justifications and
experimental results.

1)   The power supply:

The least noisy pc /er supply available, batteries, were used.
The   OP27   used   in   our   preamp specifies ±4.5V minimum supply
voltage.   We optimized the preamp noise as a function of voltage;
the   optimal   voltage   was   ±6.5V,   and 9.0 eV battery cells were
used.   Physically,   they are housed in a separate aluminium box
maintained   at   room   temperature   and connected to the preamp by
shielded coaxial cables.   By using batteries, we observed a noise
reduction   by   a factor of two compared with a typical laboratory
power supply (Global Specialties Model 1300).

The   large supply drain of 10 mA requires that a power supply
must   be   conserved by switching it off when the preamp is not is
use.   Actually,   we   used   rechargable Ni/Cd batteries; for six
batteries we expect about a week of continuous use.

2)   The design of first gain stage:

The   PMI MAT-02 dual matched transistor pair has an intrinsic
voltage   and   current   noise near the theoretical limitations for
bipolars, especially at low currents:

$$E_N^2 = \frac{2(KT)^2}{qI_C} \qquad\qquad (1) \quad \text{Per Transistor}$$

and

$$I_N{}^2 = \frac{2qIc}{h_{FC}} \qquad\qquad \text{(2) Per Transistor}$$

We verified that at T=25°C, I_C=1mA and h_{FE}=600, the MAT-2 is characterized by E_N=0.85 nV/√Hz and I_N=1pA/√Hz in accordance with PMI data sheets. At high currents, however, the effect of base spreading resistance (R_{BB}') is to make $E_N{}^2$ increase as seen in the voltage noise vs. collector current curve (see Fig. 4 reproduced from PMI data sheets). Thus:

$$EN^2 = \frac{2(KT)^2}{qI_C} + 4KTR_{BB}' + \frac{2qIc}{h_{FC}} R_{BB}' \quad \text{(3)}$$

and from a comparison of (3) with Fig. 4 we see that $R_{BB}' = b\sqrt{I_C}$, where b ≈250 and is constant. Therefore, (3) can be rewritten as

$$E_N{}^2 = \frac{2(KT)^2}{qI_C} + 4KTb\sqrt{I_C} + \frac{2bqIc^{1.5}}{h_{FE}} \qquad\qquad \text{(4)}$$

This provides a fairly accurate model for $E_N{}^2$, as was verified at I_C = 5mA, T ≈25°C, H_{FE} = 600, wherein E_N = 0.82 nV/√Hz. The min(E_N) = 0.76 nV/√Hz at I_C = 2.5mA is obtained by minimalizing (4) with respect to I_C.

From the above, the total noise from the transistor pair with source resistance R_S can be modeled as

$$E_t{}^2 = 2(E_N{}^2 + I_N{}^2R_S{}^2 + 4KTR_S) \qquad\qquad \text{(5a)}$$

$$E_t{}^2 = 2(2(KT)^2/qIc + 4KT(b\sqrt{I_C} + R_S) + 2qI_C(b\sqrt{I_C} + R_S)/h_{FE}) \qquad \text{(5b)}$$

Thus, to reduce $E_t{}^2$ we should:

1) operate at I_C = 2.5mA;
2) reduce R_{BB}' by paralleling; and
3) reduce R_S.

For N = number of parallel pairs we have

$$R_{BB}'(N) = R_{BB}'(1)/N = b\sqrt{I_C}/N \qquad\qquad \text{(6)}$$

and

$$E_T{}^2 = 2[2(KT)^2/qNF_C + 4KT(b\sqrt{I_C}/N + R_S) + 2qNI_Cb\sqrt{I_C}/(h_{FE}+N) + R_S{}^2] \qquad \text{(7)}$$

Table 1 is a comparison between theoretical values from (7) and the experimental values for different source resistances, I_C and number of pairs in parallel. Particular attention was paid to $E_N{}^2$, since R_S is expected to be low. We conclude that it is more efficient for noise and power dissipation to parallel than to increase I_C to 2.5 mA. Therefore, we decided to use 3 transistor pairs at I_C (nominal) = 1.2 mA, achieving a theoretical noise performance of E_N = 0.48=0.45nV/√Hz and I_N = 1.3-1.6 pA/√Hz, at room temperature. The calculated power dissipation is 160 mW.

Some other characteristics of this amplifier are summarized in Table 2; also part of the PMI - Application note 02 featuring a similar design is provided for comparison and/or reference.

3) Optimalization of Operating Temperature.

Equation (7) suggests a strong dependence of noise upon temperature. The OP27 and MAT-02 are specified for operation to $T = -55°C$, where the theoretical noise would be $E_N = 0.37nV/\sqrt{Hz}$ and $E_T = 0.61nV/\sqrt{Hz}$ for NF = 5 dB with $R_S = 10\Omega$. We hypothesize that since the preamplifier has fairly wide bandwidth at room temperature (640 kHz), a lower noise level can be achieved if the bandwidth does not decrease below 160 KHz at temperatures near -55°C. (Our present application only calls for 100 KHz full gain).

One experiment was to briefly immerse the preamplifier in liquid nitrogen (T ≈ 77°K) and allow it to warm through the range of temperatures from 77°K to 300°K while measuring bandwidth and noise. It was found, as expected, that the transistor did "freeze out" at liquid nitrogen; but there was a point during the warm-up where $E_T \le 0.55nV/Hz$ (see Photo 2).

The experiment was repeated at "dry ice" temperature (-78°C or 192°K): a bandwidth of 430 KHz was obtained with a total noise of $0.56nV/\sqrt{Hz}$ for $R_S = 10\Omega$ (see Photo 3), and a calculated $E_T = 0.57 nV/\sqrt{Hz}$, $E_N = .34 nV/\sqrt{Hz}$. We plan for further studies at $-193°C \le T \le -78°C$. In recent implementation, we reached $0.4mV/\sqrt{Hz}$.

We concluded that, after improvement by a factor of 4-5, the bipolar preamplifier is an attractive candidate for a DC-SQUID preamp and can compete with most FET preamplifiers.

Table 3 is a breakdown of the cost of each such preamp, in quantities of 10. Thus, the preamp is not major contribution to the price of DC-SQUID readout electronics.

Acknowledment:

Bibliography:

1) Gray Mayer, "Analog Integrated Circuits", J. Wiley.

2) Sherwin - National Semiconductor, Application Note AN 104.

3) Pease "A Low Noise Precision OP-AMP:, National Semiconductor LB52.

4) Nelson - National Semiconductor, Application Note AN202.

5) PMI, Application Note AN102.

Table 1: MAT-02 Transistor Noise; Theoretical vs. Measured Data for T = 25°C.

RS (Ω)	N	I_C (MA)	EN_t theoret. (nV/√Hz)	E_T(nV/√Hz) Theoret.	Meas.	IN(pA/√Hz) Theort.	Meas.	Comments
50	1	2.0	.76	1 50	1.48			
200	1	2.0	.76	2.70	2.67			
50	2	1.0	.59	1.41	1.48	1.00	1.28	
50	2	2.0	.54	1.40	1.42	1.46	1.34	
50	3	1.5	.45	1.36	1.39			
10	3	1.5	.45	0.73	0.78	1.55		see Photo 1
50	3	2.0	.44	1.56	1.36			
N/A	3	1.0	.48	--	--	1.26		see Table 2

Table 2: Performance Characteristics of Bipolar Low Noise Preamp (T=25°C).

Parameter	PMIAN-102	Measured	Comments
Voltage-Noise $_{RMS}$ (F=100-100KHz)	E_N=0.5/√Hz (F=1KHz)	Et=0.78nV/√Hz E_t=1.36nV/√Hz	RS=10Ω(NF=5.6dB) R_S=50.0Ω(NF=3.7dB)
IN$_{RMS}$ (F=100-100KHz)	1.5pA/√Hz --	1.5 PA/√Hz --	See Table 1
Bandwidth (G=1000)	150KHz	640KHz	Measured at -3dB point
Slew Rate	2V/µS	1.8V/µS	
Open loop gain	3×10^7	10^7	
Common Mode Rejection Ratio	130dB	140dB	
Input Bias	3µA	3.5µA	Need to balance input resistor with R_S to reduce offset.
Supply Current	10mA	9.83mA	

Table 3: Cost Estimate of Bipolar Preamplifier.

Component	Qty/Amp	Cost
Resistors (Metal Film)	10	≤ 5.00
Capacitors (NPO)	4	≤ 5.00
OP 27 AJ	1	20.00
MAT02AH	3	30.00
Box & Connectors	2	50.00
PC Board	1	25.00
Mounting	--	40.00
TOTAL		175.00

Fig. 1 Schematic of the SQUID electronics. Components within the dashed box are at liquid ^{4}He temperature.
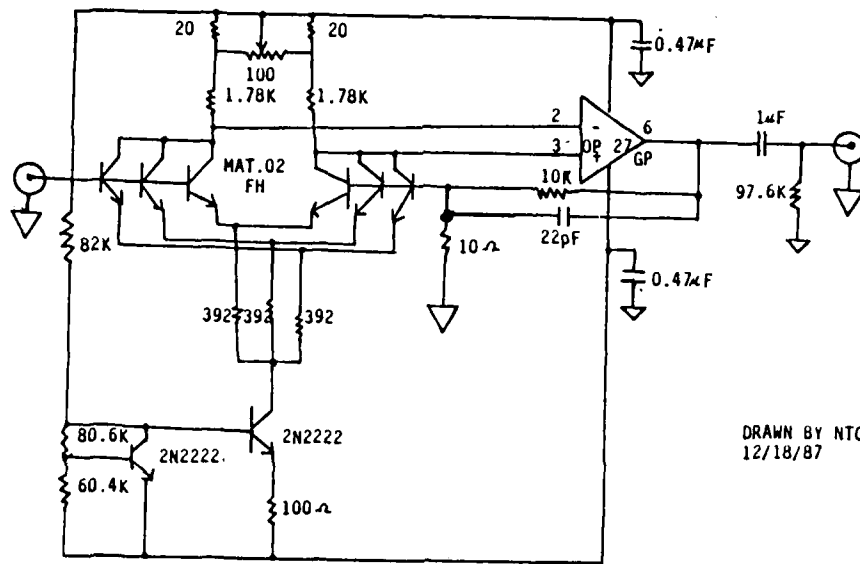

Fig.2   NBS,Boulder preamplifier

FIG. 3 SCHEMATIC: ARC LOW NOISE BIPOLAR PREAMP
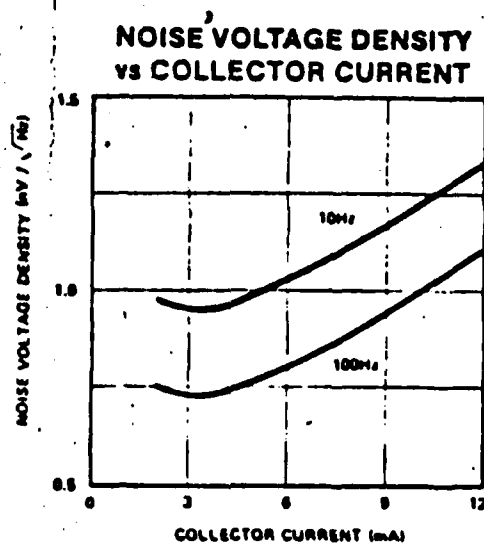
NOTE: ALL RESISTORS METAL FILM
ALL CAPACITORS NPO

Fig.4   MAT-02 characteristics (courtesy PMI).
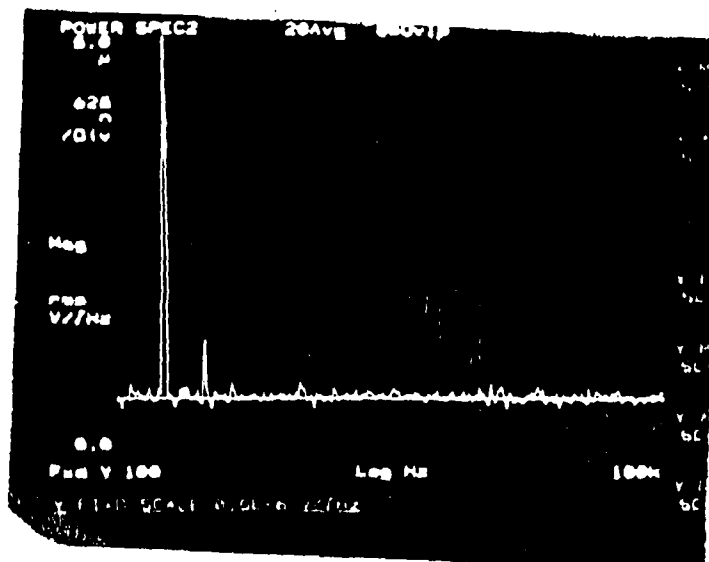
PHOTO 1:
PREAMPLIFIER
NOISE PSD
WITH 10 OHM SOURCE
T= 300K

PHOTO 2:
PREAMP MINIMUM OBSERVED
NOISE PAD
WITH 10 OHM SOURCE
70 K ≤ T ≤ 300K
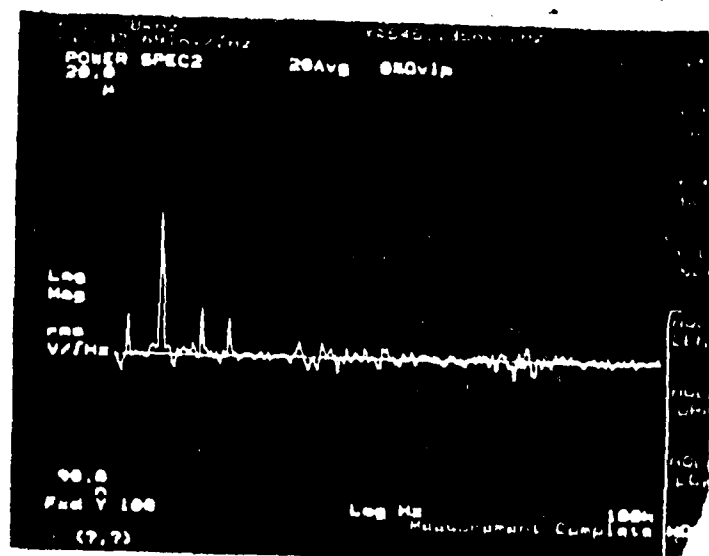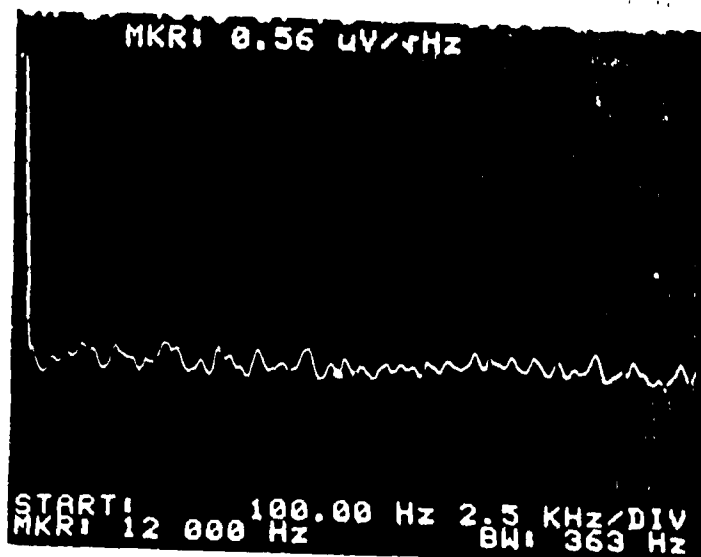
PHOTO 3:
PREAMP
NOISE PSD
WITH 10 OHM SOURCE
T= 192 K
(DRY ICE)

Appendix 5: Status of the Development of Fast Electronics by ARC/U. Md. College Park Collaboration.

A SSCD can find important applications in gamma ray detection. In fact, it is not only important but, with the exception of neutron detectors, also the simplest application of a SSCD; the total energy lost by the annihilation photon is much larger than the minimum energy threshold. Thus relatively large grains (R $\approx$ 10 µm) can be used, for which a good signal/noise ($\geq$ 10) has been achieved by at least four groups (ARC/UBC, Orsay, MPI/TU and LAPP/CERN).

The main challenge in the development of a SSCD-based γ-detector is the need for multichannel, very fast electronics able to detect single grain flips. It is our experience that the best source of relevent know-how is in high energy groups which have designed/implemented systems consisting of ten thousand channels of very fast electronics. Thus, we have accepted the offer of the high energy group of the University of Maryland, College Park to jointly develop the fast electronics for the SSCD detector. Furthermore, we obtained valuable information from the MPI f. Physik, Munich and LAPP/CERN groups which have about three years of experience in fast electronic SSCD readout.

We have decided to perform two complementary experiments using the electronics developed by LAPP/CERN group ($t_{rise} \approx 10$ nsec):

- a coincidence test using a CERN muon beam (a true time-of-flight experiment);

- a coincidence test using back-to-back annihilation photons, at ARC/U. Md. Lab.

In both experiments two physically separate SSCD's will be used. To enable the 2γ coincidence experiment, the Physics Department, U. of Maryland, College Park has provided us with a large (50 m^2) laboratory and some technical help.

We believe that the proposed experiments are clean feasibility tests of a SSCD-based detector. They are, however, somewhat more complicated and require development of both a large cryostat and of special electronics. This development is described in this Appendix; the experimental results of the "coincidence tests" are expected in the spring of 88.

The experimental set-up for the 2γ coincidence tests consists of:

- a large cryostat with gas handling system;
- a temperature and magnetic field stabilization system;
- fast electronics.

Our large, aluminum cryostat is on loan from NBS, Gaithersburg. It's large enough (ϕ_{int} = 6 inch, length = 80 inch) to house the prototype PET device to be developed in

Phase II, which will feature two 8x8 detectors (each 2 cm x. 2 cm x 1 cm) separated by 30 cm. Furthermore, the large helium volume permits a long autonomy time of 4-5 days. *In preliminary tests,* we will often use an external high energy γ-source; this is possible due to the low atomic number of the materials used in cryostat construction.

The cryostat insert is of standard construction. We predicted, however, three electronic pots which are able to accomodate up to 64 channels of readout electronics using twisted-pair readout. Furthermore, a separate pot for coaxial-cables permits precise temperature measurement/control. The electromagnet with persistant field heat-switch will be placed inside of this cryostat.

The gas handling system features precision pressure manometers (Diavac and Combivac-II, Leybold-Heraus) and a series of valves including fine control, Cartesian pressure controller (Model 329, Lake Shore Cryogenics). Furthermore, the temperature is stabilized using both the above pressure controller and Lake Shore Cryogenic Temperature Controller, with nominal temperature stability of about 1 mK.

We use a large roughing pump placed in the same room as the cryostat. This permits us to achieve T$\approx$1.1°K with our cryostat, but may lead to microphonic noise in our readout electronics. If necessary, the pump will be removed to next room.

To measure temperature, generate/measure magnetic field, and move/shield radioactive sources we opted for a general electronic system based on IEEE-488. Almost identical systems are installed in U. Md. and in our experiment in NBS, Gaithersburg. It is described in some details in the next sub-section.

The fast electronics system is based on:

- fast, room-temperature preamps developed by LAPP/CERN;
- some NIM elements (coincidence, delay, TDC etc.);
- a Canberra multichannel analyser (on loan from NRL);
- some CAMAC elements (on loan from U. Md.).

This system is still under development. If required, further information will be provided in the spring of 88.

A5.1: The description of general electronics used in U. Md. and NBS, Gaithersburg.

The purpose of this project was to use the PC-XT with IEEE-488 for data acquisition, instrument control, and testing. As a test of system performance, the linearity and short and long-term stability of measuring instrument output, and the relative stability of the Hewlett-Packard and EM ATR Power supplies, were measured.

The system was assembled as shown in Fig. 1. The IBM-compatible PC with IEEE-488 has 640K memory, a speed of 4.77 MHz, and parallel ports for communication.

The measuring devices and their specifications were:

(a) <u>Keithley 197 Autoranging Multimeter</u>, with ranges of 1µV/count to 750V, 1mΩ to 220 MΩ, and 0-10A.

(b) <u>Programmable Counter/Timer</u>, with read frequency, oven stabilized quartz, and frequency drift $\pm 10^{-8}$/day.

(c) <u>EMDP Digital Programmer</u>, the interface/control unit for use with power supplies manufactured by Electronic Measurements, Inc. This Programmer provides an accurate means for remote control of the parameters of the EM power supplies via the IEEE-488 Standard Interface. The programmer has two identical outputs. The programming range of each output is 0 to +5 volts DC.

The power supplies, shown in Fig. 1, are:

(a) <u>Hewlett Packard System DC Power Supply</u>, with ranges of 0-20V/0-5A, 100W, provides for both remote and local programming, and permits reading and setting of both voltage and current.

(b) <u>EM ATR Power Supply</u>: this supply is able to produce peak voltage/maximum current output at three operating ranges. The supply can be controlled in constant current or constant voltage modes. By "Remote Programming" the power supply output voltage or current is controlled from a remote location by means of an external voltage source or resistance.

Specialized software written in Basic on the IBM Compatible Computer using Subroutine "CALLS" directly to the onboard firmware performs the above specified functions of data acquisition, instrument control, and permits testing of the linearity and stability of the measuring devices as well as the two power supplies.

The address of each instrument must be uniquely identified in order to allow individual devices to access the general purpose interface bus (GP-IB/IEEE488) without interference. The bus address is assigned by internal switches (in our case the bus Address is 21).

The programs for data acquisition are:

(i) Program "Hysteresis", which performs the following:

(a) checks temperature stability by:

- reading a specified number (N) of resistance values, RES(I), from the multimeter at a set time interval.
- checking the stability through the following calculations:

$$Rmean = (\sum_{i=1}^{N} Res(I))/N$$

$$R_{Diff}(I) = |\ Res(I)-R_{mean}\ |$$
determines if $R_{Diff, max} \leq$ EPS, where EPS is the user-set error factor.

    (b)   tests the operation of the various instruments by:

- setting and reading current from the HP power supply, and
- reading resistance from multimeter.

  (ii) Program "Stability", which performs the following:

    (a)   checks temperature stability, by the same procedure as listed above under Hysteresis.

    (b)   checks the linearity of current from HP power supply, by recording a set of linearly increasing values of current by setting and reading the current on the HP.

    (c)   tests operation of instruments by setting and reading data at given time interval.

    (d)   checks temperature stability, by the same procedure as listed under Hysteresis.

    (e)   checks stability of frequency, by:

- reading a set value of frequency, FR(I), at a given time interval a specified number of times (N).
- calculating for stability are:

$$Fr_{mean} = (\sum_{i=1}^{N} FR(I))/N$$

$$DR_F(I) = |FR(I)-Fr_{mean}|$$

$$DRF_{max}/N \leq EPS$$

- Standard deviation calculation

The linearity/stability tests of the power supplies were performed by the following programs:

    (i)   "EMDP"

- checks temperature stability (same procedure as under Hysteresis)
- sets linearly increasing values of current on both the HP and EM power supplies.

- takes readings of measurements of current from both power supplies.
- checks temperature and frequency stability.
- reads frequency and resistance.
- checks linearity of current from both power supplies using the following calculations:

$$I_{Dmean} = (\sum_{i-1}^{N-1} I(i+1)-I(i))/N-1) \text{ for both HP \& EM supplies}$$

Compare I_{Dmean} (HP) to I_{Dmean} (EM)

- compares the linearity and stability of the HP to the EM power supply.

(ii) "EMDP #2"

- checks temperature stability (same procedure as under Hysteresis)
- sets current on the HP and EM power supplies.
- reads a set of current values at a given time interval from the HP and EM.
- checks stability of current using the following equations:

$I_{HP}(J)$ = current value from HP

N   = number of current values read

$I_{EM}(J)$ = current values for EM

$$I_{HP} \text{ Mean } = (\sum_{j=1}^{N} I_{HP}(j))/N$$

$$I_{EM} \text{ Mean } = (\sum_{j=1}^{N} I_{EM}(J))/N$$

$$Diff_{IHP}(j) = |\ I_{HP}(j)-I_{HP} \text{ Mean}|$$

$$Diff_{IEM}(j) = |\ I_{EM}(j)-I_{EM} \text{ Mean}|$$

- check if: $Diff_{IEM}$ Max $\leq$ EPS
         $Diff_{IHP}$ Max $\leq$ EPS

Hand calculations and computer output of data showed the HP power supply to have greater accuracy in measurements than the EM power supply. The HP power supply had an error of $\pm. 0006$ and the EM power supply had an error of ± 0.1 between the value set by the user and the value read from the instrument measuring devices.

Both devices show, however, satisfactory long term stability of 10^{-5} and 5×10^{-4}/hour for HP and EMP, respectively. Furthermore, using a 1.5 kΩ resistor we studied long term stability of Keithley 197 multimeter which looks O.K.; about 10^{-5}/hour. Additionally, using the program "stability" we tested the long time stability of LC oscillator at 1.2°K; it seems satisfactory $\Delta v/v \approx 10^{-6}$/10 minutes.

The acquisition of data and instrument control by the PC with IEEE-488 has been implemented using specialized software that utilized IEE488 general purpose interface bus. Program "Hysteresis" tests the operation of the HP power supply, counter, and multimeter. The program "stability" is a modification of "Hysteresis" with the tests for stability of temperature and frequency included. The programs "EMDP" and "EMDP#2" both test the HP and EM power supplies for stability and linearity of current. The comparison of the two power supplies has shown that the HP has better stability than the EM.

The above described programs will be provided on request.
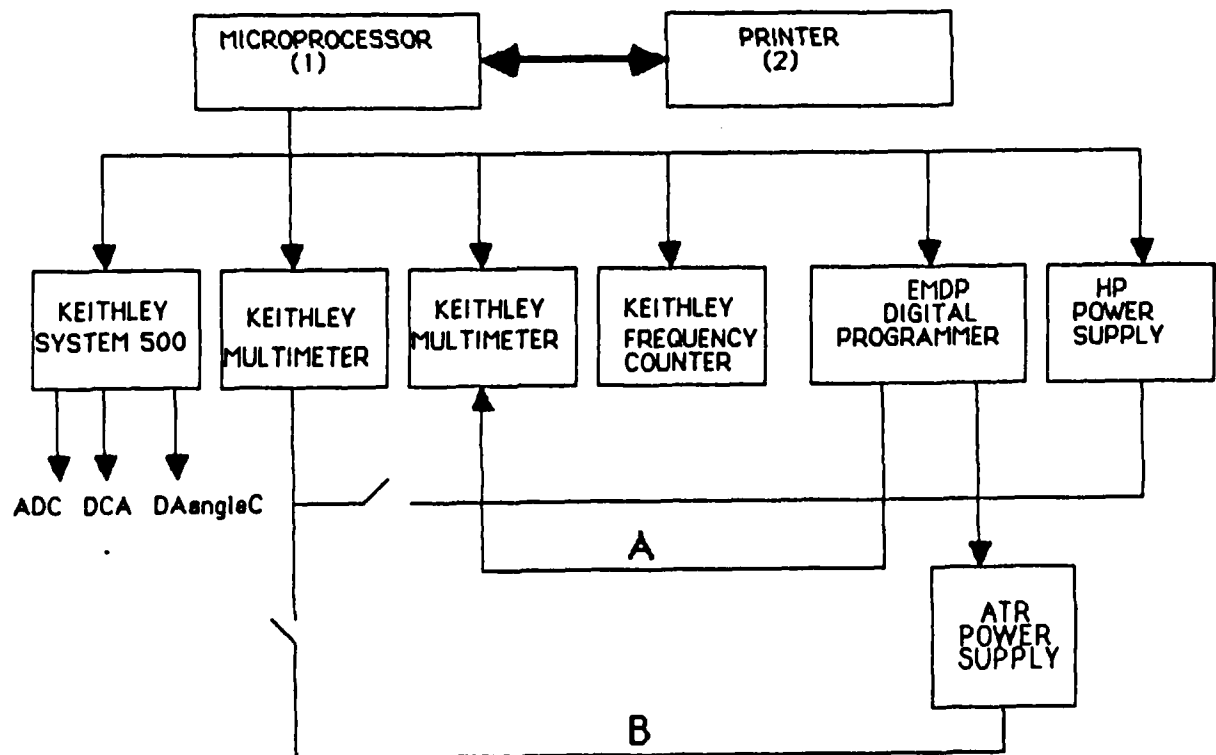
BLOCK DIAGRAM OF INSTRUMENTATION

Figure 1

APPENDIX 6: **Towards Tests of SSCD at Very Low Temperatures (T < 100 mK): Progress Report of ARC/NBS, Gaithersburg Collaboration**

The need for tests of the cryogenic SSCD detectors at very low temperatures (T ≤ 100 mK) is recognized by all groups working in this field. However, only two (H. Moseley et al, GSFC/Wisconsin; F. von Feilitzsch et al., TU Munich) have operated at temperatures below 0.3K; both have obtained results at 100≤T≤150 mK, using dilution refrigerators shared with other groups. Reaching the lowest possible temperature is judged important enough to justify the purchase of $150,000 dilution refrigerators, and the following groups have ordered new refrigerators (or are modifying their existing ones): B. Cabrera et al. (Stanford), B. Sadoulet et al. (Berkeley), F. von Feilitzsch et al. (TU Munich), L. Stodolsky et al. (MPI f. Physik, Munich), E. Fiorini et al. (Bologna/CERN), and G. Waysand et al. (Orsay/Saclay/Paris). Almost all of these groups are expected to have operational dilution refrigerators by fall 1988.

In collaboration with the Temperature Division of NBS, Gaithersburg we have reassembled and tested a dilution refrigerator to 15 mK, and have initiated modifications for very low temperature tests of cryogenic particle/radiation detectors. This gives ARC the unique advantage of having a dilution refrigerator dedicated for superconducting detector studies. Furthermore, at a total cost of about $10,000 including manpower, we now operate a dilution refrigerator which otherwise would be in mothballs.

A6.1 Goals/Sechedules

In Section 5 we argued that, by operating a SSCD at very low temperature, one can gain about two orders of magnitude in detector sensitivity. In certain applications (detection of weakly interacting particles, detection of visible/infrared photons) operation at T ≤ 100 mK may be necessary. For other applications of a SSCD, the use of very low temperature is essentially a matter of economical tradeoff. We note that a new generation of one-shot, computer-operated, relatively inexpensive (≤ $50,000) dilution refrigerators is becoming available commercially. Many applications of a SSCD will require hundreds of channels of electronic readout. Thus use of sophisticated cryogenics with simpler/less expensive electronics may be preferred to a simple liquid helium-4 cryostat with ultrasensitive, expensive electronics. We believe that this question can be studied only experimentally, and is a legitimate part of SSCD's feasibility testing.

As a result of priority changes by NBS, a dilution refrigerator (DR) was to be retired; at the same time, an RF Faraday cage housing an inoperational He-3 cryostat existed. In

an agreement reached between ARC and NBS, in which Drs.' Drukier and Girard became visiting scientists at the latter, the dilution refrigerator was reassembled within the RF cage and tested to 15 mK. Within the agreement terms, ARC provides manpower, general electronics, and direction to the research, and will financially support the experiments.

The preliminary tasks were:

1) removal of the liquid He-3 cryostat from the cage, installation of the dilution refrigerator;
2) leak/low temperature operational testing of the refrigerator;
3) development of the initial readout electronics and low temperature testing;
4) low temperature (T $\leq$ 100 mK) studies of SSCD hysteresis curves;
5) irradiation tests at T $\leq$ 100 mK).

Even with new units and full support of the manufacturer, the assembly and debugging of a dilution refrigerator typically requires six to nine months. Thus, our initial timetable for completing the above tasks was:

Tasks 1-2: January, 1987.
Tasks 3-4: February, 1988.
Tasks 5: March, 1988.

For the first series of hysteresis studies, the measurement of magnetic permeability using a low temperature LC oscillator was most convenient. According to plans, we will however implement LAPP/CERN-type fast electronics in the spring of 1988, and begin irradiation studies at T $\leq$ 100 mK. During the summer, one channel of DC-SQUID will be assembled and tested.

A6.2 Results

We have been extremely fortunate. Installation and leak testing of the DR was accomplished by the end of October; operational testing of the DR began in November, and temperatures of <15 mK were achieved in three subsequent runs.

In parallel, installation of the LC oscillator-based acquisition system was accomplished by November's end, and first measurements of SSCD hysteresis curves attempted in early December. A schematic of the experimental setup is shown in Fig. 1. For T>1K, no change in the sample permeability was observed, as anticipated. Unfortunately, at T<1K the oscillator circuit generated excessive heating of the sample, which we attributed to:

1. normal V = IR heating,

2. RF (eddy current) heating.

The first was estimated to be small relative to the second, in which case the time-averaged power delivered to the sample area is given by

$$Q = \frac{\pi^2}{64} \frac{Vd^2}{\rho} \ B^2 f^2 \ \cdot \ 10^{-16} W$$

where V, d, and ρ are the volume, diameter, and resistivity of the sample exposed to the time-averaged magnetic field (B) of the oscillator pickup coil, at frequency f. Because of the proximity of the 1.2 cm diameter X 10 cm length copper cold finger to the coil, a second test was initiated in late January using a fuzed quartz capillary of the same length but 0.7 cm external diameter. The results of these tests were however similar to those previous.

The oscillator circuit has been redesigned, as shown in Fig. 2, to operate at 100 kHz--a reduction of two orders of magnitude from that previous.
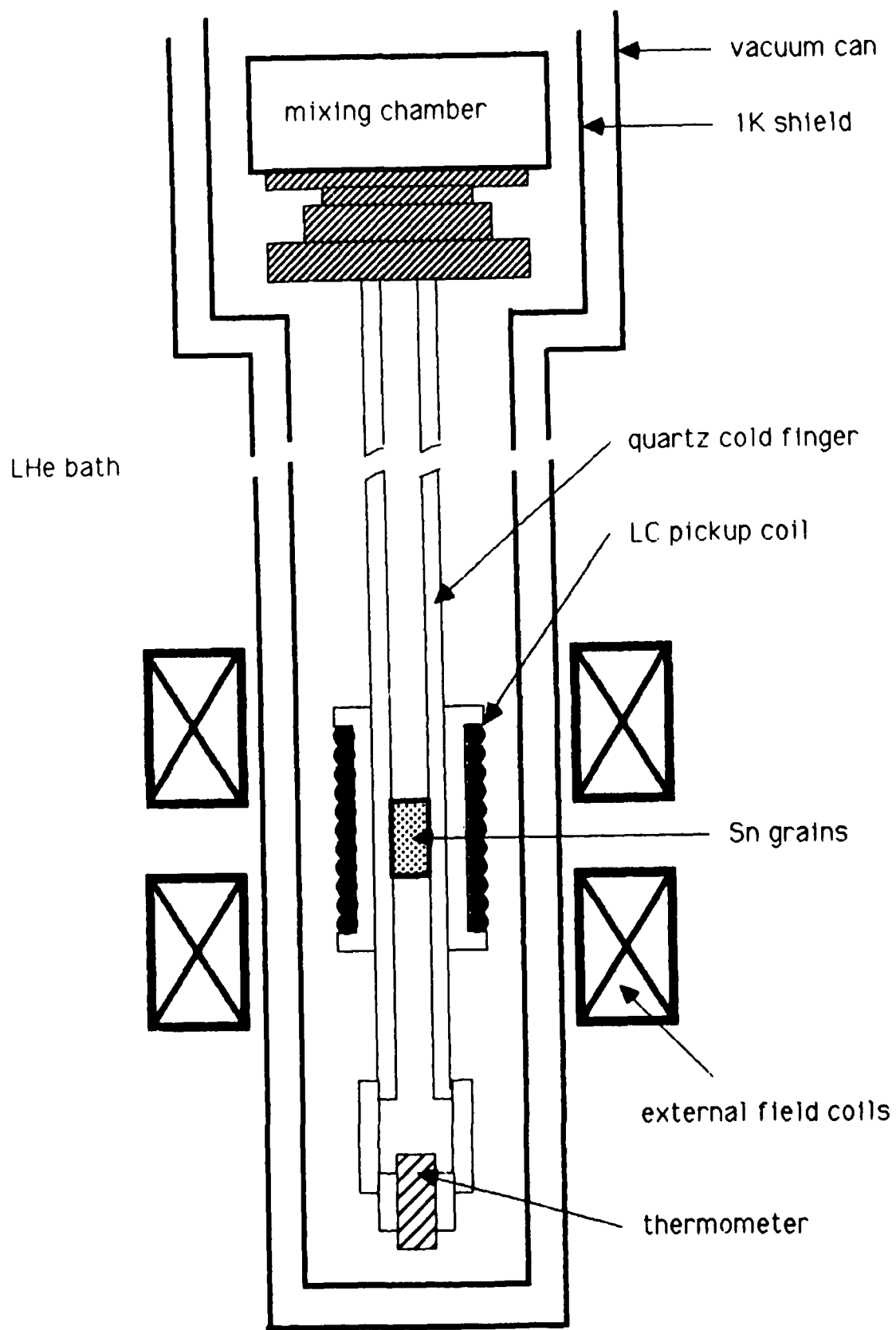
Figure 1
Experimental Set-up

4521BP

1 MΩ

560 Ω

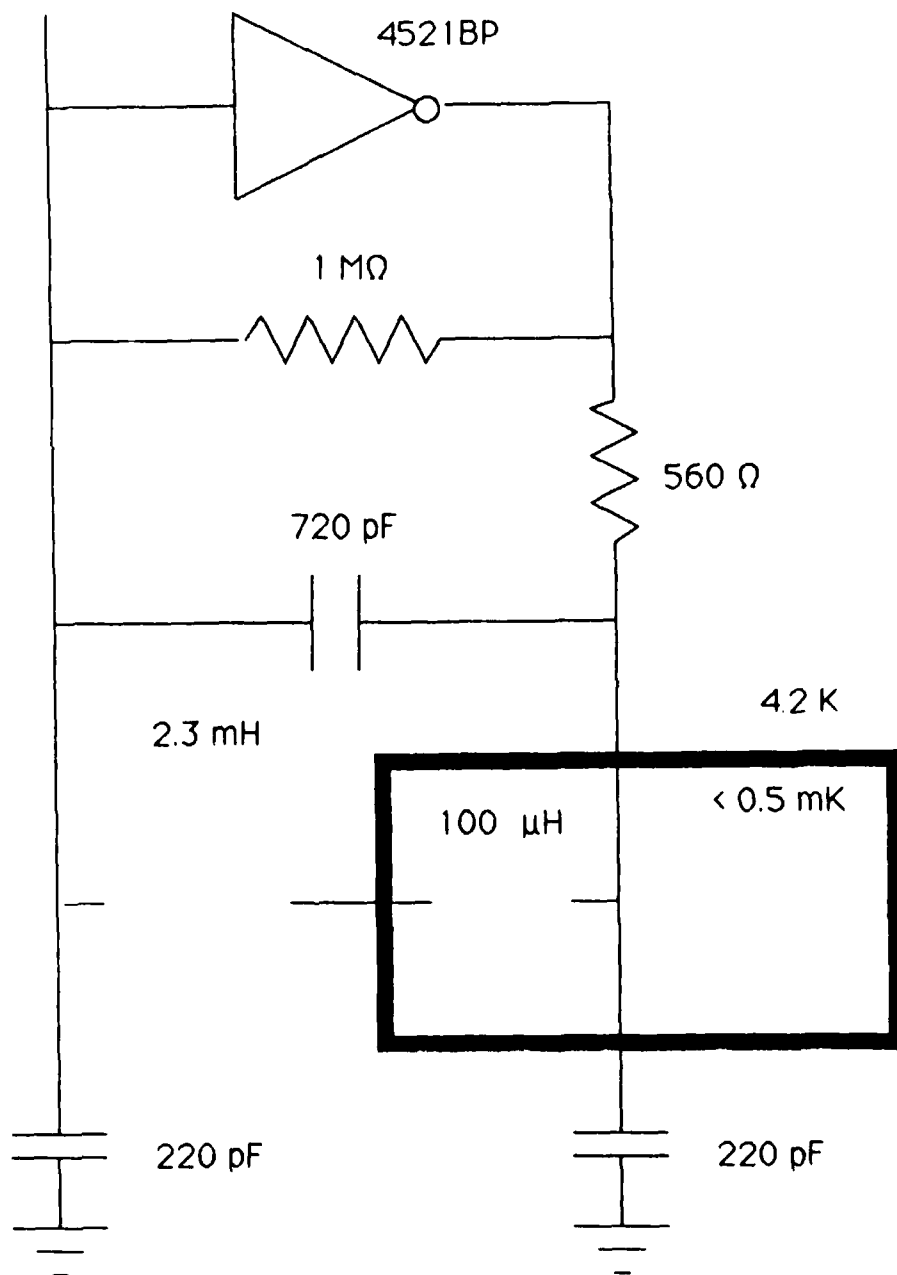720 pF

2.3 mH

4.2 K

100 µH

< 0.5 mK

220 pF

220 pF

Figure 2
Low Temperature LC Oscillator

The contractor, Applied Research Corporation hereby certifies that, to the best of its knowledge and belief, the technical data delivered herewith under Contract No N00014-87-C-0848 is complete, accurate, and complies with all requirements of the contract.

Date 11 March 88

Name and title of certifying Official _____

A.R. DRUKIER

The following people are authorized to certify in writing that the technical data is complete , accurate , and complies with all requirements of the contract.

These people are familiar with the Contractors technical data conformity procedures

Dr Andrew S. Endal, Senior Vice President for Research and Development

Dr Andrzej Drukier, Diector of Applied Technologies

Dr Anthony C. Danks, Senior Scientist.

END

DATE
FILMED

6-88
DTIC